

**The role of Macrophage Migration Inhibitory Factor (MIF) in anti-tumor
immune responses and metastatic niche formation in breast cancer**

Kristen Nicole Balogh
Durham, ME

Bachelor of Science Biology, Northeastern University, 2011

A Dissertation presented to the Graduate Faculty of the University of Virginia in
Candidacy for the Degree of Doctor of Philosophy

Experimental Pathology
University of Virginia
May, 2018

Acknowledgements

I would first like to thank my mentor Janet, for always supporting me as a person, and for constantly considering what is in my best interest in terms of my career development, and personal growth as a scientist. She has taught me how to be an independent thinker, and to recognize how and when to find the help I need when roadblocks inevitably appear. I will be forever thankful for all she has done for me.

I would also like to thank the members of my thesis committee for their unwavering enthusiasm for my work throughout my time in graduate school. I have always enjoyed meeting with my committee, and appreciate that they have always pushed me to my limits, while being extremely supportive at the same time.

I need to thank all of my “barn family” as well, as they (both human and equine) have kept me sane through the ups and downs of graduate school. I will remember each and every member of that family fondly, and will be forever grateful for everything they have done for me.

Lastly, I would like to thank my family. My parents have always been supportive of my interests, and have been instrumental in my ability to successfully follow my dreams as a scientist. My new family-in-law is also always extremely supportive of me, and it is a true gift to have them in my life. And thank you to my husband Peter, for always being there for me in every way shape and form.

Abstract

Macrophage Migration Inhibitory Factor (MIF) is an inflammatory cytokine expressed by most cell types, which functions as both a cell signaling molecule and a chemokine. MIF is known to have an intrinsic enzymatic activity as a keto-enol tautomerase, however the substrate for this activity *in vivo* is unknown, and the importance of this activity in the biological function of MIF is still debated. Overexpression of MIF has been found in both the serum and primary tumor tissue of patients with numerous cancer types, including lung, ovarian, colorectal and breast cancer, and increased expression often correlates with poor outcomes and increased risk of metastasis. Increased MIF expression has also been shown to drive tumor progression and enhance metastasis in a variety of mouse models of cancer, further supporting a role for MIF in tumor progression.

Many of the studies linking increased MIF expression to enhanced tumor progression have established MIF as an immune modulator, effectively working to dampen the anti-tumor immune response through a variety of mechanisms. Our group has demonstrated previously that MIF expression in the primary tumor leads to enhanced accumulation of the monocytic subset of immunosuppressive myeloid derived suppressor cells (MDSCs) in the primary tumor, leading to decreased T cell activation, and increased tumor growth. We have now discovered that loss of MIF expression in the 4T1 cell line also promotes the cancer cells to undergo a specific type of cell stress-induced death, termed “immunogenic cell death” (ICD). We show that loss of MIF expression enhances the ICD response specifically when cells are cultured under serum-free conditions *in vitro*.

Furthermore, we demonstrate that when implanted *in vivo*, MIF-depleted 4T1 tumors show enhanced infiltration of activated dendritic cells and T cells, indicative of an enhanced anti-tumor immune response. We suggest a model whereby MIF expression in the primary tumor protects the cancer cells from undergoing ICD *in vivo*, resulting in a dampened anti-tumor immune response, and loss of control of tumor growth.

Numerous studies, both in human cancer patients and in mouse models of cancer, also support a role for MIF in promoting metastasis. Supplementary to this, we have previously reported that depletion of MIF in the 4T1 model results in an almost complete loss of spontaneous pulmonary metastasis. However, we have since discovered that when MIF depleted tumors are permitted to grow to the same (larger) size as a MIF-expressing tumor, pulmonary metastasis is restored to the levels observed in the setting of a MIF-expressing tumor. This suggests that it is tumor size, rather than MIF expression, that is driving metastasis. In these same studies, we also analyzed whether MIF expression in the primary tumor had any effect on the generation of a metastatic niche, a process by which the primary tumor prepares a distant organ for future metastasis. Using the 4T1 model, we discovered that while loss of MIF expression in the primary tumor has no effect on collagen matrix remodeling in the lungs, loss of MIF expression does lead to a reduction in overall accumulation of CD11b⁺ myeloid cells in the lungs, both early and late during tumor development. Importantly, we found that the decrease in myeloid cells observed is not dependent on primary tumor size, suggesting that MIF expression in the tumor is directly driving this phenotype. Further analysis of the myeloid cell populations in the lungs of WT versus MIF KD tumor-bearing mice by flow cytometry revealed no

differences in the subsets analyzed. More detailed analysis of lung-infiltrating myeloid cells will need to be performed to determine which subset(s) is specifically controlled by MIF expression in the primary tumor.

We have also utilized the MMTV-PyMT murine transgenic model of breast cancer to further confirm the role of MIF in tumor progression. We observed a significant delay in tumor progression in MIF KO mice compared to WT mice using this model. We also detected a significant decrease in overall tumor burden at both 8 weeks and 5 months in MIF KO mice. However, we discovered no difference in pulmonary metastasis between WT and MIF KO mice at the late stages of tumor development, suggesting that MIF expression is important for promoting primary tumor growth, but not metastasis. Based on our previously published work, we hypothesized that MIF expression may promote tumor growth through increased accumulation of MDSCs in the tumor microenvironment in this model. However, when we analyzed tumor-infiltrating myeloid cells both early and late during tumor development, we found no significant differences in either MDSC subpopulation. This suggests that there is another mechanism by which MIF is controlling tumor growth in this model. We propose that a more detailed analysis of immune infiltrates in early stage tumors in this model, focusing on dendritic cells and macrophages, will begin to reveal the mechanism by which MIF is promoting growth. Increased dendritic and T cell activation may also suggest that MIF expression in this model is functioning to protect cancer cells from undergoing ICD, as we see in the 4T1 model, and would further support a model in which loss of MIF expression renders the primary tumor more susceptible to recognition and attack by the immune system.

Overall, our work strongly supports development of a clinical MIF inhibitor for use in the setting of treating patients with solid tumors. We show a clear role for MIF in primary tumor growth, which is reliant on interaction with the host immune response.

Immunotherapy has proven to be quite successful in treating a number of cancer types in the clinic; however, the immunosuppressive tumor microenvironment remains a challenge to overcome in patients who do not show an ideal response to these treatment modalities. Our work suggests that combination of MIF inhibition with current immunotherapeutic strategies could enhance responses, and lead to better outcomes for a large number of patients.

Table of Contents

ACKNOWLEDGEMENTS.....	2
ABSTRACT.....	3
TABLE OF CONTENTS	7
LIST OF FIGURES	9
LIST OF ABBREVIATIONS.....	12
CHAPTER ONE: GENERAL INTRODUCTION	15
DISCOVERY OF MACROPHAGE MIGRATION INHIBITORY FACTOR (MIF) AND ITS ROLE IN INFLAMMATORY DISEASES	16
MIF'S ENZYMATIC ACTIVITY AND RECEPTORS	17
DEVELOPMENT OF MIF INHIBITORS.....	20
MIF AND CANCER.....	22
THE ANTI-TUMOR IMMUNE RESPONSE	25
MYELOID DERIVED SUPPRESSOR CELLS	26
MIF AND MODULATION OF THE ANTI-TUMOR IMMUNE RESPONSE.....	30
IMMUNOGENIC CELL DEATH (ICD) AND CANCER.....	31
THE METASTATIC NICHE	33
4T1 MURINE MODEL OF BREAST CANCER	37
MMTV-PYMT TRANSGENIC MODEL OF BREAST CANCER	39
MOVING THE FIELD FORWARD.....	41
CHAPTER TWO: MACROPHAGE MIGRATION INHIBITORY FACTOR PROTECTS CANCER CELLS FROM IMMUNOGENIC CELL DEATH AND IMPAIRS ANTI-TUMOR IMMUNE RESPONSES.	43
ABSTRACT	44
INTRODUCTION	45
MATERIALS AND METHODS.....	47
RESULTS	52
DISCUSSION	65
CHAPTER THREE: A ROLE FOR MIF IN PULMONARY METASTASIS AND METASTATIC NICHE FORMATION.....	79
ABSTRACT	80
INTRODUCTION	81
MATERIALS AND METHODS	84
RESULTS	88
DISCUSSION	101
CHAPTER FOUR: MIF PROMOTES PRIMARY TUMOR GROWTH, BUT NOT METASTASIS OR MYELOID CELL ACCUMULATION IN THE MMTV-PYMT MURINE MODEL OF BREAST CANCER.	105
ABSTRACT	106
INTRODUCTION	107
MATERIALS AND METHODS.....	108
RESULTS	112
DISCUSSION	126

CHAPTER 5: DISCUSSION AND FUTURE DIRECTIONS.....	131
THE ROLE OF MIF IN TUMOR GROWTH AND METASTASIS.....	132
<i>MIF and ICD in the 4T1 model</i>	<i>133</i>
<i>Detection of ICD in vivo.....</i>	<i>136</i>
<i>MIF in combination with ICD inducers/non-inducers.....</i>	<i>137</i>
<i>Role of CD4 versus CD8 T cells in tumor control in the 4T1 model.....</i>	<i>138</i>
MIF AND THE METASTATIC NICHE.....	139
<i>Further analysis of the role of MIF on matrix remodeling in the metastatic niche.....</i>	<i>141</i>
ROLE OF MIF IN TUMOR PROGRESSION IN THE MMTV-PYMT MODEL.....	142
<i>Further dissection of immune cell subsets in WT and MIF KO MMTV-PyMT tumors</i>	<i>142</i>
<i>Analysis of ICD/anti-tumor immunity in the MMTV-PyMT model.....</i>	<i>145</i>
<i>MIF, metastasis, and the metastatic niche in the MMTV-PyMT model.....</i>	<i>146</i>
MIF AS A CELL SURVIVAL FACTOR AND TRANSLATIONAL IMPLICATIONS	147
REFERENCES.....	152

List of Figures

Figure 1.1: The metastatic cascade.....	34
Figure 1.2: Development of a metastatic niche in the lung.....	38
Figure 1.3: Summary of tumor progression in the MMTV-PyMT murine model of breast cancer.....	40
Figure 2.1: Confirmation that MIF expression promotes tumor progression in the 4T1 model of breast cancer.....	53
Figure 2.2: MIF expression promotes cell growth and protects against cell death <i>in vitro</i> in serum-free conditions.....	55
Figure 2.3: MIF expression in the primary tumor dampens anti-tumor T cell responses <i>in vivo</i>	57
Figure 2.4: Systemic depletion of CD4 ⁺ and CD8 ⁺ T cells restores MIF KD tumor growth <i>in vivo</i>	59
Figure 2.5: MIF expression in the primary tumor leads to decreased dendritic cell abundance and activation in the tumor.....	61
Figure 2.6: MIF-expressing tumor cells show decreased markers of immunogenic cell death under serum-free conditions.....	63
Figure 2.7: Experimental Model.....	66
Supplementary Figure 2.1: Confirmation of MIF depletion and re-expression in 4T1 cell lines.....	71
Supplementary Figure 2.2: MIF expression protects against cleaved caspase 3-mediated cell death <i>in vitro</i> in serum-free conditions.....	72
Supplementary Figure 2.3: Gating strategy for T cell analysis by flow cytometry.....	73
Supplementary Figure 2.4: Treatment of mice with CD4/8 depleting antibodies leads to almost complete loss of CD4/8 ⁺ T cells in the circulation during tumor growth.....	74
Supplementary Figure 2.5: MIF expression in the primary tumor does not affect total intratumoral leukocyte abundance.....	75

Supplementary Figure 2.6: Gating strategy for DC analysis by flow cytometry.....	76
Supplementary Figure 2.7: MIF-depletion in the primary tumor does not affect dendritic cell presence or activation in the draining lymph node.....	77
Supplementary Figure 2.8: <i>In vitro</i> DC activation is not achieved through treatment with WT or MIF KD CM or by co-culture with WT or MIF KD cells.....	78
Figure 3.1: MIF expression promotes tumor progression and spontaneous pulmonary metastasis in the 4T1 model of breast cancer.....	89
Figure 3.2: Tumor size, not MIF expression, directly dictates lung metastatic tumor burden in the 4T1 model.....	91
Figure 3.3: MIF expression in the primary tumor does not affect collagen crosslinking in the lungs at late stages of tumor growth.....	94
Figure 3.4: MIF expression in the primary tumor promotes accumulation of CD11b ⁺ myeloid cells in the lungs regardless of tumor size.....	95
Figure 3.5: MIF expression in the primary tumor does not affect collagen crosslinking in the lungs at early stages of tumor growth.....	97
Figure 3.6: MIF expression in the primary tumor promotes accumulation of CD11b ⁺ myeloid cells in the lungs during early tumor development.....	99
Figure 3.7: MIF expression in the primary tumor does not promote accumulation of CD11b ⁺ myeloid cells in the lungs during early tumor development by flow cytometry.....	100
Figure 4.1: MIF expression promotes tumor progression in the murine MMTV-PyMT spontaneous model of breast cancer.....	113
Figure 4.2: MIF expression does not promote spontaneous lung metastasis.....	115
Figure 4.3: MIF expression does not promote collagen cross-linking in late-stage lungs.....	117
Figure 4.4: MIF expression promotes CD11b ⁺ cell accumulation in late-stage lungs.....	119
Figure 4.5: MIF expression does not affect intra-tumoral accumulation of myeloid cell subsets at 5 months.....	121

Figure 4.6: MIF expression does not affect intra-tumoral accumulation of myeloid cell subsets at 4 months.....	123
Figure 4.7: MIF expression does not affect intra-tumoral accumulation of T cells at 4 months.....	125
Supplementary Figure 4.1: Confirmation of MIF status in WT and MIF KO MMTV-PyMT mice.....	130

List of Abbreviations

ANOVA: Analysis of Variance

APC: Antigen Presenting Cell

ATF6: Activating Transcription Factor 6

ATP: Adenosine Triphosphate

BMDC: Bone Marrow-derived Cell

CALR: Calreticulin

CHOP: C/EBP Homologous Protein

CM: Conditioned Media

CRC: Colorectal Carcinoma

CSF-1: Colony Stimulating Factor 1

CTL: Cytotoxic Lymphocyte

DAMP: Damage-associate Molecular Pattern

DC: Dendritic Cell

DHICA: D-dopachrome into 5,6-dihydroxyindole-2-carboxylic acid

ECM: Extracellular Matrix

EMT: Epithelial-Mesynchemal Transition

ER: Endoplasmic Reticulum

FMO: Fluorescence Minus One

GBM: Glioblastoma Multiforme

GM-CSF: Granulocyte-Macrophage Colony-Stimulating Factor

HCC: Hepatocellular Carcinoma

HIF1a: Hypoxia Inducible Factor 1a

HMGB1: High Mobility Group Box 1

HRE: Hypoxic Response Element

HSP: Heat-shock Protein

ICD: Immunogenic Cell Death

iNOS: Nitric Oxide Synthase

IRE1a: Inositol-requiring Enzyme 1 Alpha

KD: Knock-down

KO: Knock-out

LOX: Lysyl Oxidase

LPS: Lipopolysaccharide

MCP-1: Monocyte Chemoattractant Protein-1

MDSC: Myeloid Derived Suppressor Cell

MET: Mesenchymal-Epithelial Transition

MI: Myocardial Infarction

MIF: Macrophage Migration Inhibitory Factor

MMP: Matrix Metalloproteinase

MMTV: Mouse Mammary Tumor Virus

Mono-MDSC: Monocytic Myeloid Derived Suppressor Cell

MVD: Microvessel Density

NK: Natural Killer (cell)

NO: Nitric Oxide

NSCLC: Non-small Cell Lung Cancer

OS: Osteosarcoma

PBMC: Peripheral Blood Mononuclear Cell

PDAC: Pancreatic Ductal Adenocarcinoma

PDT: Photodynamic Therapy

PERK: Protein Kinase R-like ER Kinase

PI: Propidium Iodide

PMN-MDSC: Polymorphonuclear Myeloid Derived Suppressor Cell

PyMT: Polyoma Middle T (Antigen)

PRR: Pattern Recognition Receptor

RMS: Rhabdomyosarcoma

ROS: Reactive Oxygen Species

SFN: Sulforaphane

TAM: Tumor-associated Macrophage

TCR: T Cell Receptor

TGFbeta: Transforming Growth Factor Beta

TLR: Toll-like Receptor

Treg: Regulatory T cell

UPR: Unfolded Protein Response

VEGF: Vascular Endothelial Growth Factor

VEGFR1: Vascular Endothelial Growth Factor Receptor 1

Chapter One: General Introduction

Discovery of Macrophage Migration Inhibitory Factor (MIF) and its Role in Inflammatory Diseases

The Macrophage Migration Inhibitory Factor (MIF) is a cytokine that was first characterized in 1966 by Bloom and Bennett (1). MIF was originally shown to be secreted by T cells, and was named based on its ability to inhibit the random migration of macrophages *in vitro* (1,2). Since its discovery in lymphocytes, MIF has since been found to be expressed by a variety of other immune cell types (3–5), as well as non-immune related cells such as epithelial and endothelial cells (6,7). MIF was originally described as a pro-inflammatory cytokine based on increased concentrations of MIF observed in the circulation of patients with inflammatory disease, as well as in animal models of endotoxaemia and inflammation (8–11). MIF has also been found to stimulate production of several pro-inflammatory cytokines in an autocrine fashion, including TNF-beta, IL-1beta, and nitric oxide (5,12,13).

These discoveries have led to numerous studies on the effect of MIF expression in a wide range of inflammatory diseases. In a mouse model of sepsis, co-injection of *E. coli* with high doses of recombinant MIF lead to greater mortality by endotoxaemia than in mice challenged with *E. coli* alone. Further, high circulating levels of MIF have been found in patients experiencing severe sepsis or septic shock (14). In a mouse model of arthritis, treatment of mice with an anti-MIF antibody led to a delayed onset and decreased frequency of arthritic disease, due to suppression of autoantibody production specific to the peptide used to induce disease in this model (15). These results were confirmed a year later by Leech *et al.* in a rat model of arthritis, in which increased levels of MIF were

found in the serum of arthritic mice when compared to healthy controls, and treatment with an anti-MIF antibody significantly reduced the severity of disease (16). MIF expression by innate immune cells has also been found to promote development of colitis in mice. De Jong *et al.* reported that MIF-deficient mice were protected from development of colitis, but that when mice were reconstituted with wild-type (MIF-expressing) innate immune cells, disease was restored. This group also found increased levels of MIF in the plasma of patients with Crohn's disease, linking their findings in a mouse model to human disease (17). Furthermore, increased levels of MIF in both vascular endothelial cells and smooth muscle cells has been associated with atherogenesis in a model of high-fat diet-induced disease in rabbits (18). As recently reviewed by Dayawansa *et al.*, elevated levels of MIF have been observed in the plasma of patients experiencing myocardial infarction (MI), and increased MIF levels have been correlated with infarct size in mouse models of MI (19). Work by Rossi *et al.* revealed that eosinophils are a source of MIF in a mouse model of asthma, and that bronchoalveolar lavage fluid from patients with asthma contained increased levels of MIF when compared to healthy controls, an observation that was later confirmed in a study by Yamaguchi *et al.* (3,20). These studies broadly implicate MIF as an inflammatory mediator, and suggest that inhibition of MIF may be efficacious in a wide range of inflammatory diseases.

MIF's Enzymatic Activity and Receptors

MIF is a highly conserved protein (21), which functions in its active form as a homotrimer (11). MIF is unique in that it has several known enzymatic functions. MIF has been shown to act as a thiol oxidoreductase (22), a phenylpyruvate tautomerase (23),

and a D-dopachrome tautomerase (24). The D-dopachrome tautomerase activity allows MIF to rearrange double bonds within a molecule, and this activity can be measured *in vitro* through tautomerization of the synthetic compound D-dopachrome into 5,6-dihydroxyindole-2-carboxylic acid (DHICA), which results in a quantifiable colorimetric change (24). While this enzymatic activity of MIF can be measured *in vitro*, there is no known physiological substrate for the tautomerase activity of MIF *in vivo*. The requirement for MIF's enzymatic activity as a tautomerase in its biological function is debated, with some groups reporting no requirement for its biological function, while others report that this activity is necessary. MIF has been shown to inhibit monocyte chemoattractant protein-1 (MCP-1)-induced peripheral blood mononuclear cell (PBMC) chemotaxis *in vitro*, and enzymatically inactive MIF mutants are still able to inhibit this activity (25). Dickerhoff *et al.* also found that enzymatic inhibition of MIF through oxidation of MIF protein did not affect its ability to induce CXCL8 production from PBMCs *in vitro* (26). Conversely, Lubetsky *et al.* found that inhibition of MIF's enzymatic activity with a small molecule inhibitor prevented the ability of MIF to exert its known function of overriding glucocorticoid-based immune suppression *in vitro* (27), contradicting the findings of Bendrat *et al.* who earlier reported that mutagenesis of MIF at the active site (P1S) showed full activity in this assay (28). Another group reported that inhibition of MIF's enzymatic activity with a covalent modifier blocked both cell migration and anchorage independent cell growth in a model of lung adenocarcinoma (29). Onodera *et al.* utilized a P1A MIF mutant *in vitro*, and observed a reduction in MIF's ability to induce matrix metalloproteinase (MMP) expression by synovial fibroblasts (30). Use of a small molecule inhibitor to block MIF's enzymatic activity in a

lipopolysaccharide (LPS)-induced model of sepsis in mice resulted in decreased TNF α secretion from peritoneal macrophages, and use of the inhibitor increased survival of endotoxaemic mice (31). Our group has reported that the enzymatic activity of MIF is required for its ability to increase accumulation of immunosuppressive myeloid cells in tumors using a mouse model of breast cancer (32), and also that the enzymatic activity is required to protect those cancer cells from undergoing apoptosis *in vitro* under stress-inducing culture conditions (33). However, further investigation of the specific type of cell death occurring under cellular stress revealed that loss of the enzymatic activity resulted in intermediate expression of the markers of stress-induced cell death (33). Together, these studies point to the fact that our understanding of the role of MIF's enzymatic activity in its biological function is still partial, and discussion in the field remains highly controversial.

MIF has been described to bind a number of cell surface receptors, the first being the class II-associated invariant chain, CD74 (34). In this study, MIF was found to promote macrophage proliferation through binding to cell-surface CD74, followed by downstream activation of the MAPK pathway. This signaling activation requires colocalization of CD74 with CD44, as CD74 lacks an intracellular signaling domain (35). Since the discovery of CD74 as a MIF receptor, others have found that MIF functions as a non-cognate ligand for the chemokine receptors CXCR2, CXCR4, and CXCR7. Bernhagen *et al.* discovered that MIF is capable of competing with the cognate chemokine ligands for both CXCR2 and CXCR4, and this interaction leads to chemotaxis and arrest of monocytes and T cells in the setting of atherosclerosis (36). Recently, Lacy *et al.* reported

that an Arg-Leu-Arg (RLR) sequence in the 87-89 amino acid region of MIF is necessary for binding to CXCR4, and disruption of this interaction leads to loss of MIF/CXCR4 signaling, as well as the chemotactic responses to that interaction (37). Tarnowski *et al.* has also described the ability of MIF to functionally bind CXCR4, and added that MIF can bind CXCR7 in a model of rhabdomyosarcoma (RMS). This group concluded that binding of MIF to both of these receptors enhanced the adhesiveness of RMS cells *in vitro* (38).

Development of MIF inhibitors

While the role of MIF's enzymatic activity in its biological function remains controversial, targeting this activity with small molecule inhibitors has been the major focus in the development of MIF inhibitors. Zhang *et al.* developed the first inhibitors of MIF in 1999 in a study to better understand the biological role of MIF's enzymatic activity. These inhibitors were based on structural analogues of D-dopachrome methyl ester (a known substrate of MIF *in vitro*) (39). Since these initial studies, a number of small molecule inhibitors targeting MIF's enzymatic activity have been developed. One such inhibitor, ISO-1, competes with the substrate by binding at the active site of MIF, and has been shown to potently inhibit MIF's tautomerase activity (27,31). Another inhibitor, 4-iodo-6-phenylpyrimidine (4-IPP) has been well characterized as a covalent modifier of the proline residue (Pro¹) required for MIF's enzymatic activity (29).

As recently reviewed by Garai *et al.*, a number of other small molecule inhibitors of MIF have been described, including NAPQI (an acetaminophen derivative), phenylpyruvic

acid derivatives, cinnamates, acetylenic compounds, and a number of plant-derived products including curcumin, caffeic acid, resveratrol and dietary isothiocyanates (40). Our group discovered that the broccoli derived isothiocyanate sulforaphane (SFN) covalently inhibits MIF at the N-terminal proline, resulting in potent inhibition of MIF's tautomerase activity (41). This activity is shared with members of the isothiocyanate class of cancer preventives present in other cruciferous vegetables (41). We have also demonstrated that treatment of mice with SFN in a mouse model of breast cancer recapitulates the decreased accumulation of immunosuppressive myeloid cells we observe using a MIF knock-down (KD) version of the breast cancer cell line, supporting the importance of MIF's tautomerase activity in its biological function (32).

Other groups have focused on the interaction of MIF with its receptors, including Bai *et al.* who discovered an allosteric inhibitor of MIF. This compound, p425, is a sulfonated azo compound, which blocks the interaction of MIF with CD74, leading to a loss of MIF's proinflammatory properties *in vitro* (42). Schinagl *et al.* have also generated antibodies specific to the oxidized form of MIF, and treatment with these antibodies reduced prostate cancer cell growth both *in vitro* and *in vivo* (43). Another anti-MIF antibody developed by Shire was recently in Phase II clinical trials in the setting of colorectal carcinoma, but the trial was terminated in June of 2017 for as-of-yet undisclosed reasons (Clinicaltrials.gov/NCT01765790).

While studies with many of these inhibitors provide proof-of-concept support for the use of MIF inhibitors to treat a number of diseases, the lack of successful drugs in the clinic

points to the need for more work in this area. Small molecule inhibitors often have poor pharmacological properties once moved *in vivo*, and commonly have greater off-target effects and toxicities than monoclonal antibodies. However, the promiscuity of MIF as a ligand may make targeting its interaction with its multiple receptors challenging as well. Development of therapeutics that can both inhibit MIF's enzymatic activity and general receptor binding will likely yield the most promising results.

MIF and Cancer

MIF has been implicated in enhanced tumor growth and poor outcomes in a number of cancer types. MIF expression in tissue samples from patients with cervical adenocarcinoma has been positively correlated with primary tumor size and presence of lymph node metastases (44). MIF protein expression in the serum and gastric epithelium of patients with gastric cancer was positively correlated with tumor grade, with lowest expression being found in samples from healthy controls (45). Increased MIF mRNA and protein have been observed in tumor tissue from patients with lung adenocarcinoma compared to lung tissue from healthy controls. Interestingly, this study also demonstrated that MIF expression in the nuclei (as opposed to the cytoplasm) of tumor cells correlated with an increased overall survival, suggesting that the intracellular localization of MIF may play a role in tumorigenesis (46). A second study in patients with lung adenocarcinoma found that MIF levels in tumor tissue positively correlated with increased expression of pro-angiogenic chemokines and increased vessel density (47). Hagemann *et al.* reported that MIF protein levels are increased in ovarian carcinoma patient samples when compared to normal ovarian tissue, and the same study found

higher levels of MIF in malignant ascites fluid compared to cirrhotic (sterile) ascites (48). In a study of patients with colorectal carcinoma (CRC), serum MIF levels were positively correlated with increased risk of liver metastasis. This same study found increased MIF expression in both the primary tumor and in the metastatic tissue when compared to healthy controls and adjacent normal tissue in cancer patients (49). High MIF expression in tumor tissue from patients with hepatocellular carcinoma (HCC) was positively correlated with poor disease-free survival and tumor recurrence (though MIF expression did not correlate with overall survival) (50). Increased MIF mRNA expression in tumors from patients with pancreatic ductal adenocarcinoma (PDAC) has also been positively correlated with poor overall survival (51). Recently, Wang *et al.* performed a study of patients with osteosarcoma (OS) and found that increased MIF expression in serum and tumor tissue was positively correlated with primary tumor size, presence of pulmonary metastasis, and overall survival (52). Together, these studies strongly suggest a link between MIF expression and poor outcomes in the setting of solid cancers in general.

Mechanistically, MIF has been shown to inhibit accumulation of the tumor suppressor p53, leading to tumorigenesis through enhanced proliferation and protection from cell death (9,53). As discussed above, MIF signaling through CD74 also activates members of the MAPK pathway, leading to increased cellular proliferation in cancer cells (34). MIF has also been linked to increased angiogenesis, with MIF expression shown to correlate with the pro-angiogenic factors vascular endothelial growth factor (VEGF) and IL-8 in multiple breast cancer cell lines (54). Similarly, cytoplasmic MIF expression has been

strongly correlated with increased microvessel density (MVD) in a cohort of breast cancer patients (55).

MIF has been linked to the hypoxic response in a number of solid cancer models, with hypoxia being a known state in which cancer cells are able to better survive expansive growth when angiogenic development isn't able to keep up with rapid tumor growth. Interestingly, in a model of PDAC, MIF expression is both induced under hypoxic conditions, and necessary for maximal hypoxia inducible factor 1a (HIF1a) expression (56). Similarly, in models of glioblastoma multiforme (GBM) and cervical carcinoma, MIF expression is induced under hypoxic conditions (57,58). The MIF gene has also been described to contain a hypoxic response element (HRE) in the 5'UTR, suggesting that MIF is a direct transcriptional target of HIF (58,59).

Lastly, MIF has been shown to enhance metastasis by a number of groups. MIF enhanced epithelial-to-mesenchymal transition (EMT) in a model of breast cancer through activation of the RAS/MAPK signaling pathway (60). MIF has also been found to promote invasion of colon carcinoma cells by acting as a CXCR4 ligand (61).

Interestingly, MIF expression has also been found in tumor-secreted exosomes in a model of pancreatic cancer, and shRNA-based MIF depletion completely blocked liver metastasis in this model (62). Our group has also shown that depletion of MIF expression in the 4T1 murine model of breast cancer almost completely blocks spontaneous metastasis to the lungs (32). Together, this work suggests a multifunctional role for MIF in solid tumor growth, survival, and metastasis.

The Anti-Tumor Immune Response

The immune system as a whole is responsible for responding to “self” versus “non-self”, and defending against foreign material and pathogens. In the setting of cancer, the immune system is sometimes able to recognize oncogenic cells, which arise from “self tissue”, mainly through mutation of antigens that occurs as the tumor continues to grow and accumulate more genetic alterations. Uptake of tumor antigens by antigen presenting cells (APCs) leads to priming and activation of cytotoxic lymphocytes (CTLs) and helper T cells in the draining lymph nodes. Activated T cells are then able to travel back to the site of the tumor, invade the tumor tissue, and mount a cytotoxic response specifically to tumor cells expressing the mutated antigens.

However, it has become clear that cancers often develop evasive techniques to avoid immune detection. This process has been termed “immunoediting”, and has been described to involve three distinct steps. The first is the elimination phase, in which the immune system works to eradicate any tumor cells expressing foreign, or “non-self” antigens. This leads to the equilibrium phase, in which selection for survival of tumor cells with less immunogenic potential occurs, leading to a tumor which is highly resistant to immune detection and attack. During this phase, tumor cells are often quiescent, and can lay dormant for long periods of time. The final phase is the escape phase, where certain tumor cell clones have survived the long period of immune pressure and are now able to grow in an unrestrained fashion, leading to a clinically detectable tumor (63).

Cancers have developed other mechanisms to suppress the immune response outside of selection for non-immunogenic antigens as well. One of these mechanisms is secretion of immunosuppressive cytokines by both cancer cells and stromal cells in the tumor microenvironment. Some of the major cytokines responsible for immunosuppression in this setting include TGF-beta, IL-10 and GM-CSF (64). Tumors have also evolved mechanisms to recruit immunosuppressive immune cell subsets, such as regulatory T cells (Tregs), M2-like macrophages/tumor-associated macrophages (TAMs), and myeloid derived suppressor cells (MDSCs), which all work to impede the ability of anti-tumor immune cells to attack cancer cells (65–67). Tumors have also been found to commonly upregulate expression of the ligand for PD-1, a cell-surface protein found on activated T cells (68). Engagement of PD-1 with its ligand, PD-L1, functions as a “checkpoint” signal in activated T cells, leading to T cell anergy, apoptosis or exhaustion (69–71). Therefore, upregulation of PD-L1 by tumors functions as a potent inhibitory mechanism to control the anti-tumor response by tumor-infiltrating T cells. As recently reviewed by Chen *et al.*, targeting the interaction between PD-1/PD-L1 with monoclonal antibodies has proven to be very successful in treating patients with a number of solid cancer types, including metastatic melanoma, non-small-cell lung cancer (NSCLC), and metastatic renal cell carcinoma (72).

Myeloid Derived Suppressor Cells

Myeloid derived suppressor cells (MDSCs) are a heterogeneous population of immature myeloid cells, which have been shown to arise specifically during periods of chronic inflammation (73). During normal myeloid cell development, immature myeloid cells

leave the bone marrow and differentiate rapidly into mature subsets such as macrophages and dendritic cells upon arrival at distant sites such as the skin and lymph nodes.

However, in the setting of chronic inflammation, immature myeloid cells can be halted in their differentiation process, resulting in a population of MDSCs. These cells acquire an immunosuppressive phenotype by upregulating expression of molecules including arginase-1, nitric oxide synthase (iNOS), reactive oxygen species (ROS), and peroxynitrite, which utilize unique mechanisms to inhibit T cell activation and function (74–77). As reviewed by both Bronte and Rodriguez, L-arginine is a critical amino acid required for the survival of T cells, which can be depleted by both arginase and iNOS generated by MDSCs (78,79). Upon depletion of L-arginine, T cells down-regulate expression of the cell signal-initiating T cell receptor (TCR) zeta chain, resulting in decreased production of IL-2 and IFN γ (74,80). Nitric oxide (NO), a product of the utilization of L-arginine by iNOS, has been shown to inhibit the function of JAK3/STAT5 signaling in T cells and down-regulate MHC class II expression (75,76). Gehed *et al.* also reported that iNOS-generated NO can down-regulate E-selectin expression on endothelial cells, which may decrease the ability of T cells to enter the tumor-draining lymph nodes (81). ROS production has also been shown to inhibit CD3 zeta-chain expression and IFN γ production by T cells, as well as to generally inhibit antigen-specific CD8⁺ T cell responses (77,82). Peroxynitrite has more recently been shown to cause nitration of the TCR-CD8 complex, which leads to a reduced capacity of T cells to bind to the peptide-MHC I complex on APCs, leaving T cells unable to be stimulated in an antigen-specific manner (83).

Beyond their ability to suppress T cell activation, proliferation and function through the mechanisms described above, MDSCs have been shown to promote tumor growth and metastasis through a variety of other mechanisms. MDSCs have been shown to support tumor growth and invasion by promoting EMT in cancer cells, as well as by degrading the extracellular matrix at the peripheral edge of the tumor (84–86). MDSCs have also been shown to utilize expression of the S100A8/A9 family of proteins in an autocrine fashion for their retention in tumor tissues by both secreting these proteins into the circulation, and expressing their receptors. Furthermore, blockade of the receptors for S100A8/A9 leads to decreased accumulation of MDSCs in the circulation and lymphoid tissues of tumor-bearing mice (87). A second study reported that mice lacking expression of S100A8/A9 have reduced tumor burden, metastasis, and infiltration of MDSCs in tumor tissues and pre-metastatic sites (88). More recently, exosomal expression of S100A8/A9 originating from MDSCs has been shown to polarize macrophages into the pro-tumorigenic “M2-like” phenotype, further supporting the role of these proteins in MDSC biology in tumor tissue (89). A study by Shi *et al.* found increased numbers of MDSCs in pre-metastatic lungs in a mouse model of melanoma, and those MDSCs upregulated IL-1beta expression in the lungs. The increase in IL-1beta resulted in increased expression of E-selectin on endothelial cells in pre-metastatic sites, which promoted arrest of tumor cells at these sites, and increased overall retention of tumor cells in the lungs (90). MDSCs have also been shown to generate an immunosuppressive environment through upregulation of PD-L1 expression on their cell surface (91), induction of Treg development (92), and inhibition of natural killer (NK) cell activity (93).

MDSCs were initially described and characterized in a variety of mouse models of cancer, in which expansion of MDSCs was observed (94–97). In mice, MDSCs have been defined as expressing both CD11b and GR-1 (98). GR-1 consists of two epitopes, Ly6G and Ly6C, each of which can be recognized by specific antibodies (98). Analysis of expression of these two epitopes on MDSCs *in vivo* has revealed two subsets: monocytic MDSCs (mono-MDSC) and polymorphonuclear MDSCs (PMN-MDSC). Mono-MDSCs are generally described as being CD11b⁺Ly6G⁻Ly6C^{hi}, while PMN-MDSCs are described as being CD11b⁺Ly6G⁺Ly6C^{low} (99).

Since their discovery in mice, immunosuppressive MDSCs have been found in the circulation, as well as in primary tumor and metastatic tissue, of cancer patients. In human PBMCs, the mono-MDSC subset is defined as CD11b⁺CD14⁺HLA-DR^{-/low}CD15⁻, and the PMN-MDSC subset is defined as CD11b⁺CD14⁻CD15⁺ or CD11b⁺CD14⁻CD66b⁺ (99). Increased frequencies of MDSCs have been reported in both the circulation and tumor tissue of patients with colorectal carcinoma, and frequency of MDSCs in the tumor positively correlated with increased tumor stage and metastasis (100). Similarly, in a study of breast cancer patients, increased circulating numbers of MDSCs were detected in cancer patients versus healthy controls, and MDSC numbers positively correlated with increased clinical stage (101). A study of gastric cancer patients found increased numbers of circulating MDSCs in diseased patients compared to healthy controls, and increased numbers of MDSCs correlated with increased staging and poor survival. This study also found that MDSCs from these patients expressed high levels of arginase-1, and were able

to potentially inhibit T cell proliferation and IFN γ production *ex vivo* (102). Arihara *et al.* reported that increased MDSC frequency in HCC patients positively correlated with tumor progression, as well as increased circulating levels of IL-10, IL-13, and VEGF, all of which are important in the regulation of MDSC expansion (103). Studies of circulating MDSCs in PDAC and bladder cancer patients revealed that an increase in only the PMN-MDSC subset (and not the mono-MDSC subset) was seen relative to healthy controls (104,105). Alternatively, a study of patients with NSCLC found an increase in the mono-MDSC subset in the circulation of cancer patients compared to healthy controls, which also positively correlated with increased metastasis and decreased progression-free survival (106). These studies suggest that there may be differential regulation of the two subsets of MDSCs in different cancer types. Together, all of these studies suggest that MDSCs play an important role in tumor progression and metastasis, and targeting depletion or functional inhibition of these cells may significantly enhance the efficacy of immunotherapeutic techniques currently used in the clinic.

MIF and Modulation of the Anti-Tumor Immune Response

Our group and many others have published numerous studies linking tumor-derived MIF expression to dampened anti-tumor immune responses in cancer. We have previously published that MIF expression in the primary tumor in the 4T1 mouse model of breast cancer (more detailed discussion of this model can be found below) leads to an accumulation of mono-MDSCs in the tumor microenvironment, and that these cells are able to inhibit T cell proliferation *ex vivo* (32). MIF expression has also been linked to inhibition of T cell activation in a mouse model of neuroblastoma (107,108).

Additionally, in a mouse model of colorectal carcinoma, MIF knock-out (KO) mice were shown to have a significant reduction in immunosuppressive regulatory T cell accumulation in both the tumor and spleen (109).

MIF expression has also been linked to modulation of conventional myeloid cell populations by several studies. Inhibition of MIF promotes conversion of patient-derived MDSCs to dendritic cells (DCs), and addition of recombinant MIF inhibits maturation and migration of immature DC cultures (110,111). Furthermore, inhibition of MIF promotes conversion of M2-like macrophages to an M1-like phenotype in a mouse model of glioma (112). These studies suggest that MIF blocks immature myeloid cells from developing into populations capable of functioning to initiate an anti-tumor immune response.

Lastly, MIF has been shown to enhance immune escape in studies of ovarian cancer and glioma by down-regulating expression of the NK cell activation ligand NKG2D (113,114). These studies suggest that increased MIF expression in the setting of cancer leads to protection of cancer cells through a number of immune modulatory mechanisms, and inhibition of MIF could release the suppressed immune response to a large degree, and from many angles.

Immunogenic cell death (ICD) and cancer

Recent work in the field of cell death has uncovered that apoptotic cell death, long believed to be a highly controlled and non-immunogenic process, can actually be

immunogenic under certain conditions of cell stress. This type of cell death has been termed “immunogenic cell death” (ICD), and detection relies on exposure of several immunogenic signals by dying cancer cells. These signals include secretion of adenosine triphosphate (ATP) and high mobility group 1 (HMGB1) into the extracellular space, as well as exposure of the endoplasmic reticulum (ER) chaperone protein calreticulin (CALR) and heat-shock proteins 70 and 90 (HSP70/90) on the cell surface (115–122). These molecules serve as damage-associated molecular patterns (DAMPs), and are recognized by the host immune system through binding to pattern recognition receptors (PRRs) (123). Recognition of these molecules specifically by APCs leads to IL-1 β secretion, which is responsible for initiating IFN γ production by CD8⁺ T cells, finally resulting in a robust anti-tumor immune response (124).

ICD induction has been shown to be cell-stress dependent, with induction relying on an intact ER stress response (125). Several *in vitro* screens of current anti-cancer therapies have identified a number of strong ICD inducers, as well as therapies that do not induce this type of cell death. Several chemotherapies have been identified as ICD inducers, including anthracyclines, mitoxantrone, cyclophosphamide, and oxaliplatin, while others such as etoposide and mitomycin c do not (120). Therapies that exert physical effects on cancer cells, such as radiation and photodynamic therapy (PDT), have also been identified as strong inducers of ICD (121,126–128). While these therapeutic modalities have very different effects on cancer cells in terms of the mechanisms by which cell death pathways are activated, they are each able to initiate an ER stress response, leading

to the downstream exposure of the critical DAMP signals discussed above, leading to anti-tumor immunity *in vivo*.

The Metastatic Niche

The process of metastasis consists of several consecutive steps culminating in the successful outgrowth of a macrometastasis at a distant site from the location of the primary tumor. This process begins with cancer cells in the primary tumor acquiring an invasive phenotype, allowing them to intravasate into the local vasculature of the tumor. These cells then travel through the circulation, where they must avoid attack from the host immune system before they can extravasate at distant sites. Upon extravasation, the cancer cells then must adhere to the new tissue, seeding a micrometastasis. Finally, the newly re-located tumor cells must successfully proliferate in order to form a macrometastasis (172). This process is depicted in **Figure 1.1**.

Steven Paget's "seed and soil" hypothesis, voiced over 100 years ago, suggested that the "seed" (tumor cells from the primary tumor) would only colonize the "soil" (distant organ site) if that distant site harbored the proper microenvironment to support growth of the "seed" tumor cells (129). Paget's work also established that certain cancer types tend to metastasize with organ preference. For example, breast cancers tend to metastasize to brain, bone, liver and lung (129). This early work to better understand the process by which cancers metastasize led to the hypothesis that primary tumors are actually able to alter distant sites ahead of the arrival of metastatic cells, helping ensure their survival at this new site. Work by Kaplan *et al.* in 2005 was the first to clearly demonstrate this

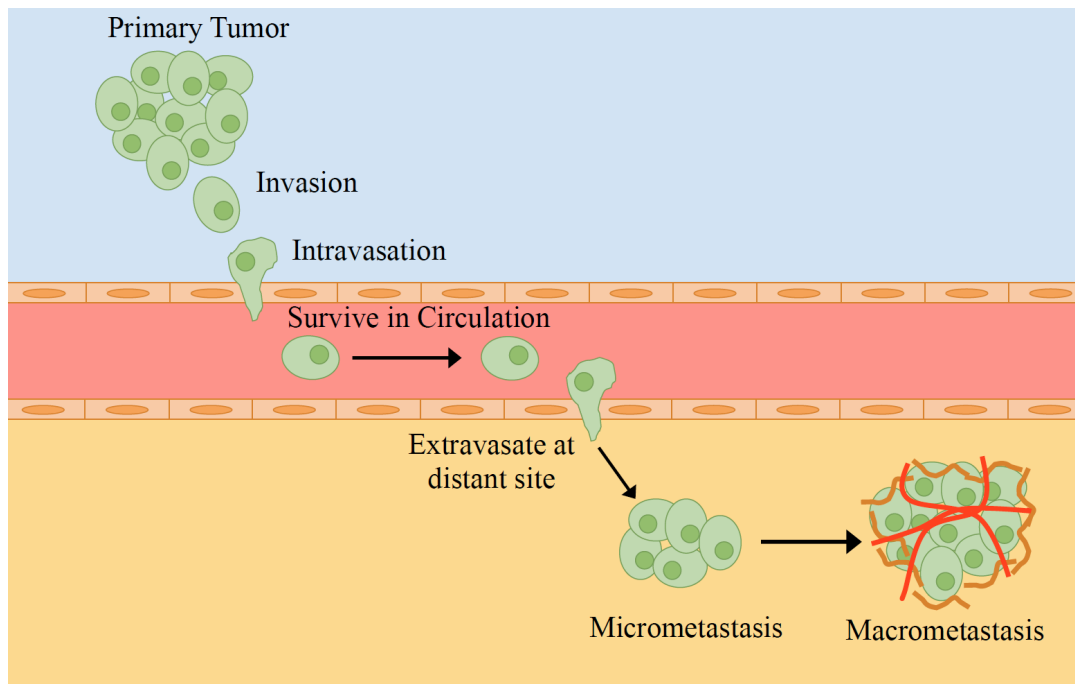


Figure 1.1: The metastatic cascade. In order for a primary to metastasize to a distant organ, a specific series of events must take place, starting with invasion of tumor cells at the edge of the primary tumor. These invasive cells must intravasate, and survive in the circulation as they travel to distant sites. Once they reach the target organ, the cells must extravasate into the new tissue, and seed a micrometastasis consisting of few very cells. This micrometastasis must then be able to start proliferating in order to form a detectable macrometastasis.

process *in vivo*, now referred to as establishment of a “pre-metastatic niche”. This study demonstrated that vascular endothelial growth factor receptor 1-positive (VEGFR1+) bone marrow-derived cells (BMDCs) formed clusters in the lung prior to the arrival of disseminated tumor cells, and recruitment of BMDCs was dependent on VEGF secretion from the primary tumor. These VEGFR1+ cells interacted with lung-resident fibroblasts to produce fibronectin, which was supportive of the seeding of tumor cells (130). Another important aspect of this study demonstrated that conditioned media from a melanoma cell line induced a mouse model of lung cancer to metastasize to organs typical of melanoma metastasis, rather than lung cancer metastasis (130). This experiment strongly supports the concept that certain cancer types metastasize with organ preference, which is determined by tumor-derived factors specific to each tumor type.

Since the seminal work by Kaplan *et al.*, a number of other key factors have been discovered to play a role in formation of a pre-metastatic niche. A number of studies have linked primary tumor hypoxia to successful niche formation. Hypoxia consists of a reduction in tissue oxygenation, and is a process that will occur in any tumor greater than 1cm³ due to lack of blood supply in the abnormal vasculature that often forms in tumors (131). HIFs are the downstream regulators of the hypoxia response, and expression of HIF1alpha has been associated with increased tumor growth and metastasis in a number of solid tumor types in both animal models and in cancer patients (132).

One hypoxia-induced gene that has been shown to be important in formation of the pre-metastatic niche is the lysyl oxidase (LOX) family of proteins. LOX functions in niche

formation by crosslinking collagen IV, which has been shown to both increase the stiffness of the extracellular matrix at pre-metastatic sites, as well as promoting recruitment of BMDCs (133,134). Inhibition of LOX expression in the primary tumor in a mouse model of breast cancer abrogates both seeding of BMDCs in the lung, as well as overall metastasis, suggesting that LOX's role in niche formation in this model is critical for successful metastasis to occur (134,135). LOX expression has also been found to be upregulated in a number of cancer types, including breast, and head and neck, and increased expression correlates with poor outcomes (136,137).

Recruitment of BMDCs to sites of pre-metastatic niche formation has also been shown to be critical in successful outgrowth of metastases (134,138,139). BMDCs travelling to distant sites can give rise to a variety of myeloid cell types, including neutrophils, macrophages, DCs and MDSCs (140). MDSCs have been found to accumulate in sites of pre-metastatic niche formation by a number of studies (138,139,141–143). MDSCs are thought to enable formation of metastases through several mechanisms. MDSCs can enhance recruitment of tumor cells through secretion of tumor cell chemoattractants such as S100A8/A9, MMP9, and Bv8 (139). MDSCs can also promote tumor cells to undergo a mesenchymal to epithelial transition (MET), supporting the seeding of cancer cells in a micrometastasis (144). As discussed previously, MDSCs are also known to create an immunosuppressed microenvironment, allowing newly seeded tumor cells to evade immune attack (74–77,93).

The process of metastasis is a complex, multistep progression, which requires secretion of specific factors by the primary tumor itself, modifications to the extracellular matrix at distant organ sites, recruitment of BMDCs that render the new site permissible to disseminated tumor cells, as well as successful outgrowth of metastatic cells upon seeding in this newly modified niche (**Figure 1.2**).

4T1 Murine Model of Breast Cancer

The 4T1 cell line was originally isolated from a single spontaneously arising mammary tumor from a Balb/cfC₃H mouse (145). This tumor cell line has become a highly utilized model for studying breast cancer *in vivo* due to several key characteristics. First, the 4T1 cell line was found to grow well both *in vitro*, as well as when implanted specifically into the mammary fat pad of a Balb/c host, allowing for study of tumor development in its site of origin (145). Second, the primary tumor in this model can be easily removed surgically due to its location close to the surface of the skin, with no critical organs in the way to render the procedure more challenging. This allows for analysis of metastatic disease and further treatment after primary tumor resection. The majority of patients undergoing treatment for breast cancer will undergo some version of tumor resection, followed by adjuvant therapy, making the 4T1 model an excellent tool for translational studies (146). Last, and perhaps most importantly, this model closely follows disease progression as found in the setting of human disease. The primary tumor in this model consistently spontaneously metastasizes to the draining lymph nodes, followed by spread to distal organs in a similar pattern to human disease, including to the lungs, liver, brain and bone (147,148).

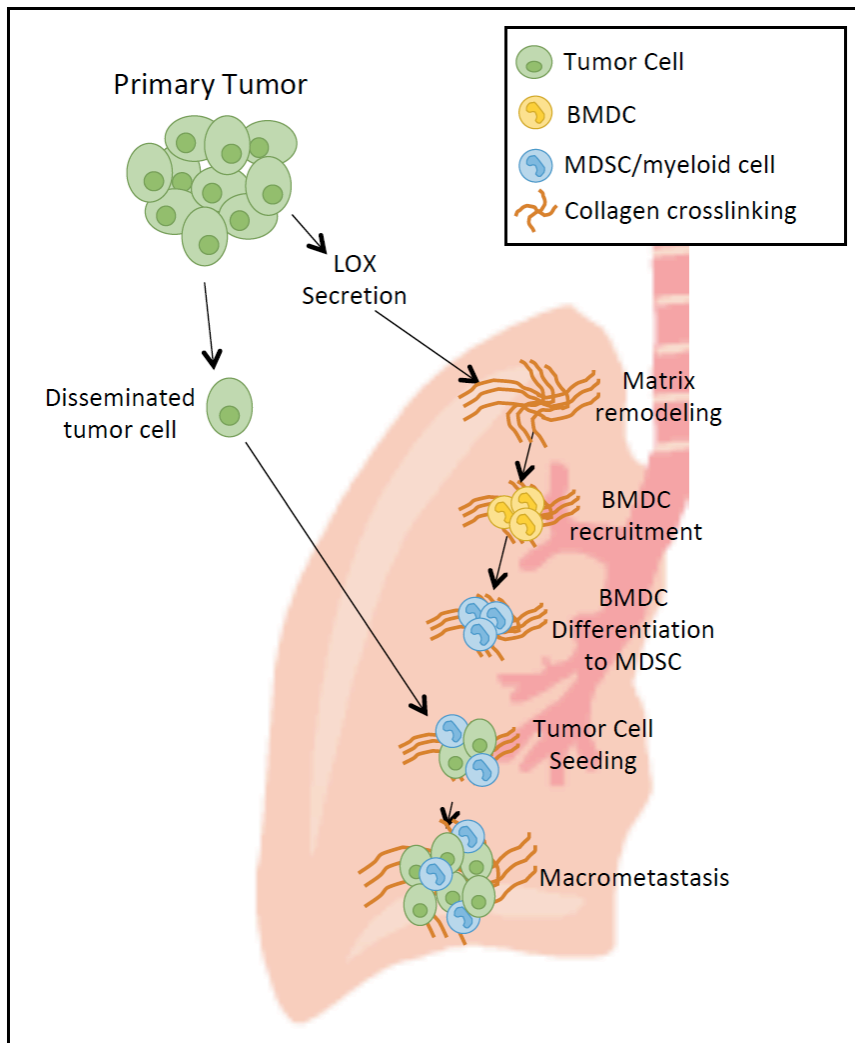


Figure 1.2: Development of a metastatic niche in the lung. Formation of a metastatic niche in the setting of breast cancer metastasis to the lung involves a consecutive set of steps, beginning with secretion of tumor-derived factors from the primary tumor, which travel through the circulation to the lungs. These factors, such as LOX, begin to remodel the extracellular matrix in the lung, rendering it more conducive to seeding of BMDCs, which have mobilized from the bone marrow in response to the presence of a tumor. These BMDCs differentiate into immunosuppressive myeloid cells, such as MDSCs, which creates a permissive, immunosuppressive microenvironment in which tumor cells can seed, begin to proliferate, and form a functional metastasis.

MMTV-PyMT Transgenic Model of Breast Cancer

The MMTV-PyMT murine model of breast cancer is widely used due to its genetically controlled nature, which is considered to be more clinically relevant than many implantable models. In this model, the polyoma virus middle T oncogene is expressed under the transcriptional control of the mouse mammary tumor virus (MMTV) promoter, leading to development of adenocarcinomas in multiple mammary fat pads of female mice carrying the transgene (149). As a membrane-bound protein, the polyoma virus middle T antigen (PyMT) functions as a scaffolding protein, to which Shc family proteins can bind, leading to activation of the MAP kinase and PI3K/AKT pathways (150). This activity makes the PyMT antigen a strong oncogene, and therefore a useful tool in development of genetic models of cancer.

The MMTV-PyMT model closely mimics the progression of human breast cancer, advancing from hyperplasia through poorly differentiated adenocarcinoma over a time course of approximately five months after birth, as depicted in the figure shown from Fluck *et al.* (**Fig 1.3**) (151). Lesions first arise very close to the nipple, making the earliest stages of tumorigenesis easy to locate and study histologically. However, as these mice and their mammary ducts mature, more lesions arise throughout the length of the mammary duct, quickly making it difficult to study individual tumor foci (151). Another benefit of this model is that the primary tumors spontaneously metastasize to the lungs, as is seen in human disease progression (149). Lung metastasis can often be seen macroscopically at the late stages of tumor growth, but can also be detected and quantified early through qRT-PCR for the MMTV-PyMT transgene. Lastly, the genetic

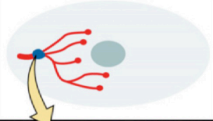
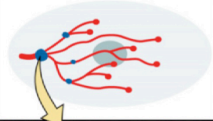
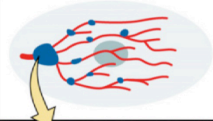
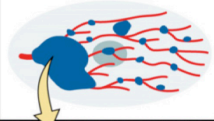
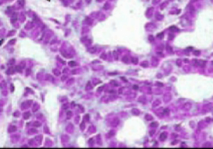
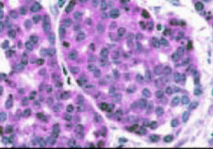
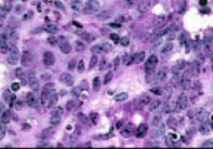
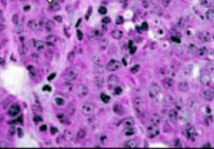
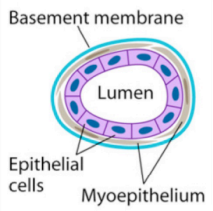
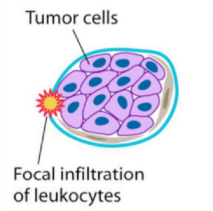
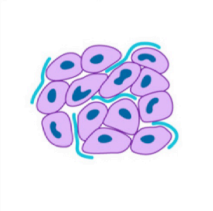
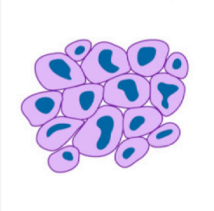
Stage	Hyperplasia	Adenoma/MIN	Early carcinoma	Late carcinoma
Gross				
H&E				
Cellular morphology				

Figure 1.3: Summary of tumor progression in the MMTV-PyMT murine model of breast cancer. The gross panel presents diagrams of the four stages of tumor progression, beginning in the pre-pubertal ducts through overtaking of the entire mammary gland (tumors are labeled as blue dots). H&E images are representative of each of the four stages of tumor progression. The cellular morphology panel depicts changes in the basement membrane and epithelial layer, as well as local inflammation during progression in this model (151).

background of this model is generally either FvB/N or C57Bl/6, both fully immunocompetent murine strains with many tools for modulating the immune system, such as Rag-/- crosses (151). This allows for analysis of specific aspects of the immune response in breast cancer progression, which is proving to be an exciting and successful avenue in terms of new treatment options. Together, these characteristics make the MMTV-PyMT model highly attractive for studying a variety of aspects of breast cancer progression.

Moving the Field Forward

Accumulating evidence supports MIF as a pro-tumorigenic factor that functions through both enhancing tumor cell-intrinsic survival, as well as dampening the anti-tumor immune response. However, while both of these phenotypes have been reported numerous times as discussed above, no link has been made between the two observed phenotypes. I hypothesized that these two observations are actually closely linked, and that the increase in cell death observed in MIF-deficient tumor cells may in fact be responsible for the enhanced immune activation observed upon loss of MIF expression in tumor cells. It has become appreciated more recently that cancer cell death can in fact be immunogenic under the correct conditions (such as under ER stress) (161). Therefore, the ability of MIF expression to intrinsically promote cancer cell survival may translate to a less robust activation of the immune response *in vivo* when compared to that which would be observed when MIF expression is lost. The work presented here aims to better

understand the MIF-dependent mechanism(s) linking cell death and the anti-tumor immune response.

**Chapter Two: Macrophage Migration Inhibitory Factor
protects cancer cells from immunogenic cell death and impairs
anti-tumor immune responses.**

Kristen N. Balogh, Dennis J. Templeton, Janet V. Cross

Modified from submission to PLoS ONE

Abstract

The Macrophage Migration Inhibitory Factor (MIF) is an inflammatory cytokine that is overexpressed in a number of cancer types, with increased MIF expression often correlating with tumor aggressiveness and poor patient outcomes. In this study, we aimed to better understand the link between primary tumor expression of MIF and increased tumor growth. We first confirmed our previous observation that higher MIF expression supported tumor growth in the 4T1 murine model of breast cancer. We subsequently discovered that loss of MIF expression in 4T1 cells led to decreased cell numbers and increased apoptosis *in vitro* under reduced serum culture conditions. We hypothesized that this increase in cell death would promote detection by the host immune system *in vivo*, which could explain the observed impairment in tumor growth. Supporting this, we demonstrated that loss of MIF expression in the primary tumor led to an increased abundance of intra-tumoral IFN γ -producing CD4⁺ and CD8⁺ T cells, and that depletion of T cells from mice bearing MIF-deficient tumors restored growth to the level of MIF-expressing tumors. Furthermore, we found that MIF depletion from the tumor cells resulted in greater numbers of activated intra-tumoral dendritic cells (DCs). Lastly, we demonstrated that loss of MIF expression led to a robust induction of a specialized form of cell death, immunogenic cell death (ICD), *in vitro*. Together, our data suggests a model in which MIF expression in the primary tumor dampens the anti-tumor immune response, promoting tumor growth.

Introduction

The Macrophage Migration Inhibitory Factor (MIF) was first described in the 1960's as a T cell secreted factor capable of inhibiting the random migration of macrophages *in vitro* (1,2). MIF has since been characterized as an inflammatory cytokine implicated in a number of diseases, including colitis and arthritis (17,152). Moreover, MIF has been broadly implicated in cancer, with overexpression shown in a number of solid tumor types (45,55,153–155). Importantly, MIF overexpression in the serum of cancer patients and in tumor biopsies has been correlated with enhanced tumor progression and metastasis (46,50,156,157). The MIF protein has an enzymatic activity, functioning as a keto-enol tautomerase, with the N-terminal proline required for this activity (158). While no physiological substrate has been discovered, our work and the work of others have indicated the biological importance of the enzymatic activity through use of point mutations and/or inhibitors that specifically target the active site of MIF (27,32,159). However, this conclusion remains controversial, as others have suggested that the enzymatic activity is dispensable for at least some of the biological functions of MIF (25,26).

Recently, several studies, including our own, strongly suggest that MIF exerts its pro-tumorigenic effects through modulation of the immunosuppressive tumor microenvironment. We published previously that, in the 4T1 model of breast cancer, MIF expression promotes tumor growth only in a host with a fully intact immune system capable of mounting an adaptive immune response (32). Work by several other groups has shown that MIF expression suppresses dendritic cell (DC) maturation *in vitro*, as well

as dampens T cell activation *in vivo* (107,108,111). This suggests that MIF is an important mediator in establishment of an immunosuppressive tumor microenvironment.

One mechanism to overcome immunosuppression in the context of the tumor microenvironment is the induction of a specialized type of cell death in cancer cells termed immunogenic cell death (ICD). As recently reviewed by Dudek *et al*, this type of cell death can be induced specifically in cancer cells through treatment with certain classes of chemotherapeutics, radiation therapy, and photodynamic therapy (PDT) (126). Cancer cells undergoing ICD exhibit cellular release of ATP and exposure of certain ER chaperones on the cell surface, including calreticulin (CALR) and HSP70 (117,119–121). Expression of these molecules on even a low number of cancer cells can be recognized by the host immune system through several mechanisms, leading to a robust anti-tumor immune response as well as immunological memory against the tumor (123).

In this study, we demonstrate that depletion of MIF expression in the 4T1 model of breast cancer strongly promotes ICD *in vitro* under serum-free conditions. We present evidence supporting a model in which depletion of MIF expression in the primary tumor *in vivo* leads to a robust anti-tumor immune response marked by enhanced DC maturation, followed by increased IFN γ -producing T cells in the tumor. This leads to greater tumor control in MIF-depleted tumors.

Materials and Methods

Cell lines

The 4T1 cell line was obtained directly from Caliper Life Sciences. The 4T1 cell line tested negative for mycoplasma at the University of Virginia, most recently on May 11, 2017. Cells were cultured under the conditions recommended by the ATCC. All cell lines were cultured no more than 10 passages before use in *in vivo* or *in vitro* experiments. The method for the generation of the MIF knock-down (MIF KD) 4T1 cells was published previously (32). For reconstituted cell lines, the coding region for wild-type (WT) human MIF or mutant human P2G MIF was inserted into the pQCXI-neo vector and was used to generate retroviruses. MIF-depleted 4T1 cells were infected with WT MIF or P2G MIF-expressing viruses (or empty vector) and selected with 500ug/mL neomycin. Efficient MIF depletion and subsequent re-expression of MIF in the reconstituted cell lines was confirmed by immunoblot (Santa Cruz, #sc-20121) (**Supplementary Figure 2.1A-B**).

Antibodies and Flow Cytometry

For immunoblotting, anti-cleaved caspase 3 (Cell Signaling, #9661S) was used, as well as anti-tubulin (Sigma, #T9026) as a housekeeping control. For flow cytometry analysis, cells were stained with propidium iodide (PI) (eBiosciences), Live/Dead Fixable Yellow Dead Cell Stain (Invitrogen), as well as with the list of antibodies shown in **Table 1** according to the manufacturers recommendations. All gating on cell surface markers was based on fluorescence minus one (FMO) controls. The cells were analyzed with the Beckman Coulter CyAN ADP LX 9 Color Flow Cytometer.

Table 1:

Antibody Name	Fluor	Vendor	Clone
Annexin V	FITC	BioLegend	N/A
Cleaved Caspase 3	PE	Cell Signaling	5A1E
CD3e	FITC	eBioscience	145-2C11
CD8a	efluor-450	eBioscience	53-6.7
CD4	APC efluor780	eBioscience	GK1.5
IFN γ	APC	Biolegend	XMG1.2
CD45	PerCP	BD Bioscience	30-F11
CD11b	Pacific Blue	Invitrogen	M1/70.15
CD11c	APCCy7	BioLegend	N418
CD8a	Pacific Orange	Invitrogen	5H10
CD103	FITC	BioLegend	2E7
MHCII	PE	eBioscience	M5/114.15.2
CD86	PECy7	BioLegend	GL-1
CD40	APC	BioLegend	3/23
Calreticulin	Alexafluor647	AbCam	EPR3924
HSP70	PE	Miltenyi Biotec	REA349
CD16/32 (blocking)	N/A	BioLegend	93

Mouse tumor models and tumor dissociation

Female 16-18 gram BALB/c mice were purchased from Charles River Laboratories.

1.0×10^4 WT or MIF KD 4T1 cells were injected into the mammary fat pad and monitored every other day for tumor growth starting 7 days after tumor implant. One hundred percent of mice develop tumors in this model using this approach. All animal studies were conducted in accordance with the University of Virginia Animal Care and Use Committee (ACUC) under protocol approval #4039 and all efforts were made to minimize suffering of animals in all experiments.

Using calipers, tumor volumes were estimated from two perpendicular measurements using the formula $V = 0.4 \times L \times W^2$. Tumors were excised from the mammary fat pad,

weighed, and then digested with 10,000 U collagenase I (Worthington Biochemical) for 60 min at 37°C, followed by addition of 30U of DNase (Qiagen) for 10 minutes at RT. Cell suspensions were strained through a 70-um screen before use in experiments.

***Ex Vivo* T cell Stimulation**

On day 10 of 4T1 tumor growth, tumors were excised and digested as described above. The digested material was incubated in triplicate *in vitro* for 4 hours with brefeldin A (BFA) (eBioscience) in anti-CD3-coated (eBioscience) 96-well plates. Cells were then stained by flow cytometry for extracellular T cell surface markers followed by intracellular staining for IFN γ .

T cell Depletion

Beginning two days before 4T1 cell tumor implantation, mice were treated with intraperitoneal injection of an initial dose of 200ug/mouse of anti-CD4 (clone GK1.5, BioXCell) and anti-CD8 (clone 2.43, BioXCell) antibodies in PBS, followed by similar dosing with 100ug/mouse every 4 days throughout the course of tumor growth. Tumors were excised on day 20 and weighed.

Intratumoral and Lymph Node Dendritic Cell (DC) Analysis

On day 8 of 4T1 tumor growth, tumors were excised and digested as described above. Draining inguinal and non-draining axillary lymph nodes were removed, manually dissociated using a blade, and strained through a 70-um screen. The digested/dissociated material was stained by flow cytometry for expression of dendritic cell surface markers.

Growth curve

5.0×10^4 4T1 WT or MIF KD 4T1 cells were plated in triplicate in 6-well dishes in RPMI media containing 10% fetal bovine serum (FBS) (HyClone). After 24 hours, medium was washed off and replaced with 1% serum or serum-free RPMI. The number of cells per well was counted each day up to three days after culture in 1% or serum-free media by hemocytometer.

Cell death and ICD cell surface marker analysis

5.0×10^4 WT or MIF KD 4T1 cells were plated in triplicate in 6-well dishes in 10% serum-containing RPMI. After 24 hours, media was washed off and replaced with serum-free RPMI. After a further 48 hours in serum-free media, cells were harvested and stained for Annexin V and propidium iodide (PI), cleaved caspase 3 or calreticulin and HSP70 by flow cytometry, or lysed in Laemmli sample buffer for cleaved caspase 3 analysis by immunoblot.

ATP Assay

5.0×10^4 WT or MIF KD 4T1 cells were plated in triplicate in 6-well dishes in 10% serum-containing RPMI. After 24 hours, media was washed off and replaced with serum-free RPMI. After a further 24 hours, media was sampled by removing 100uL from each well. ATP was measured in the media using the ATP Bioluminescence Assay Kit HS II (Roche) and the concentration was determined by comparing to a standard curve.

***In vitro* DC activation with 4T1 Conditioned Media (CM)**

CM was generated by removing the media from WT or MIF KD 4T1 cells grown in serum-free media for 48 hours. Bone marrow-derived DCs were generated *in vitro* by culturing 5×10^5 naïve bone marrow cells in 6-well dishes with media containing 20ng/mL GM-CSF and 10ng/mL IL-4. On days 2 and 5, cells were supplemented with fresh media plus cytokines, and on day 5 1ug/mL LPS was added as a positive control, or 500uL of CM was added (only fresh media was added to the unstimulated cells). On day 8, cells were harvested and analyzed for expression of DC activation markers.

***In vitro* DC activation with 4T1 co-culture**

Bone marrow-derived DCs were generated *in vitro* using the protocol described above. On day 5, the DC cultures were harvested by gently scraping the cells off the plates with a cell scraper, and DCs were moved to cultures containing WT or MIF KD 4T1 cells grown in serum-free media for 48 hours. 1ug/mL LPS was added to positive control cells, and media containing only cytokines was added to the unstimulated cells. On day 8, cells were harvested and analyzed for expression of DC activation markers.

Statistical Analysis

Data are presented as mean +/- SEM. Data was analyzed either by Student's t-test or one-way ANOVA using the Graph-Pad Prism analysis software. P values are represented in the figures as * $p < 0.05$, ** $p < 0.01$, *** $p < 0.001$, **** $p < 0.0001$.

Results

Confirmation that MIF expression promotes tumor progression in the 4T1 model of breast cancer.

We have previously demonstrated that depletion of MIF in the 4T1 model results in delayed tumor growth and impaired metastasis (32). The 4T1 cell line is an orthotopic model of triple-negative breast cancer syngeneic to Balb/c mice (146), in which tumors spontaneously metastasize to the lungs, bone, brain and liver, similar to the metastatic profile seen in human breast cancer (160). To confirm the tumor growth observations we have observed previously, MIF knock-down (MIF KD) and MIF-expressing (WT) 4T1 cells were implanted in the mammary fat pad of Balb/c mice, and tumor growth was monitored over the course of 21 days. Consistent with our previous work, loss of MIF expression in the primary tumor reduced tumor growth in the 4T1 model (**Fig 2.1 A-B**).

MIF expression promotes cell growth and protects against cell death *in vitro* in serum-free conditions.

We previously reported that the *in vitro* growth of 4T1 cells was not altered following depletion of MIF under standard cell culture conditions with 10% serum (32). In order to more closely mimic the more nutrient-deficient microenvironment murine tumor cells might experience upon orthotopic implant into the mammary fat pad, WT or MIF KD 4T1 cells were cultured *in vitro* in 1% serum or serum-free media. Cells were counted each day for 3 days after the media was changed, and compared to standard 10% serum growth conditions. As expected, equal numbers of WT and MIF KD cells were observed

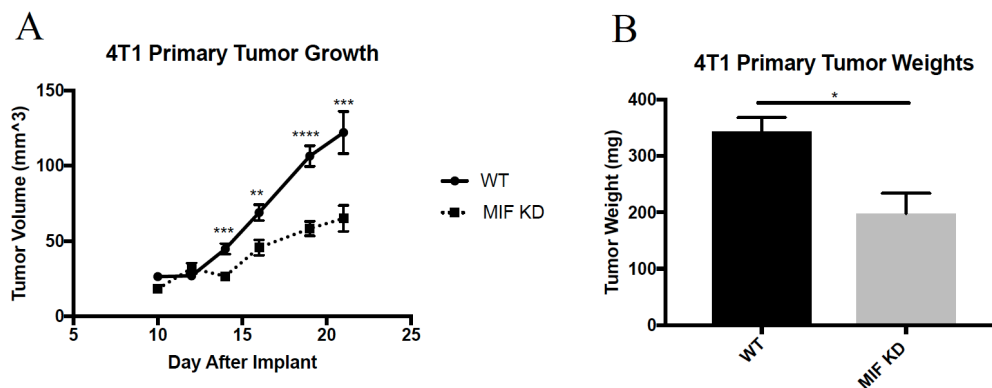


Figure 2.1: Confirmation that MIF expression promotes tumor progression in the 4T1 model of breast cancer. **A**, 1.0×10^4 WT or MIF KD 4T1 cells were implanted in the mammary fat pad of female Balb/c mice and tumor size was monitored starting at day 10 by caliper measurement. **B**, Tumors were harvested at day 22 of tumor growth post implantation and weighed. Data in **A** and **B** are representative of three independent experiments, with n=5 mice/group in each experiment. One-way ANOVA. *p<0.05, ** p<0.01, *** p<0.001 **** p<0.0001.

when cultured in 10% serum (**Fig 2.2A**). However, when the serum concentration was reduced to 1% or the cells were cultured in serum-free media, the MIF KD cells showed a significant reduction in cell number when compared to the WT cells (**Fig 2.2A**).

To determine if the decreased cell numbers in the MIF KD cultures under serum-free conditions was due to increased cell death, we measured this using several approaches. Annexin V and propidium iodide (PI) co-staining revealed that MIF-depletion led to an increased abundance of cells undergoing both early apoptosis (Annexin V⁺/PI) and late apoptosis/necrosis (Annexin V⁺/PI⁺) after 48 hours in serum-free media. In contrast, no differences were observed when the WT and MIF KD cells were cultured in 10% serum (**Fig 2.2B**). Cleaved caspase-3, a marker of late apoptosis, was also increased in the MIF KD cells after 48 hours in serum-free conditions, as detected by both flow cytometry (**Fig 2.2C**) and immunoblot (**Supplementary Figure 2.2**).

To confirm that the reduction in cell numbers observed in the MIF KD cultures was indeed due to loss of MIF expression, we reconstituted the MIF KD cells with WT MIF. In parallel, to determine whether the enzymatic activity of MIF is involved in this phenotype, we reconstituted the MIF KD cells with the enzymatically inactive point mutant form of MIF (MIF P2G). MIF KD cells engineered to re-express WT MIF, but not P2G MIF, led to increased cell numbers in serum-free conditions (**Fig 2.2D, bottom**). As expected, no difference in cell number was seen between these three cell lines in 10% serum (**Fig 2.2D top**). These data confirm that loss of MIF expression leads to a disadvantage when cells are cultured in low serum conditions, and demonstrates the r

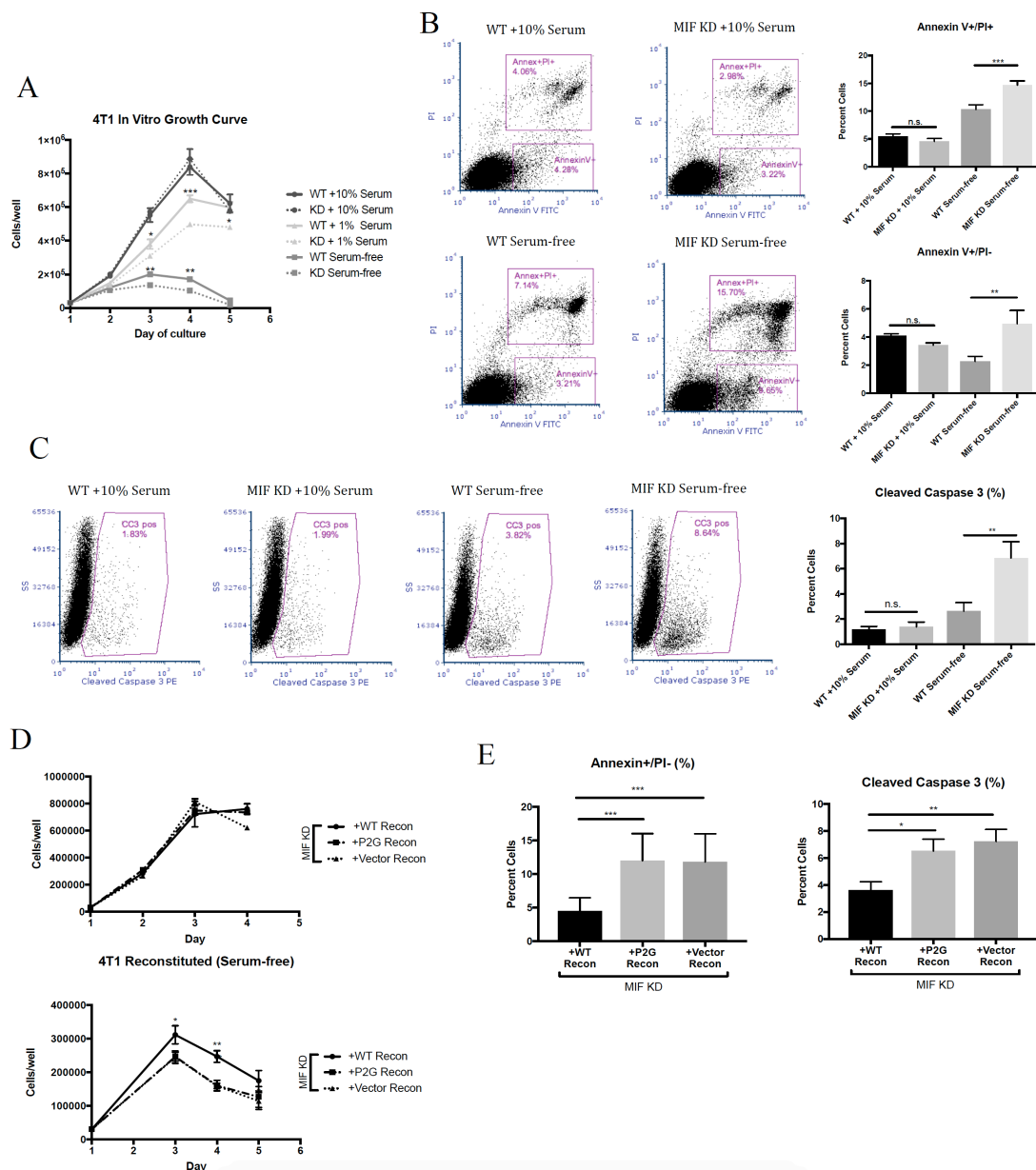


Figure 2.2: MIF expression promotes cell growth and protects against cell death *in vitro* in serum-free conditions. **A**, WT or MIF KD 4T1 cells were grown in 10% serum-containing media overnight, and then switched to fresh 10%, serum, 1% serum, or serum-free media. Cells were counted using a hemocytometer every day for 3 days. **B**, WT or MIF KD 4T1 cells were grown in 10% serum-containing media overnight, and then switched to fresh 10% or serum-free media for a further 48 hours. Cells were then stained for Annexin V and PI using flow cytometry, or **C**, stained for cleaved caspase 3 by flow cytometry. **D**, MIF KD 4T1 cells were reconstituted (recon) with WT MIF, P2G MIF or with an empty vector as a control and were grown in 10% serum-containing media overnight, and then switched to fresh 10% media (top) or serum-free media (bottom) and counted using a hemocytometer every day for 3 days. **E**, After 48 hours in fresh 10% or serum-free media, cells were stained for Annexin V and PI (left) or cleaved caspase 3 (right) using flow cytometry. Data is the mean of 3 independent experiments with 3 replicates per experiment. One-way ANOVA. * $p < 0.05$, ** $p < 0.01$, *** $p < 0.001$.

requirement for the enzymatic tautomerase activity for this biological function. Similarly, reconstitution of MIF KD cells with WT MIF only (but not P2G MIF) reduced the cell death observed in serum-free conditions (**Fig 2.2E**). Taken together, these results show that MIF-depletion leads to increased cell death when cells are cultured under serum-free conditions.

MIF expression in the primary tumor dampens anti-tumor T cell responses *in vivo*.

A recent report suggests that cancer cells that are dying due to cellular stress can elicit a strong anti-tumor immune response (161). Therefore, we next asked whether loss of MIF expression was associated with a heightened anti-tumor immune response *in vivo*. We analyzed T cell infiltration and activation in day 10 WT and MIF KD 4T1 tumors. This time point was selected because it is the earliest time point at which a statistically significant difference in tumor size between WT and MIF KD tumors is detectable (**Fig 2.3A**). MIF KD tumors contained significantly more tumor-infiltrating CD8⁺ T cells, both as a percent of total CD3⁺ T cells and by absolute cell number (**Fig 2.3B**). The MIF KD tumors also contained significantly fewer CD4⁺ T cells by percent. However, no significant difference was observed in the total number of CD4⁺ T cells (**Fig 2.3B**). Interestingly, both populations of tumor-infiltrating T cells in the MIF KD tumors were more activated, as exhibited by the ability of both CD8⁺ and CD4⁺ T cells to express IFN γ after *ex vivo* re-stimulation (**Fig 2.3C**). The gating strategy for the described T cell analysis is shown in Supplementary Figure 2.3, and the placement of all gates was determined based on the fluorescence minus one (FMO) controls shown (**Supplementary Figure 2.3**). Collectively, these results suggest that loss of MIF expression in the primary

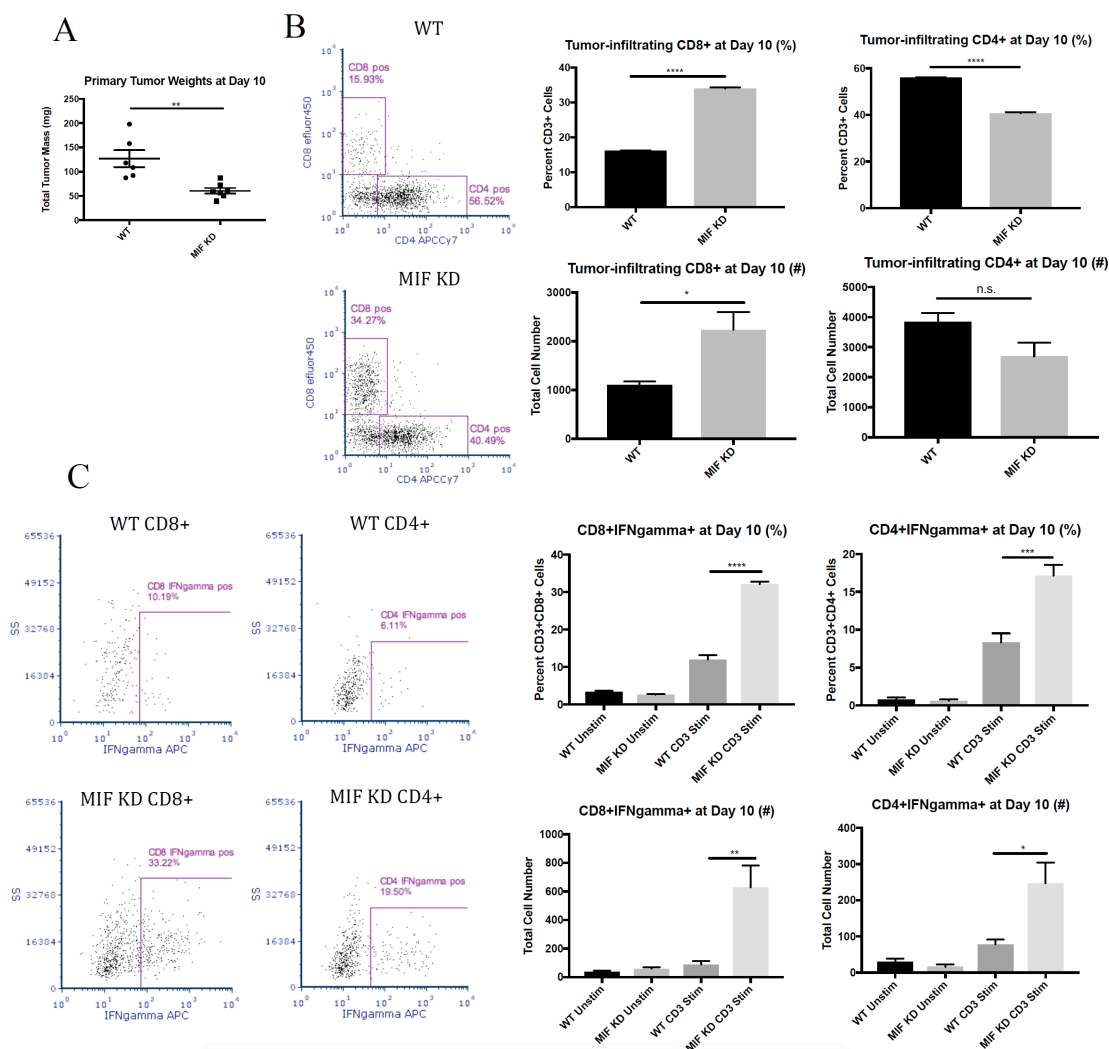


Figure 2.3: MIF expression in the primary tumor dampens anti-tumor T cell responses *in vivo*. 1.0×10^4 WT or MIF KD 4T1 cells were implanted in the mammary fat pad of female Balb/c mice. **A**, Tumors were harvested at day 10 of tumor growth and weighed. Tumors were then digested and dissociated, and cells were cultured *in vitro* for 4 hours in the presence of BFA +/- anti-CD3 stimulation. Cells were stained for CD4 and CD8 surface expression (**B**) and intracellular IFN γ (**C**) by flow cytometry. Data shown are representative of one of three independent experiments, with n=6 mice/group. One-way ANOVA. * p<0.05, ** p<0.01, ***p<0.001, **** p<0.0001.

tumor results in an enhanced early anti-tumor T cell response, leading to decreased tumor outgrowth.

Systemic depletion of CD4⁺ and CD8⁺ T cells restores MIF KD tumor growth *in vivo*.

In order to confirm that T cells are required for control of MIF KD tumors, we performed a T cell depletion experiment by treating WT and MIF KD 4T1 tumor-bearing mice with CD4 and CD8 depleting antibodies or isotype control antibodies (cIgG) throughout the course of tumor growth. Given that both CD4⁺ and CD8⁺ T cells exhibited enhanced IFN γ production in MIF KD tumors indicating enhanced functionality, we hypothesized that both populations are important in controlling growth in these tumors. Therefore, we depleted the CD4⁺ and CD8⁺ T cells simultaneously in the same mice (**Fig 2.3C**). The T cell depletion was highly effective, as confirmed at the time of tumor harvest by measuring T cell numbers in the circulation (**Supplementary Figure 2.4**). Depletion of T cells from mice bearing MIF KD tumors (dotted triangle) restored primary tumor growth to the level of WT tumors (solid circle) throughout the course of tumor growth. In contrast, depletion of T cells from mice bearing WT tumors (solid triangle) had a minimal, though still statistically significant, effect on tumor growth rate measured by calipers (**Fig 2.4A**). However, at the time of harvest, the tumor weight difference did not achieve statistical significance (**Fig 2.4B**). Nonetheless, this small difference suggests that there is some amount of T-cell mediated tumor growth control even in the setting of MIF-expressing tumors, but that this effect is very modest compared to the impact of T cells on the growth of MIF KD tumors. Cumulatively, these data confirm that the reduced

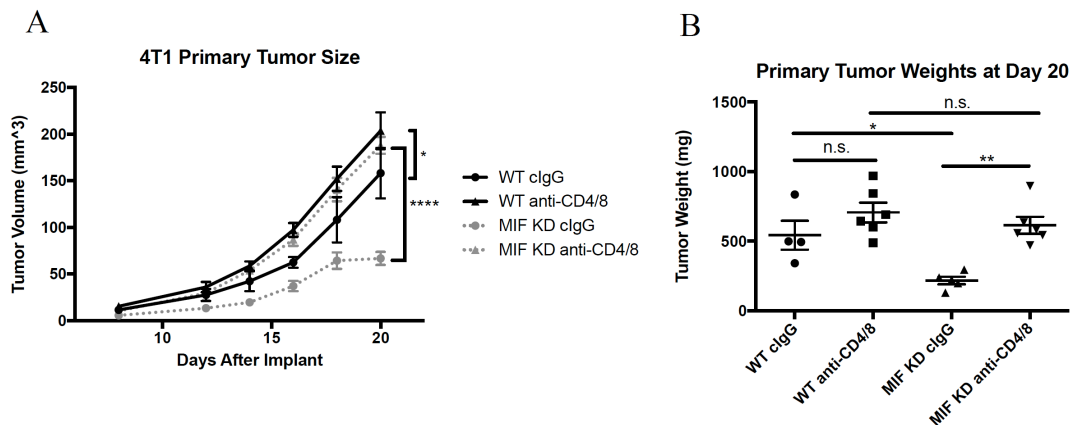


Figure 2.4: Systemic depletion of CD4⁺ and CD8⁺ T cells restores MIF KD tumor growth *in vivo*. 1.0×10^4 WT or MIF KD 4T1 cells were implanted in the mammary fat pad of female Balb/c mice. Mice were treated with CD4/8 depleting antibodies starting 2 days before tumor implantation and every 4 days thereafter. **A**, Tumor size was monitored starting at day 8 by caliper measurement. **B**, Tumors were harvested and weighed at day 20 of tumor growth. n=6 mice per group. One-way ANOVA. * p<0.05, ** p<0.01, **** p<0.0001.

growth rate of 4T1 tumors derived from cells that are depleted of MIF is dependent on an intact T cell response.

MIF expression in the primary tumor leads to decreased dendritic cell abundance and activation in the tumor.

We next hypothesized that the increased T cell abundance and activation in MIF KD tumors is due to enhanced activation of dendritic cells (DCs) either in the draining lymph nodes or the tumor. To test this, we examined WT and MIF KD 4T1 tumor-bearing mice for the presence and activation status of tumor-infiltrating and lymph node DCs. Because the difference in activated T cells was apparent at day 10, we examined DCs at day 8, as peak DC activation would be expected to occur slightly before T cell activation. No difference in primary tumor size was observed between WT and MIF KD tumors at this time point (**Fig 2.5A**). We also did not observe a statistically significant increase in total tumor-infiltrating leukocytes based on CD45 staining at this time point (**Supplementary Figure 2.5**). However, the abundance of CD11c⁺ DCs was increased in MIF KD tumors. Within this CD11c⁺ population, we also observed an increase in an unexpected population of CD103⁺CD8⁺ DCs in the MIF KD tumors (**Fig 2.5B**). We also examined the activation state of intratumoral DCs based on expression of MHCII, CD40 and CD86, with all gating determined based on the FMO controls shown in flow plots in **Fig 2.5C**. MIF KD tumors contained both a greater percentage of activated DCs, as well as a greater number per mg of tumor when compared to MIF expressing tumors (**Fig 2.5C**). DCs in MIF KD tumors also had higher expression of these activation markers on a per-cell basis as quantified by mean fluorescence intensity (MFI) (**Fig 2.5C**). The gating

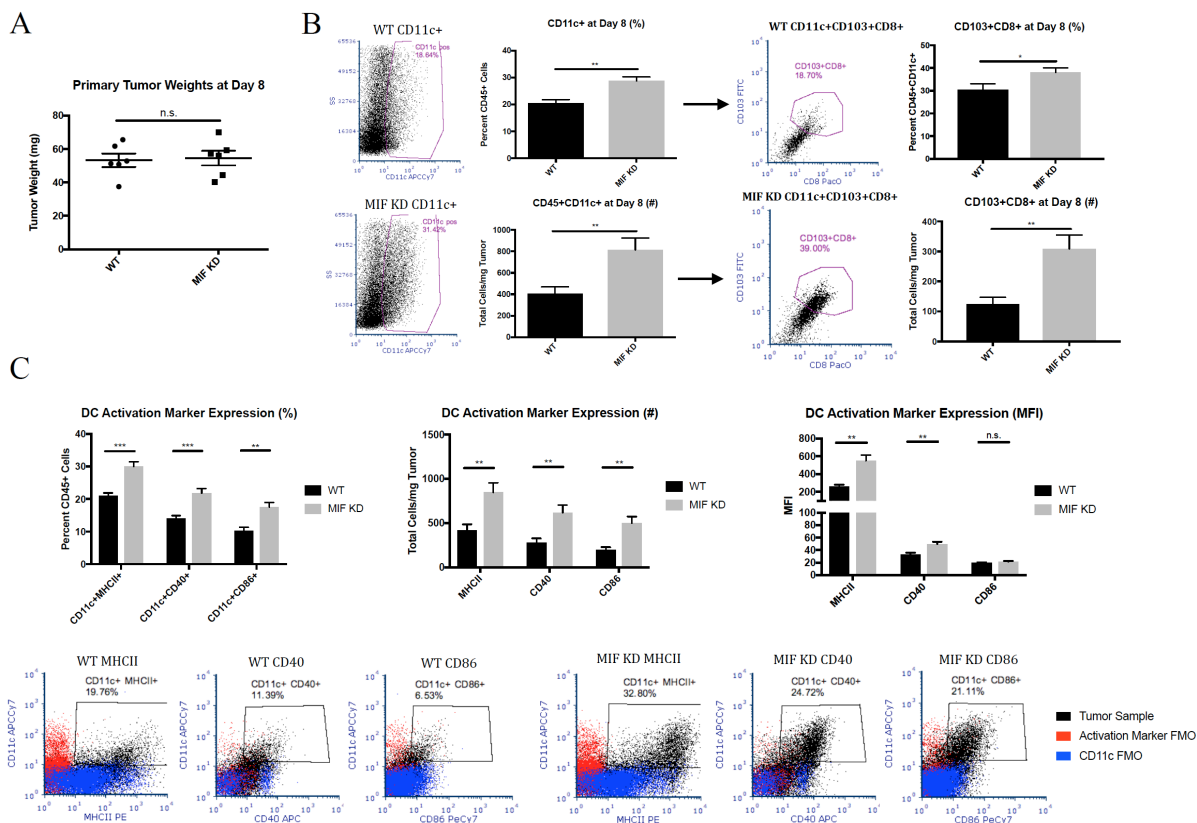


Figure 2.5: MIF expression in the primary tumor leads to decreased dendritic cell abundance and activation in the tumor. 1.0×10^4 WT or MIF KD 4T1 cells were implanted in the mammary fat pad of female Balb/c mice. **A**, Tumors were harvested and weighed at day 8 of tumor growth, which is the first point at which palpable tumors are detectable. Tumors were digested and analyzed by flow cytometry for infiltration of dendritic cells by cell surface markers (**B**) and activation markers (**C**). Representative flow plots are shown in panels B and C. $n=6$ mice per group. One-way ANOVA. * $p<0.05$, ** $p<0.01$, *** $p<0.001$

strategy for the described DC analysis is shown in Supplementary Figure 2.6 (**Supplementary Figure 2.6**). In contrast to the observation in tumors, the draining lymph nodes of mice bearing WT or MIF KD tumors showed no differences in DC numbers or activation status (**Supplementary Figure 2.7**) Taken together, these data suggest that MIF depletion results in an increased abundance and activation of DCs specifically in the tumor.

MIF-expressing tumor cells show decreased markers of immunogenic cell death under serum-free conditions.

Recent literature has characterized a specialized type of cell death, termed “immunogenic cell death” (ICD), in which the cell death process itself renders cancer cells susceptible to detection by the immune system (120,162,163). We hypothesized that loss of MIF expression in the 4T1 cancer cells would promote ICD, which could explain the enhanced immune response observed in the MIF KD tumors. Several standard markers of ICD have been established, including extracellular ATP release and exposure of calreticulin (CALR) and certain heat-shock proteins, including HSP70, on the cell surface (119,120,128). When cultured under serum-free conditions, we found that MIF KD cells exhibit an increase in all of these markers of ICD when compared to MIF expressing cells (**Fig 2.6A-C**). This suggests that depletion of MIF promotes ICD when cells are exposed to challenging growth conditions. Reconstitution of MIF KD cells with WT MIF reduced the expression of these ICD markers in serum-free culture conditions (**Fig 2.6D-F**), demonstrating that the phenotype is due to loss of MIF expression. Interestingly, reconstitution of MIF KD cells with the mutant P2G MIF resulted in an intermediate

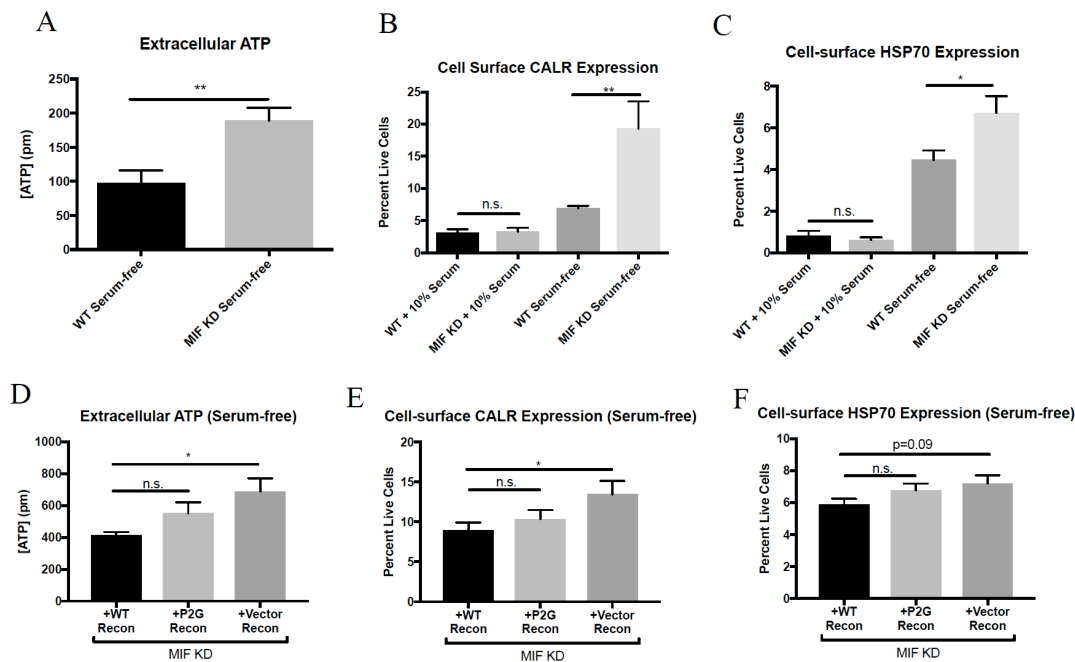


Figure 2.6: MIF-expressing tumor cells show decreased markers of immunogenic cell death under serum-free conditions. A-C, WT or MIF KD 4T1 cells were grown in 10% serum-containing media overnight, and then media was replaced with fresh 10% serum or serum-free media. After 24 hours, media was sampled and tested for extracellular ATP. After 48 hours, cells were harvested and stained by flow cytometry for cell surface expression of calreticulin or HSP70. D-F, MIF KD 4T1 cells reconstituted (recon) with WT MIF, P2G MIF, or with an empty vector as a control were grown in 10% serum-containing media overnight, and then switched to serum-free media. After 48 hours, media was sampled and tested for extracellular ATP and cells were harvested and stained by flow cytometry for cell surface expression of calreticulin or HSP70. Data shown are the means of 3 independent experiments, with 3 replicates per experiment. A, Student's t-test, B-F, one-way ANOVA. * $p < 0.05$, ** $p < 0.01$.

phenotype, suggesting that the enzymatic activity of MIF is only partially responsible for protection from the ICD response observed under serum-free conditions (**Fig 2.6D-F**).

In an effort to link our *in vitro* findings with the enhanced DC activation phenotype observed in MIF KD tumors *in vivo*, we cultured *in vitro*-derived DCs with conditioned media (CM) from WT or MIF KD 4T1 cells cultured in serum-free media. We hypothesized that the enhanced ICD response in MIF KD cells would lead to the presence of immunogenic molecules (such as ATP) in the CM, and that this would result in an enhanced DC activation phenotype when compared to culture with WT CM. However, we observed no stimulation of DCs upon culture with either WT or MIF KD CM. In contrast, LPS strongly stimulated the DCs (**Supplementary Figure 2.8A**). We next hypothesized that cell-cell contact may be required for proper DC activation through HSP70/CALR expression on the tumor cell surface. However, upon co-culture of DCs with WT or MIF KD 4T1 cells grown under serum-free conditions for 48 hours, we found even less DC activation than our un-stimulated control cells (**Supplementary Figure 2.8B**). From this, we conclude that neither CM nor co-culture of DCs with the tumor cells is sufficient to stimulate DC activation *in vitro*. This suggests there are additional cellular or soluble components required for DC activation that are missing in this culture system. Due to the lack of stimulation observed in our experimental conditions, we cannot conclude that MIF expression in the tumor cells is actively dampening DC activation, or that loss of MIF expression enhances activation. Future experiments will focus on addition of stronger stimulation signals (by adding LPS, for example) in the CM or co-culture conditions in order to get a baseline activation level.

This will allow us to determine if the enhanced cell death phenotype observed in MIF KD cells under serum-free conditions directly leads to an enhanced DC activation. If we do not observe a difference in DC activation between WT and MIF KD conditions, this would suggest that the phenotype observed *in vivo* is not the direct effect of ICD induction as hypothesized.

Discussion

Our results demonstrate that tumor cell-derived MIF is responsible for several aspects of the anti-tumor immune response in tumor-bearing animals. Specifically, MIF expression in the tumor cells reduces the abundance of activated DCs in the tumor microenvironment, and also suppresses the increase in IFN-gamma producing CD4⁺ and CD8⁺ T cells within the tumor. *In vitro*, MIF expression prevents ICD and also suppresses markers of apoptosis in serum-starved tumor cells. Based on these observations, we propose a model (**Fig 2.7**) whereby MIF-deficient 4T1 cells undergo ICD, leading to an enhanced abundance and activation of DCs in the tumor microenvironment. This results in an enhanced T cell-mediated anti-tumor immune response and better control of tumor growth, leading to the observed reduction in overall tumor burden observed in mice bearing MIF-deficient tumors. The corollary of this model is that an evolving tumor can overcome the growth suppressing anti-tumor effects through mechanisms that increase MIF expression. This is in agreement with the

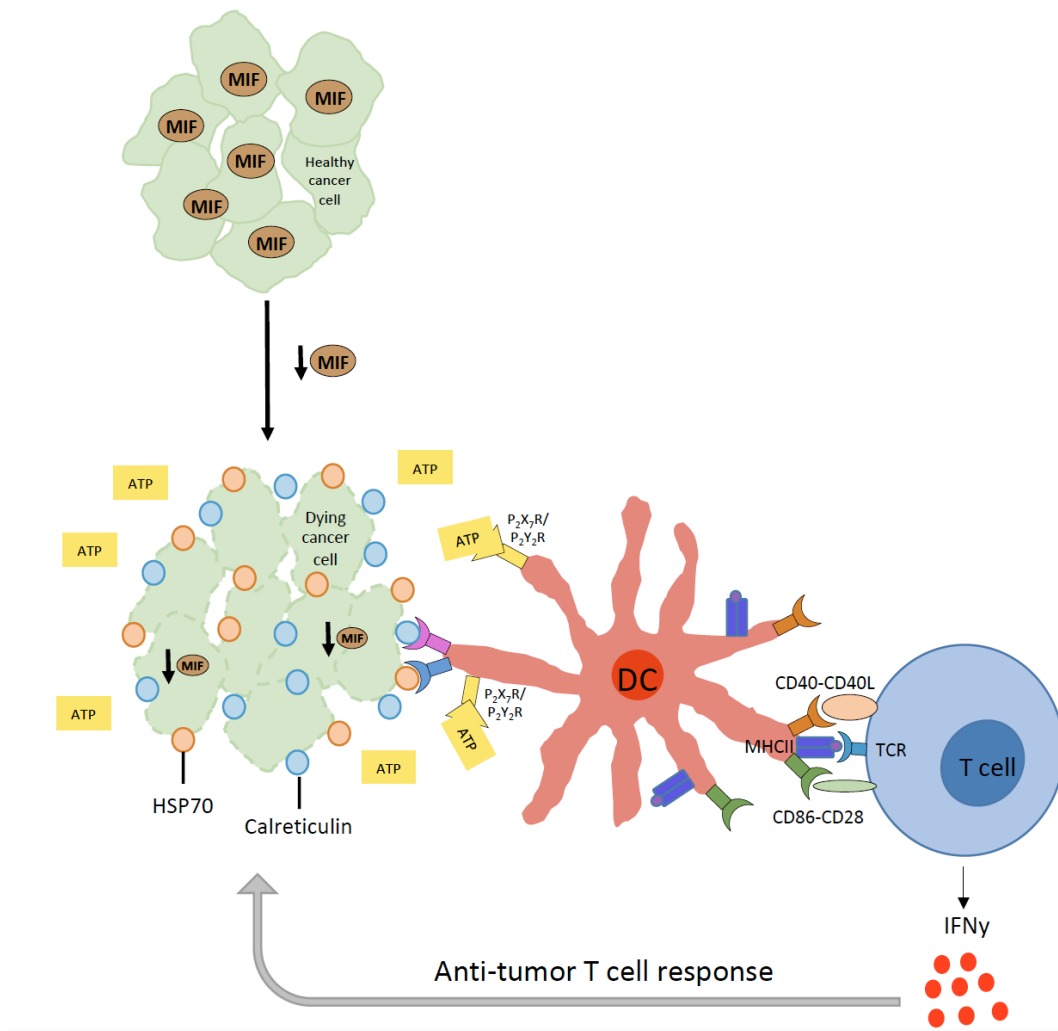


Figure 2.7: Experimental Model. Upon loss of MIF expression in the tumor, cancer cells undergo ICD. This leads to an increased abundance and activation of DCs in the tumor microenvironment, resulting in an enhanced T cell-mediated anti-tumor immune response through secretion of IFN γ in the tumor microenvironment.

common observation that expression of MIF correlates with tumor aggressiveness in patients

In the setting of pathogenic infection, ICD has likely evolved as a mechanism to alert the immune system to infection. Death of a small number of infected cells can lead to a robust immune response based on expression of damage-associated molecular patterns (DAMPs), recognized by cells such as dendritic cells, monocytes, and macrophages (117). ER chaperones such as calreticulin and certain heat-shock proteins, including HSP70, are exposed on the cancer cell surface, serving as DAMPs or “eat me” signals to be recognized by the immune system (119,120,128). Extracellular ATP released by cells undergoing ICD interacts with the immune system by signaling through purinergic receptors on antigen-presenting cells (APCs) (117). Activation of these receptors on APCs initiates the signaling processes involved in IL-1 β secretion, which is further responsible for inducing IFN γ -producing CD8⁺ T cells and the anti-tumor immune response (124).

As introduced above, ICD is induced by a number of mechanisms, including treatment with certain classes of chemotherapeutics, radiation therapy, and photodynamic therapy (PDT) (126). Our work suggests that when combined with MIF-depletion, removal of serum from *in vitro* culture conditions can also induce ICD. We hypothesize that removal of serum *in vitro* more closely mimics the stressful tumor microenvironment experienced by cancer cells *in vivo*. Therefore, our observations suggest that ICD could be induced by

inhibiting MIF, which would represent another means to increase tumor immunogenicity beyond the previously identified therapeutic approaches.

MIF overexpression has been observed in a number of human cancer types, and several reports support MIF's role in protection from apoptosis *in vitro*, including in models of lung cancer and cervical adenocarcinoma (44,164). Recently, Johler *et al.* demonstrated that MIF expression is induced *in vitro* in Rhabdomyosarcoma (RMS) cell lines upon treatment with cytotoxic agents such as Doxorubicin, Vincristine and Etoposide, further linking MIF to the cell stress response (165). Therefore, MIF overexpression may be a protective mechanism used by cancer cells to prevent cell death and overcome the immune response under the stressful conditions experienced within the tumor microenvironment.

Several previously published studies also strongly link MIF expression to dampened anti-tumor immune responses in cancer, which may be indirect evidence of the suppression of ICD. In a neuroblastoma model, MIF inhibits T cell activation *in vivo* (107,108), and MIF inhibition has been shown to promote conversion of melanoma patient-derived MDSCs into a more DC-like phenotype *in vitro* (110). Similarly, addition of recombinant MIF to immature DC cultures differentiated from CD14⁺ monocytes has been shown to inhibit both DC maturation and migration *in vitro* (111). In addition, we have previously published that MIF expression in the primary tumor leads to an increased abundance of intratumoral monocytic myeloid-derived suppressor cells (MDSCs), contributing to establishment of an immunosuppressive microenvironment (32). However, this study

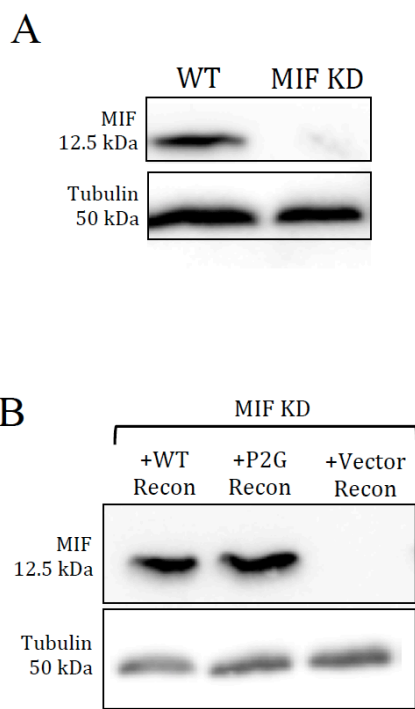
focused on tumor-infiltrating MDSCs in late-stage 4T1 tumors, and we do not see a MIF-dependent difference in MDSCs at the early time points used in the current study. This suggests that MIF may be involved in two distinct mechanisms leading to immunosuppression in the tumor microenvironment depending on the time of tumor growth. All of these studies, when taken together, suggest that MIF is an important mediator of the immunosuppressive tumor microenvironment.

We have demonstrated that, in the 4T1 model, loss of MIF expression leads to a robust increase in activated DCs intratumorally by day 8 of tumor growth. Within the CD11c⁺ DC population, we observed an increase in an unusual population of dendritic cells expressing both CD103 and CD8 in mice bearing MIF KD tumors. A similar population of DCs has been previously characterized in the spleen as being highly efficient at phagocytosis of circulating apoptotic cells, as well as cross-presentation of antigens (166). While this population of cells was shown by Qiu *et al.* to be tolerogenic in the setting of the spleen, this population of cells is not well-described intratumorally, and may serve as a mechanism of T cell activation via antigen uptake and presentation in the tumor microenvironment.

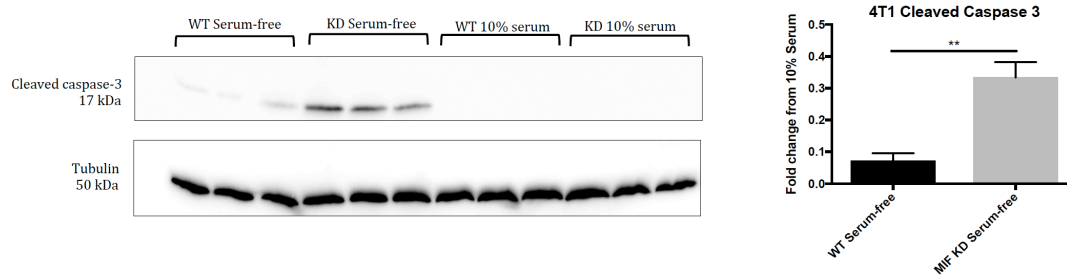
At day 10 of tumor growth, the MIF-deficient tumors contain significantly more IFN γ -producing CD8⁺ and CD4⁺ T cells. IFN γ has been established as a critical cytokine involved in the trafficking of activated T cells from the draining lymph nodes to the tumor (167), differentiation of cytotoxic immune cell subsets capable of direct tumoricidal activity (168), as well as directly inducing tumor cell growth arrest

(169–171). This suggests that the observed increase in IFN γ -producing T cells in the tumor microenvironment may explain the decreased growth of the MIF-deficient tumors in immune competent animals. We confirmed that the T cells are important by demonstrating that simultaneous depletion of CD4 and CD8 T cells restored the growth of MIF KD tumors to parallel that observed in MIF-expressing tumors. Further dissection of the relative contribution of CD4 versus CD8 cells to the MIF-dependent immune-mediated control of tumor growth will be of interest in future studies.

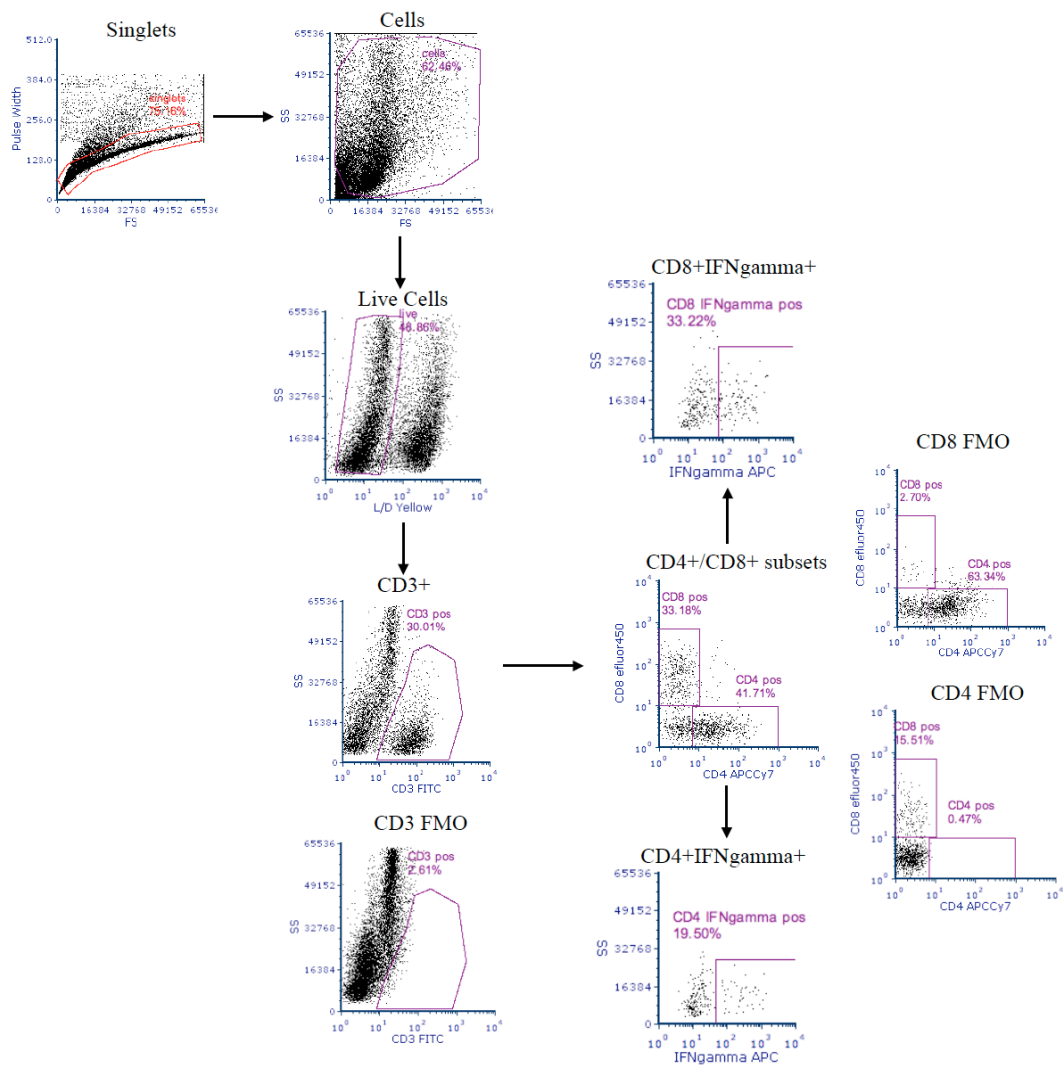
Our work proposes a novel mechanism through which MIF controls cancer growth and progression through manipulation of the host immune system. When combined with earlier work by our group and others, this suggests inhibition of MIF may be a valuable therapeutic approach. Combination of a potent MIF inhibitor with any of the promising immunotherapy options already in the clinic, or those in the developmental pipeline could lead to robust, long-lasting immunity in the setting of cancer.



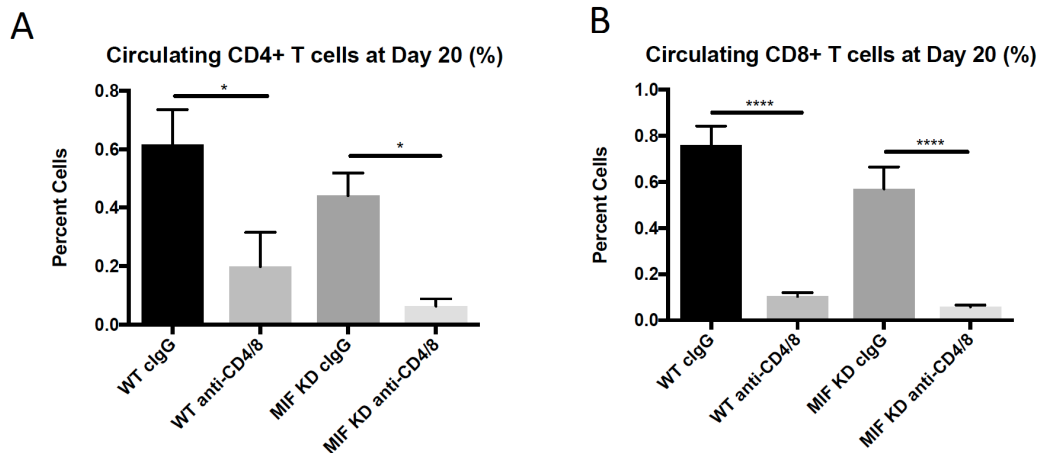
Supplementary Figure 2.1: Confirmation of MIF depletion and re-expression in 4T1 cell lines. MIF expression was detected by immunoblot in cell lysates from **A**, WT and MIF KD 4T1 cell lines and **B**, in the MIF KD cell line reconstituted with either WT MIF, P2G MIF or a vector control.



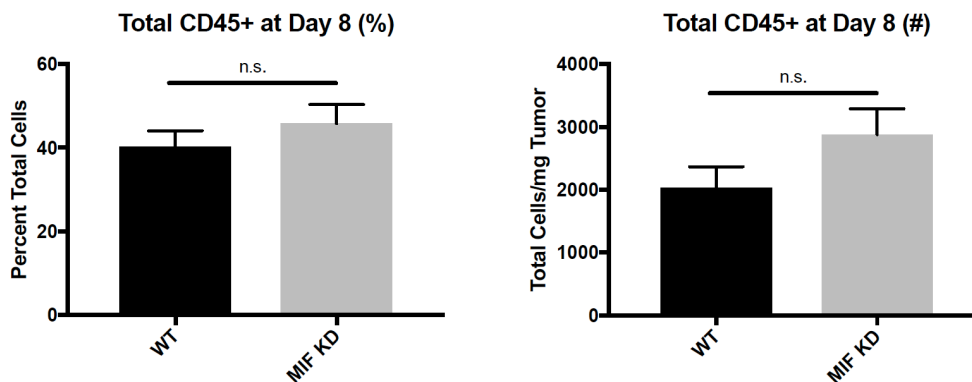
Supplementary Figure 2.2: MIF expression protects against cleaved caspase 3-mediated cell death *in vitro* in serum-free conditions. WT or MIF KD 4T1 cells were grown in 10% serum-containing media overnight, and then switched to fresh 10% serum-containing media or serum-free media for a further 48 hours. Lysates were prepared and immunoblots were performed to quantify cleaved caspase 3 expression. Data are from one experiment with 3 replicate samples and the data shown is representative of 3 independent experiments. Student's t-test. ** $p < 0.01$.



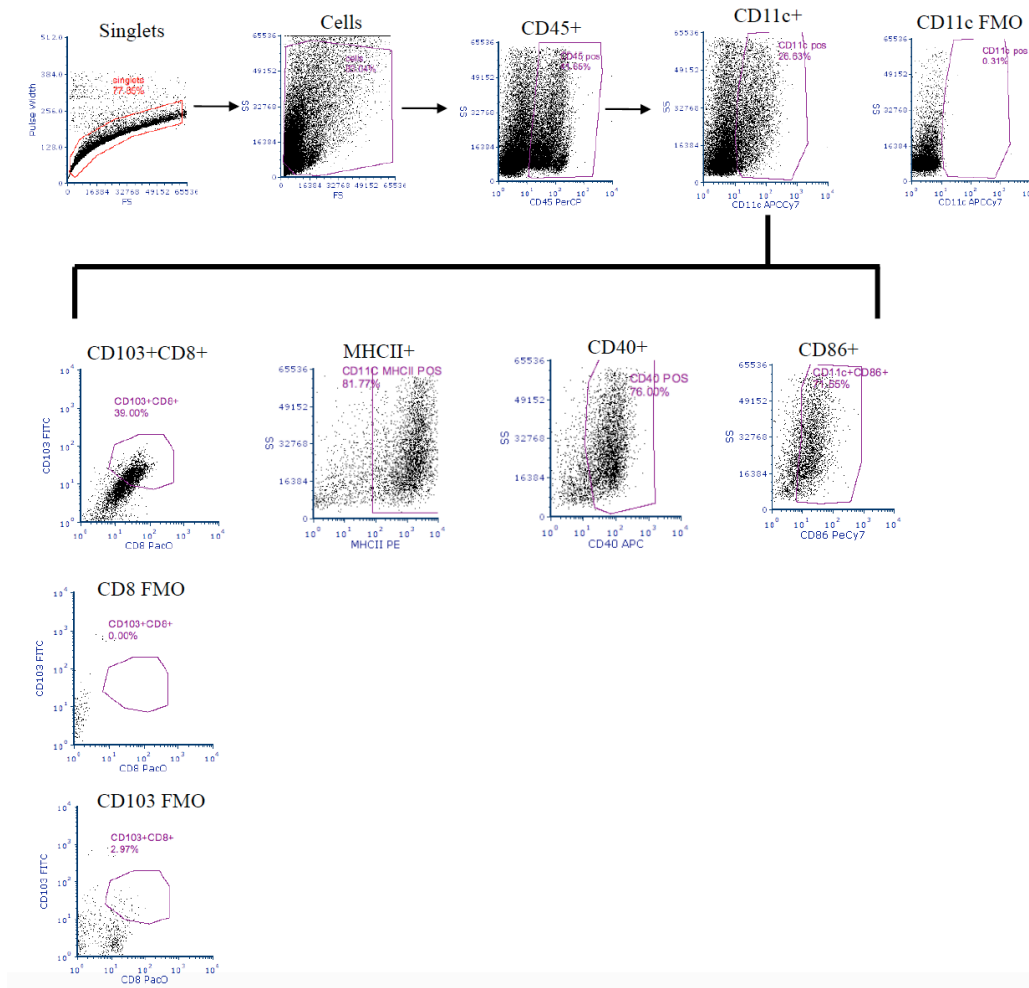
Supplementary Figure 2.3: Gating strategy for T cell analysis by flow cytometry. Single cells were selected first, followed by gating out of cellular debris by FSC vs. SSC. Next, dead cells were excluded by live/dead viability dye. T cells were gated using CD3 positivity. CD4+ and CD8+ subsets were gated, and IFNgamma positivity was assessed within each T cell subset. All populations gated on FMOs as shown.



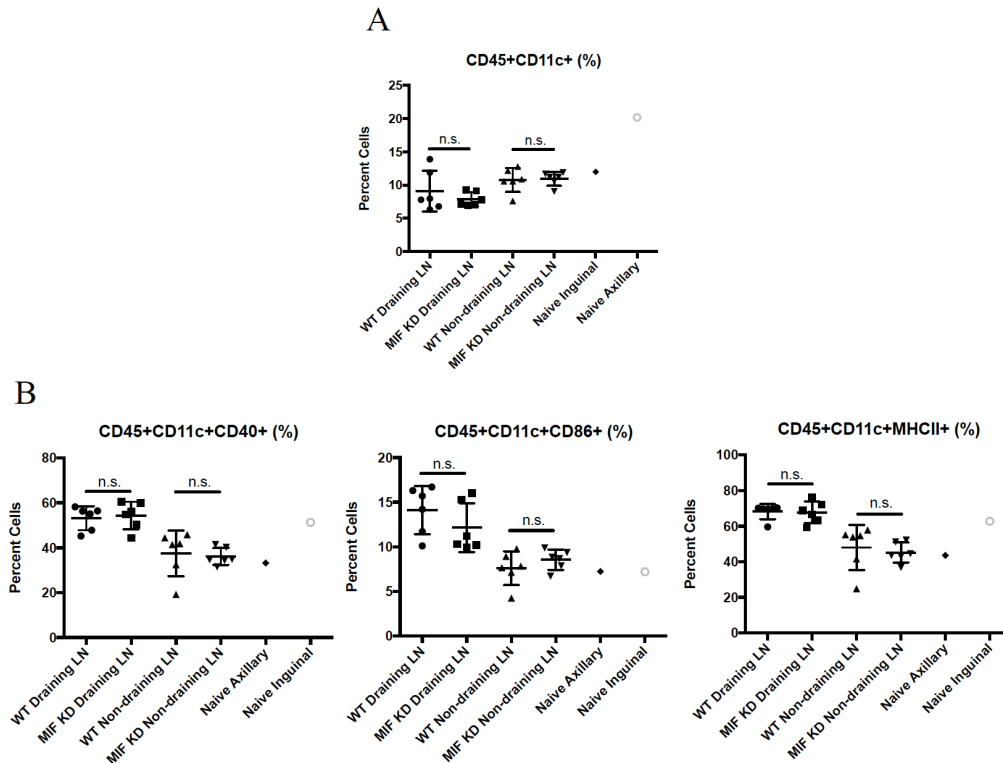
Supplementary Figure 2.4: Treatment of mice with CD4/8 depleting antibodies leads to almost complete loss of CD4/8+ T cells in the circulation during tumor growth. 1.0×10^4 WT or MIF KD 4T1 cells were implanted in the mammary fat pad of female Balb/c mice. Mice were treated with CD4/8 depleting antibodies starting 2 days before tumor implantation and every 4 days thereafter. Blood was harvested on day 20, at the time of tumor harvest and analyzed by flow cytometry for the presence of **A**, CD4+ and **B**, CD8+ T cells. Cells were pre-gated through live, CD45+ and CD3+ parameters. n=6 mice per group. One-way ANOVA. * p<0.05, **** p<0.0001.



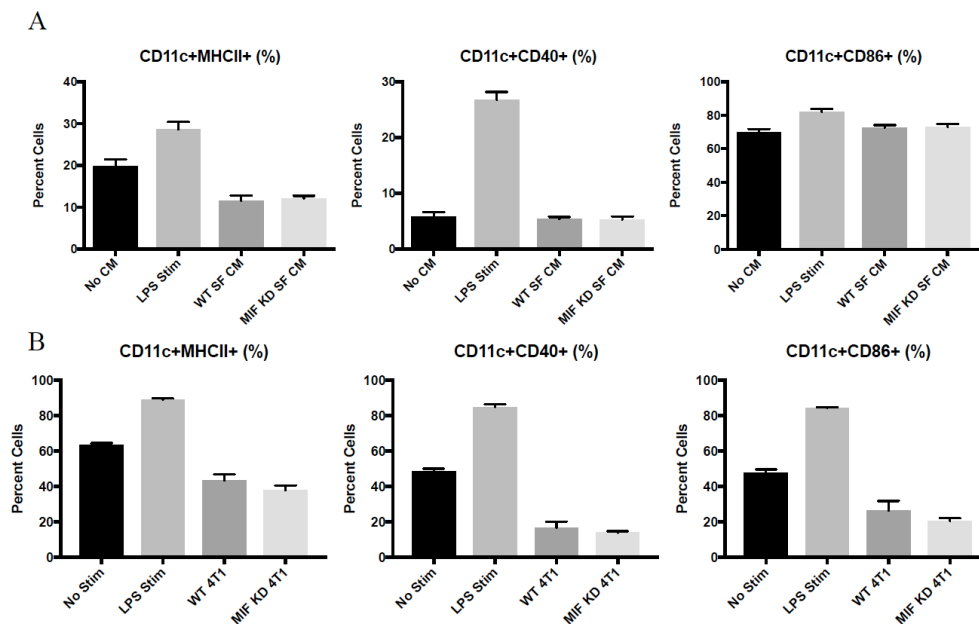
Supplementary Figure 2.5: MIF expression in the primary tumor does not affect total intratumoral leukocyte abundance. 1.0×10^4 WT or MIF KD 4T1 cells were implanted in the mammary fat pad of female Balb/c mice. Tumors were digested and analyzed by flow cytometry for infiltration of leukocytes using the cell surface marker CD45. Student's t-test revealed no statistically significant differences in CD45+ cell abundance as a function of MIF expression in the tumor.



Supplementary Figure 2.6: Gating strategy for DC analysis by flow cytometry. Single cells were selected first, followed by gating out of cellular debris by FSC vs. SSC. Next, CD45⁺ cells were selected, followed by CD11c⁺ positive cells. CD8⁺ and CD103⁺ DC subsets were gated through CD11c⁺ cells. MHCII, CD86 and CD40 activation markers were gated through CD11c⁺ cells as well. All populations gated on FMOs as shown.



Supplementary Figure 2.7: MIF-depletion in the primary tumor does not affect dendritic cell presence or activation in the draining lymph node. 1.0×10^4 WT or MIF KD 4T1 cells were implanted in the mammary fat pad of female Balb/c mice. Draining (inguinal) and non-draining (axillary) lymph nodes were harvested at day 8 of tumor growth. Lymph nodes were dissociated and analyzed by flow cytometry for infiltration of dendritic cells by **A**, cell surface markers and **B**, activation markers. A non-tumor bearing naïve mouse was used as a control. $n=6$ mice per group. One-way ANOVA.



Supplementary Figure 2.8: *In vitro* DC activation is not achieved through treatment with WT or MIF KD CM or by co-culture with WT or MIF KD cells. Bone marrow-derived DCs were generated *in vitro* using IL-4 and GM-CSF-containing media. On day 5 of culture, **A**, CM was added from WT or MIF KD 4T1 cells grown under serum-free conditions for 48 hours, or **B**, DCs were added to cultures of WT or MIF KD cells grown under serum-free conditions for 4 hours. 1 μ g/mL LPS was added as a positive control. On day 8, DCs were stained for activation markers by flow cytometry. Statistical analysis revealed no significant differences between WT and MIF KD conditions.

**Chapter Three: A role for MIF in pulmonary metastasis and
metastatic niche formation.**

Abstract

Metastatic disease accounts for the majority of mortality in patients with solid tumors. The cytokine Macrophage Migration Inhibitory Factor (MIF) has been implicated in enhancing both primary tumor growth and the metastatic process in a number of human cancer types, as well as mouse models of cancer. Here, I aimed to gain a better understanding of the mechanism by which MIF is controlling these processes using the spontaneously metastatic 4T1 model of breast cancer. I hypothesized that MIF may be controlling formation of a pre-metastatic niche by remodeling the extracellular matrix and/or by modulating accumulation of immunosuppressive myeloid cells in the lungs, thereby promoting metastasis. Interestingly, my studies revealed that increased tumor size, rather than MIF expression, dictated an increase in pulmonary metastasis in this model. Upon further analysis of the pre-metastatic niche in the lungs of WT and MIF knockdown tumor-bearing mice, I found that MIF expression in the primary tumor had no effect on matrix remodeling. However, MIF expression did promote accumulation of myeloid cells in lungs regardless of primary tumor size, suggesting that increased myeloid cell accumulation may not be responsible for an overall increase in metastatic burden in the lungs in this model. When phenotyping the myeloid cells accumulated in the lungs, I found no differences in the populations analyzed, which were mainly comprised of myeloid-derived suppressor cell (MDSC) subsets. Additional analysis of other myeloid cell subsets, such as tumor-associated macrophages, may elucidate which cells are accumulating in response to MIF expression in the primary tumor.

Introduction

Metastasis accounts for 90% of cancer-related deaths in patients with solid tumor types, necessitating a rapid, focused move towards better understanding the process of metastasis and discovering new ways of disrupting this process (172). The “metastatic cascade” consists of several consecutive steps, starting with acquisition of an invasive phenotype. Next, cancer cells must intravasate into the nearby vasculature and lymphatic vessels, and move through the circulation while evading the host immune response. Lastly, cells must extravasate at distant sites, seed micrometastases, and proliferate into macrometastases (173).

Macrophage Migration Inhibitory Factor (MIF) expression has been implicated in the process of metastasis by our group and by several others (32,52,60–62,174,175), suggesting that inhibition of MIF in the setting of solid tumors may be an efficacious therapeutic method to inhibit metastasis. Wang *et al.* observed a MIF-dependent increase in metastasis in a mouse model of osteosarcoma and suggested activation of the RAS/MAPK pathway as a mechanism by which MIF enhances proliferation and migration of cancer cells (52). Similarly, Lv *et al.* reported that MIF enhanced metastasis through ERK-mediated HMGB1 release, and activation of the epithelial-to-mesenchymal transition (EMT) (60). Ren *et al.* has associated MIF with enhanced metastasis via N-myc, RAS and c-Met signaling in a mouse model of neuroblastoma (174). siRNA-induced loss of MIF expression was also shown to delay metastasis in multiple murine breast cancer models through activation of a systemic anti-tumor immune response involving loss of MDSCs and enhancement of M1-like macrophages in the tumor

microenvironment and circulation (176). This later study supported our previous work suggesting that MIF expression promotes tumor growth and metastasis through increased accumulation of the monocytic subset of MDSCs in the primary tumor microenvironment (32).

As the process of metastasis is studied in more detail, a concept that was first introduced over 100 years ago by Steven Paget has been shown to be largely accurate. This concept, termed the “seed and soil hypothesis”, establishes that cancers tend to metastasize with certain organ-preference. For example, breast cancer tends to metastasize to the brain, bone, liver and lung specifically (129). As our understanding of where cancers metastasize and how they do so has increased, it has become clear that the primary tumor is able to exert effects on distant organs, priming that site for future metastasis. Seminal work supporting the concept of the “pre-metastatic niche” was described in a mouse model of breast cancer by Kaplan *et al* in 2005, when they showed that VEGFR1⁺ hematopoietic/bone-marrow derived cells (BMDCs) formed clusters in lung tissue, and this recruitment was dependent on VEGF secretion by the primary tumor (130). These VEGFR1⁺ BMDCs interacted with local fibroblasts to produce fibronectin, which was supportive for future seeding tumor cells (130).

Since the seminal publication by Kaplan *et al.*, collagen crosslinking has also been found to be a major component in the formation of a pre-metastatic niche (134). Primary tumors induce crosslinking of collagen IV in distant sites, such as the lung, through expression of the lysyl oxidase (LOX) family of proteins. These LOX proteins, secreted by the tumor

cells, then travel to distant sites through the circulation. The enzymatic activity of LOX (and its family members) has been shown to promote seeding of CD11b⁺ BMDCs to pre-metastatic sites (134).

Myeloid derived suppressor cells (MDSCs) constitute one major subpopulation of BMDCs found in sites of pre-metastatic niche formation (141,142). MDSCs are found at increased frequencies in numerous mouse models of cancer relative to a healthy mouse control (98) as well as in the circulation and primary tumors of human patients (67,80,100,101,177–182). MDSCs mobilize in the setting of chronic inflammation, and have been shown to dampen anti-tumor T cell responses, leading to an immunosuppressed tumor microenvironment (67,96,183,184). Recruitment of these immunosuppressive cells to sites of pre-metastatic niche formation sets up a permissive microenvironment for isolated tumor cells to avoid immune detection and immune-mediated killing at a metastatic site.

We have shown previously that MIF expression in the primary tumor enhances tumor growth and metastasis through recruitment of immunosuppressive MDSCs to the primary tumor using the 4T1 model (32). We also have unpublished data showing that WT and MIF KD 4T1 cells injected intravenously colonize the lungs equally. These two studies suggest that the presence of a primary tumor is important for MIF's ability to promote metastasis. Based on these results, I hypothesized that MIF may be involved in formation of a pre-metastatic niche, which is missing in the experimental model of metastasis through intravenous injection of tumors cells. However, upon analysis of pre- and post-

metastatic lungs, I found that while MIF expression in the primary tumor does correlate with myeloid cell accumulation in the lungs, MIF expression does not dictate matrix remodeling. Furthermore, primary tumor size is responsible for differences in lung metastasis rather than a direct effect of primary tumor MIF expression.

Materials and methods

4T1 Cell Line

The 4T1-luciferase labeled cell line (from here on referred to as “4T1-luc”) was obtained from Caliper Life Sciences. The 4T1-luc cell line tested negative for mycoplasma at the University of Virginia, most recently on May 11, 2017. Cells were cultured under the conditions recommended by the ATCC. Cells were cultured no more than 10 passages before use in experiments. The method for the generation of the MIF knock-down (MIF KD) 4T1-luc cells was published previously (32).

4T1-luc Mouse Tumor Model

Female 16-18 gram BALB/c mice were purchased from Charles River Laboratories. 1.0×10^4 WT or MIF KD 4T1-luc cells (or 1.5×10^5 MIF KD 4T1-luc cells for “MIF KD Hi” conditions) were injected into the mammary fat pad and monitored every other day for tumor growth starting 7 days after tumor implant. All animal studies were conducted in accordance with the University of Virginia Animal Care and Use Committee (ACUC) under protocol approval #4039 and all efforts were made to minimize suffering of animals in all experiments.

Using calipers, tumor volumes were estimated from two perpendicular measurements using the formula $V = 0.4 \times L \times W^2$. At the time of euthanasia, tumors were excised from the mammary fat pad, spleens were removed from the abdominal cavity, and all organ weights were recorded.

Ex Vivo Lung Imaging

Five minutes before euthanasia, 200uL of 15mg/mL Luciferin (GoldBio) in sterile PBS was injected intraperitoneally into each mouse. Following euthanasia, lungs were excised and stored in 5mL PBS in a 6-well dish until ready to image. Five minutes before imaging, each lung was moved to an individual well of a 12-well dish, and 1mL of 300ug/mL luciferin in PBS was added to each well. Lungs were imaged using the IVIS Spectrum *In Vivo* Imaging System (PerkinElmer).

Lung Sectioning

Lungs were removed from each mouse, cut in half, and flash frozen in liquid nitrogen. After freezing, lung pieces were stored at -80C until sectioned. Lungs were embedded in optimum cutting temperature (OCT) medium (VWR) and sectioned onto slides using a Leica CM3050 Research Cryostat.

Picrosirius Red Staining

Slides with frozen lung sections were fixed for 10 minutes in 10% formalin, followed by a rinse with deionized (DI) H₂O. Slides were then stained with 0.1% picrosirius red stain (AbCam) for 90 minutes. Slides were then rinsed with 0.01N HCl in water for 1 minute,

followed by another rinse in DI H₂O. Slides were dehydrated with 70% EtOH for 30 seconds, and then cover slipped for storage until imaged. Slides were imaged using the Olympus BX51 high magnification microscope with the polarizing light filter attached.

CD11b Immunofluorescent (IF) Staining

Slides with frozen lung sections were fixed for 20 minutes in an ice-cold solution of 1:1 acetone and 100% EtOH, followed by two PBS washes. Slides were then blocked with an avidin-biotin blocking kit (Vector Labs) in 3% BSA in PBS according to the manufacturers instructions. Slides were washed with PBS, and stained with primary anti-CD11b PE antibody (1:200, eBiosciences) for 45 minutes. Slides were then washed, and stained with secondary anti-rat biotinylated antibody for 30 minutes (1:200, BD Biosciences). Slides were washed, and stained with a Texas Red neutral avidin antibody (1:500, Southern Biotech) for 30 minutes. Slides were washed, and mounted with Vectashield plus DAPI mounting medium (Vector Labs) according to the manufacturers instructions. All staining was performed at room temperature. Following staining, slides were imaged with a Nikon Microphot-FXA fluorescent microscope and Nikon HB-10101AF Mercury Lamp and Olympus Q-Color5 camera.

Lung Digestion and Flow Cytometry Analysis

Following euthanasia, the chest cavity was opened and lungs were perfused with 10mL of PBS per mouse. Lungs were then harvested from naïve and tumor-bearing mice, minced, and dissociated at 4C for 75 minutes in a solution of 2mg/mL collagenase IV (Worthington Biochemical) and 6U/mL of elastase (Calbiochem) in a volume of 5mL

of HBS per lung. After digest, 30U of DNase (Qiagen) was added to each lung for 5 minutes at room temperature. Cell suspensions were strained through a 70-um screen before use in experiments.

For flow cytometry analysis, cells were stained with Live/Dead Fixable Yellow Dead Cell Stain (Invitrogen), as well as CD45-PerCP (1:100, BD Bioscience), CD11b-PacBlue (1:100, Invitrogen), Ly6G-FITC (1:200, Biolegend), Ly6C-APC (1:200, Biolegend) and CD11c-PeCy7 (1:200, Biolegend). All gating on cell surface markers was based on fluorescence minus one (FMO) controls. The cells were analyzed with the Beckman Coulter CyAN ADP LX 9 Color Flow Cytometer.

Image Quantification and Statistical Analysis

CD11b IF images were quantified using ImageJ software by calculating the area of mean pixel intensity of each image, with n=2 images per lung. For early-stage lungs, images were also counted by eye in a blinded fashion for number of CD11b⁺ cells/image. All data are presented as mean +/- SEM. Data was analyzed either by Student's t-test or one-way ANOVA using the Graph-Pad Prism analysis software. P values are represented in the figures as * p<0.05, ** p<0.01, *** p<0.001, **** p<0.0001.

Results

MIF expression promotes tumor progression and spontaneous pulmonary metastasis in the 4T1 model of breast cancer.

To study the role of MIF in metastasis, I utilized the 4T1 model of murine breast cancer, which spontaneously metastasizes to the lungs. By using a luciferase-labeled version of this cell line, I was able to quantify lung metastasis *ex vivo* using IVIS imaging, with metastasis becoming detectable at approximately day 20-25 of tumor growth. As described previously, when comparing primary tumor growth of mice bearing WT versus MIF KD tumors, I consistently found that WT tumors grew more rapidly than MIF KD tumors (**Fig 3.1A and B**). When I analyzed lung metastasis *ex vivo* on day 22 of tumor growth, I found that mice bearing MIF KD primary tumors had significantly less lung metastatic burden compared to mice with WT primary tumors (**Fig 3.1C**).

Tumor size, not MIF expression, dictates lung metastatic tumor burden in the 4T1 model.

When studying metastasis in mouse models of cancer, it is important to consider the effect of primary tumor size on metastasis, regardless of any genetic manipulation of tumor cells or treatment of mice with anti-cancer therapies. In order to determine if a decrease in primary tumor size (due to loss of MIF expression), rather than loss of MIF expression itself, was affecting lung metastasis, I compared tumor growth and metastasis in an additional group of mice. This third group (referred to from here on as “MIF KD Hi”) involved injecting mice with a greater number of MIF KD cells in order to allow

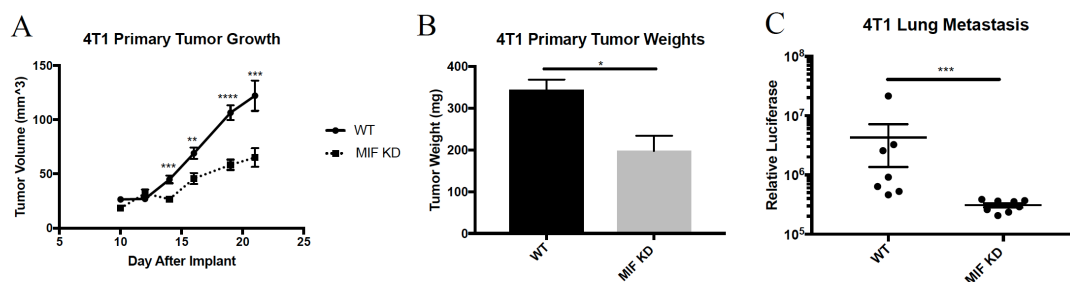


Figure 3.1: MIF expression promotes tumor progression and spontaneous pulmonary metastasis in the 4T1 model of breast cancer. **A**, 1.0×10^4 WT or MIF KD 4T1-luc cells were implanted in the mammary fat pad of female Balb/c mice and tumor size was monitored starting at day 10 by caliper measurement. **B**, Tumors were harvested at day 22 of tumor growth post implantation and weighed. **C**, Lungs were harvested at day 22 of tumor growth and imaged *ex vivo* using the IVIS imager. Lung metastasis was quantified based on relative luciferase expression in the lungs. Data are representative of three independent experiments, with $n=5$ mice/group in each experiment. One-way ANOVA. * $p<0.05$, ** $p<0.01$, *** $p<0.001$ **** $p<0.0001$.

MIF KD tumors to reach a comparable size to WT tumors over the same time course of tumor growth. I determined that injecting 1.5×10^5 MIF KD cells resulted in a MIF KD tumor with similar growth kinetics to a WT tumor, as well as more comparable tumor weights at the time of harvest on day 24 (**Fig 3.2A**). As a control, I also injected mice with our standard 1×10^4 MIF KD cells (referred to as “MIF KD lo”), which resulted in the expected reduction in primary tumor size compared to mice injected with 1×10^4 WT tumor cells (**Fig 3.2A**). I also weighed the spleens from each mouse, which generally correlates with tumor size in this model (**Fig 3.2B**) (185). When I imaged the lungs *ex vivo* to quantify lung metastatic burden, I found no statistically significant difference in metastasis between the mice with WT tumors and with the “MIF KD-hi” tumors (**Fig 3.2C**). The mice with “MIF KD lo” tumors did have significantly less metastatic burden than mice with WT tumors, as we have seen previously (**Fig 3.2C**) (32). Because the injection of a greater number of MIF KD cells in the “MIF KD-hi” condition could result in enhanced metastasis due to the difference in the initial tumor growth rate, I performed a similar experiment in which “MIF KD-lo” tumors were permitted to grow for a longer period of time in order to generate MIF KD tumors comparable in size to WT tumors (“MIF KD Long”). Tumor growth and metastasis in these mice was compared to control WT tumor-bearing mice, and mice bearing smaller MIF KD tumors harvested at the same time point as WT tumors (“MIF KD Short”). This experiment generated MIF KD tumors that were comparable in size to WT tumors at the “Long” time point (**Fig 3.2D**), and the mice bearing these large MIF KD tumors exhibited similar burden of lung metastasis as the mice bearing wild type tumors (Figure 3.2E). While the lung metastasis in the “MIF KD Short” tumor-bearing mice was not significantly lower than the “MIF KD Long” and

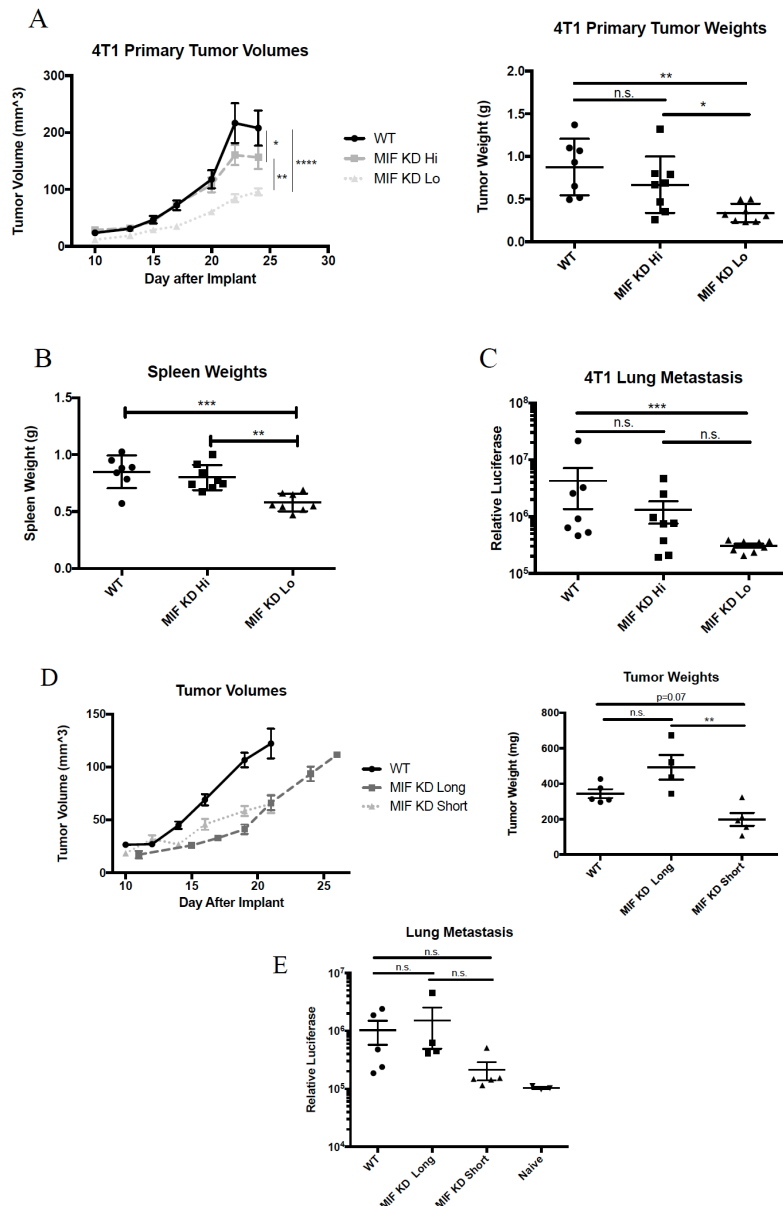


Figure 3.2: Tumor size, not MIF expression directly dictates lung metastatic tumor burden in the 4T1 model. 1.0×10^4 WT or MIF KD 4T1-luc cells (MIF KD Lo), or 1.5×10^5 MIF KD 4T1-luc cells (MIF KD Hi) were implanted in the mammary fat pad of female Balb/c mice. **A**, Tumor size was monitored over the course of tumor growth. Mice were euthanized at day 24 and tumors were excised and weighed. **B**, Spleens were excised and weighed. **C**, Lungs were excised and imaged *ex vivo* using IVIS luminescent imaging to quantify lung metastatic burden. Data is representative of 2 independent experiments with $n=8$ mice per group. **D**, 1.0×10^4 WT or MIF KD 4T1-luc cells were implanted in the mammary fat pad and tumor size was monitored over the course of tumor growth, with the “MIF KD Long” tumors permitted to grow until they reached the size of WT tumors. **E**, Lungs were excised and imaged *ex vivo* using IVIS luminescent imaging to quantify lung metastatic burden. Data is from one experiment with $n=5$ mice per group. One-way ANOVA. * $p < 0.05$. ** $p < 0.01$. *** $p < 0.001$. **** $p < 0.0001$.

the MIF WT tumor-bearing mice, the data are trending towards significance (**Fig 3.2E**). These results suggest that it is in fact primary tumor size dictating metastatic burden in this model, rather than the loss of MIF expression in the primary tumor directly. Moving forward, analysis of tumor cell numbers in the circulation will be important in order to determine if there are any differences in tumor cell shedding or escape from the primary tumor. I hypothesize that no difference would be observed based on the fact that there is no difference in overall metastatic outgrowth in the lungs. However, if differences in the number of circulating WT and MIF KD tumor cells (from equally sized tumors) are observed, this would suggest that while the tumor cells are able to colonize the lungs equally, there may be a difference in the ability of WT versus MIF KD cells to detach from the primary tumor. This result would suggest the importance of more detailed analysis of other metastatic sites, such as the liver and brain, to determine if cell seeding at other distant sites is affected by MIF expression.

MIF expression in the primary tumor does not affect collagen crosslinking in the lungs at late stages of tumor growth.

While my results suggest that MIF expression does not directly affect total metastatic burden at late stages of tumor growth, I hypothesized that MIF may still play a role in formation of a metastatic niche. This hypothesis is based on our previously published work showing that MIF expression in the primary tumor promotes accumulation of immunosuppressive monocytic MDSCs (32). Other groups have reported that accumulation of these and other immunosuppressive myeloid cell subsets at metastatic

sites (such as in the lung) promotes seeding of circulating tumor cells and therefore formation of micrometastases (141,186–188).

In the lung, one of the first steps in establishment of the metastatic niche that leads to recruitment of immunosuppressive myeloid cells is thought to be alterations to the extracellular matrix, in particular collagen crosslinking through activation of LOX in the primary tumor (134). This activity can be visualized in the lung by staining lung sections with picrosirius red, followed by imaging with a polarized light microscope. When I analyzed the lungs from the three groups described in **Figure 3.2**, (WT, MIF KD Hi, and MIF KD Lo) I found no difference in collagen crosslinking between groups (**Fig 3.3B**). When compared to a naïve mouse (which has never experienced a tumor), I did observe increased collagen crosslinking, suggesting that the presence of a primary tumor was altering the lung microenvironment as expected (**Fig 3.3A**). These results suggest that neither MIF expression in the primary tumor, nor reduced tumor size, has a major effect on collagen cross-linking in the lung.

MIF expression in the primary tumor promotes accumulation of CD11b⁺ myeloid cells in the lungs regardless of tumor size.

Based on our previous work involving MIF and monocytic MDSCs, I hypothesized that MIF may in fact play a role in accumulation of myeloid cells in the lung (32). I analyzed accumulation of myeloid cells first by immunofluorescent staining for CD11b on frozen lung sections from naïve mice (**Fig 3.4A**), as well as the WT, MIF KD Hi, and MIF KD lo groups. Representative images from each group are shown in **Figure 3.4B**. When I

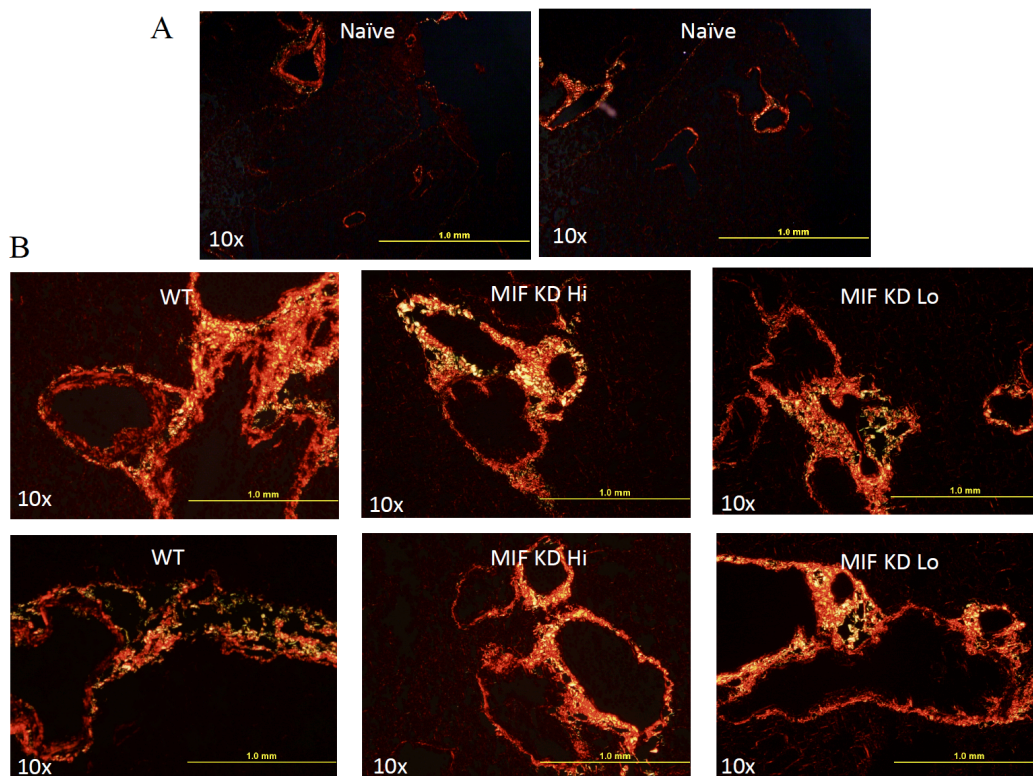


Figure 3.3: MIF expression in the primary tumor does not affect collagen crosslinking in the lungs at late stages of tumor growth. 1.0×10^4 WT or MIF KD 4T1-luc cells (MIF KD Lo), or 1.5×10^5 MIF KD 4T1-luc cells (MIF KD Hi) were implanted in the mammary fat pad of female Balb/c mice. **A**, Naïve (non-tumor-bearing) mouse lungs were removed, frozen sections were made, and stained with picosirius red as a control. **B**, Lungs from tumor-bearing mice were removed at day 24 of tumor growth, frozen sections were made, and stained with picosirius red. All images were acquired using a polarized light microscope.

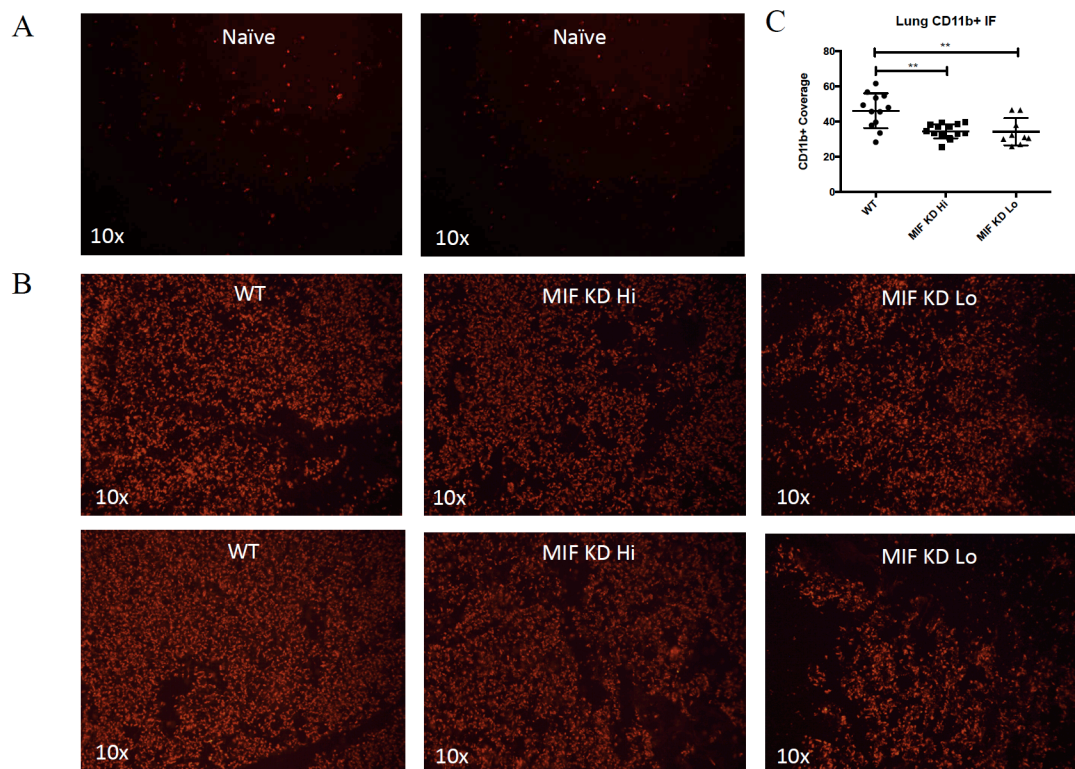


Figure 3.4: MIF expression in the primary tumor promotes accumulation of CD11b+ myeloid cells in the lungs regardless of tumor size. 1.0×10^4 WT or MIF KD 4T1-luc cells (MIF KD Lo), or 1.5×10^5 MIF KD 4T1-luc cells (MIF KD Hi) were implanted in the mammary fat pad of female Balb/c mice. **A**, Naïve (non-tumor-bearing) mouse lungs were removed, frozen sections were made, and stained for CD11b as a control. **B**, Lungs from tumor-bearing mice were removed at day 24 of tumor growth, frozen sections were made, and stained for CD11b. All images were acquired using a fluorescent light microscope **C**, Images were quantified for amount of CD11b positivity/image using ImageJ. Images and quantification are representative of 2 independent experiments with $n=8$ mice/group, and 2 images/mouse. One-way ANOVA. ** $p<0.01$.

quantified CD11b coverage in the lungs, I found that regardless of tumor size, loss of MIF expression in the primary tumor led to a reduced accumulation of CD11b⁺ myeloid cells in the lungs (**Fig 3.4C**). These data suggests that, while MIF expression in the primary tumor does not affect matrix remodeling in the metastatic niche, it does promote accumulation of myeloid cells in the lung.

MIF expression in the primary tumor does not affect collagen crosslinking in the lungs at early stages of tumor growth.

While I observed differences in some markers of metastatic niche formation in the lungs late during tumor development, I was also interested in analyzing these markers early during tumor development, before differences in primary tumor size based on MIF expression arise (the “pre-metastatic” niche specifically). I chose day 12 of tumor growth, as this is a time point at which we observe no difference in tumor size between WT and MIF KD tumors, but which is still late enough that some changes can be observed in the lung microenvironment (increased collagen crosslinking is seen in the day 12 lungs compared to the naïve controls shown in **Figure 3.3A**). When I analyzed lungs of day 12 tumor-bearing mice by staining lung sections with picrosirius red, I again found that there was no difference in collagen crosslinking between lungs from mice with WT or MIF KD primary tumors (**Fig 3.5**). This result supports my finding in **Figure 3.3** in which I saw no difference in collagen crosslinking in lungs of late-stage tumor-bearing mice.

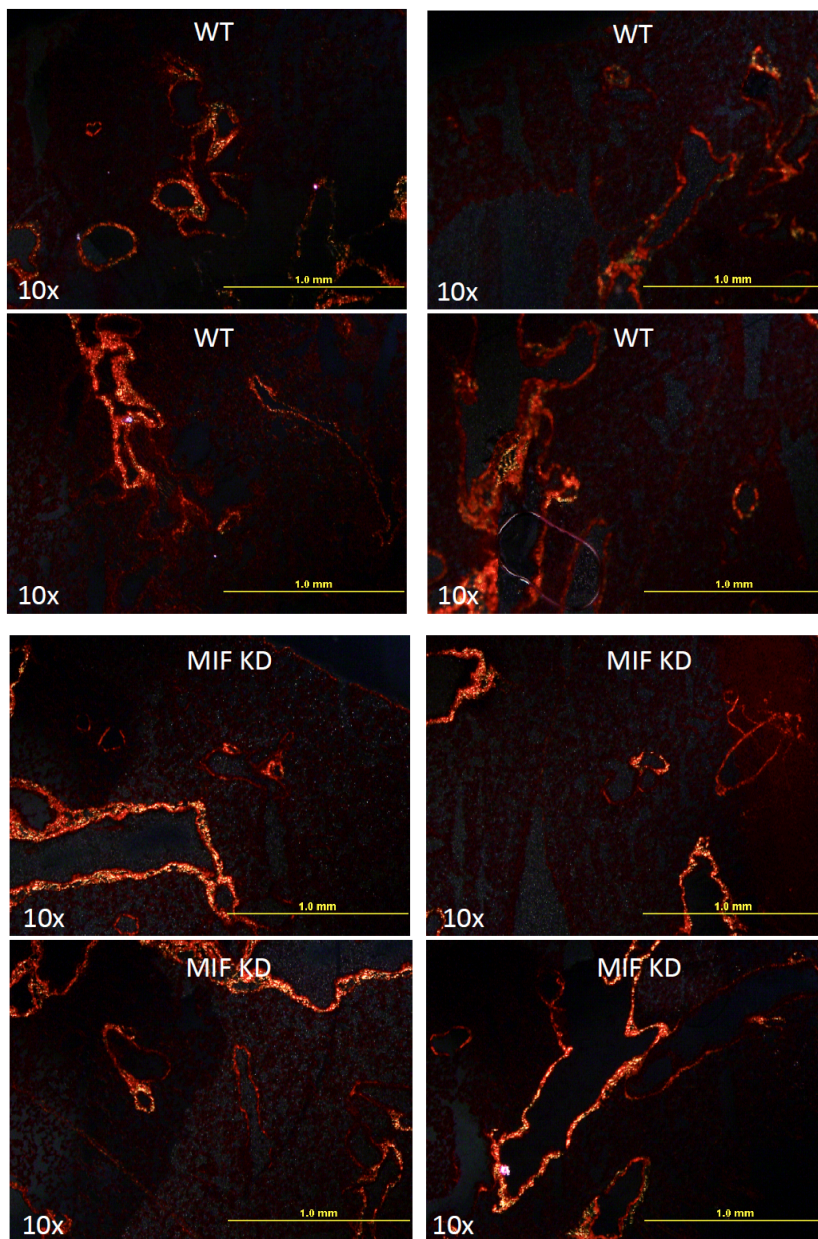


Figure 3.5: MIF expression in the primary tumor does not affect collagen crosslinking in the lungs at early stages of tumor growth. 1.0×10^4 WT or MIF KD 4T1-luc cells were implanted in the mammary fat pad of female Balb/c mice. Lungs from tumor-bearing mice were removed at day 12 of tumor growth, frozen sections were made, and stained with picrosirius red. All images were acquired using a polarized light microscope. n=8 mice/group.

MIF expression in the primary tumor promotes accumulation of CD11b⁺ myeloid cells in the lungs during early tumor development.

I also analyzed accumulation of CD11b⁺ myeloid cells in the lungs of WT and MIF KD tumor-bearing mice at day 12 by immunofluorescence. Consistent with my collagen crosslinking observations at day 12, I observed an increase in CD11b⁺ cells in lungs of tumor-bearing mice compared to naïve lungs (compare **Figure 3.6** to **Figure 3.4A**), suggesting that at day 12 of tumor growth, the pre-metastatic niche has begun to form. When I quantified the CD11b⁺ cells both using ImageJ for CD11b coverage, as well as by counting cells per image, I found that the lungs of mice bearing WT primary tumors had significantly more CD11b⁺ cells than lungs of mice with MIF KD tumors (**Fig 3.6B,C**).

MIF expression in the primary tumor does not promote accumulation of CD11b⁺ myeloid cells in the lungs by flow cytometry analysis during early tumor development.

In order to better phenotype the accumulated CD11b⁺ cells in the lungs detected by immunofluorescence, I analyzed lungs of mice with day 12 tumors by flow cytometry. I specifically analyzed markers for MDSC subsets given our previous work linking MIF expression with abundance of this cell type in the primary tumor (32). As described previously, no difference in primary tumor size was observed at this time point (**Fig 3.7A**). When I analyzed total CD11b⁺ cells in the lungs I found no statistically significant difference between WT and MIF KD tumor-bearing animals, though the data is trending towards the phenotype I see by immunofluorescence, with MIF KD tumor-bearing mice having fewer CD11b⁺ cells in the lungs (**Fig 3.7B**). Interestingly, when correlating

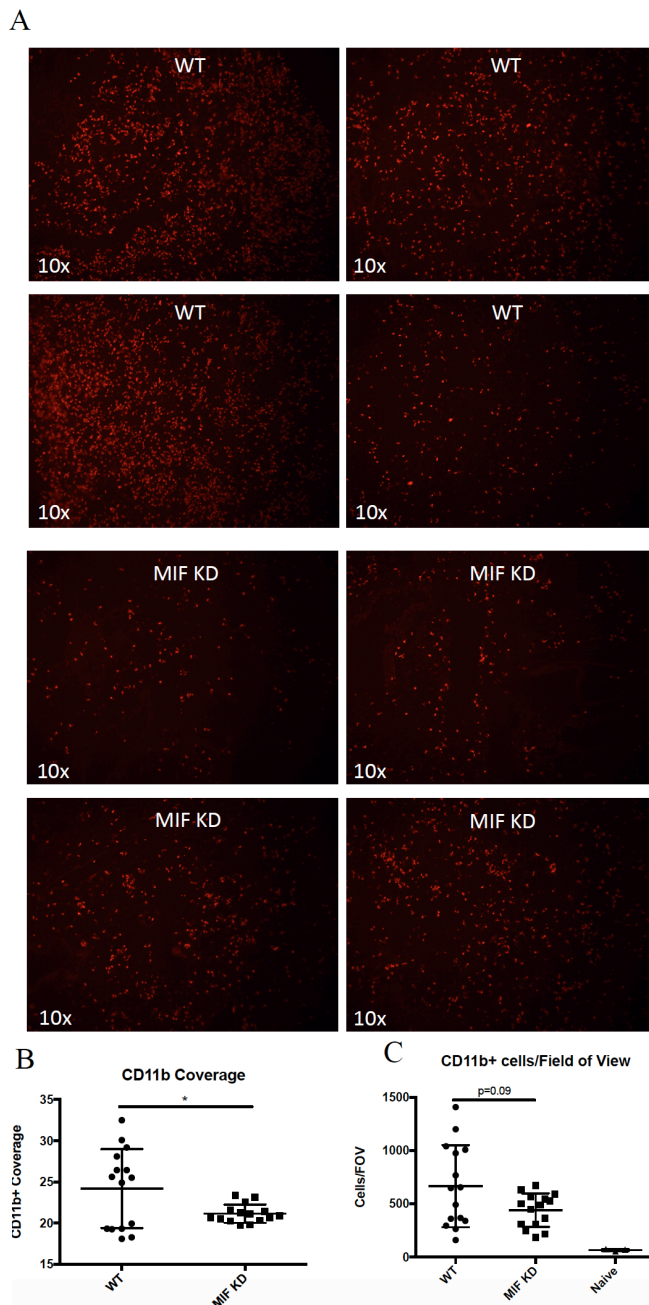


Figure 3.6: MIF expression in the primary tumor promotes accumulation of CD11b⁺ myeloid cells in the lungs during early tumor development.

1.0×10^4 WT or MIF KD 4T1-luc cells were implanted in the mammary fat pad of female Balb/c mice. **A**, Lungs from tumor-bearing mice were removed at day 12 of tumor growth, frozen sections were made, and stained for CD11b. All images were acquired using a fluorescent light microscope. **B**, Images were quantified for amount of CD11b positivity/image using ImageJ. **C**, Images were counted for the number of CD11b⁺ cells/field of view. One-way ANOVA, n=8 mice/group. Image analysis based on 2 images/mouse. *p<0.05.

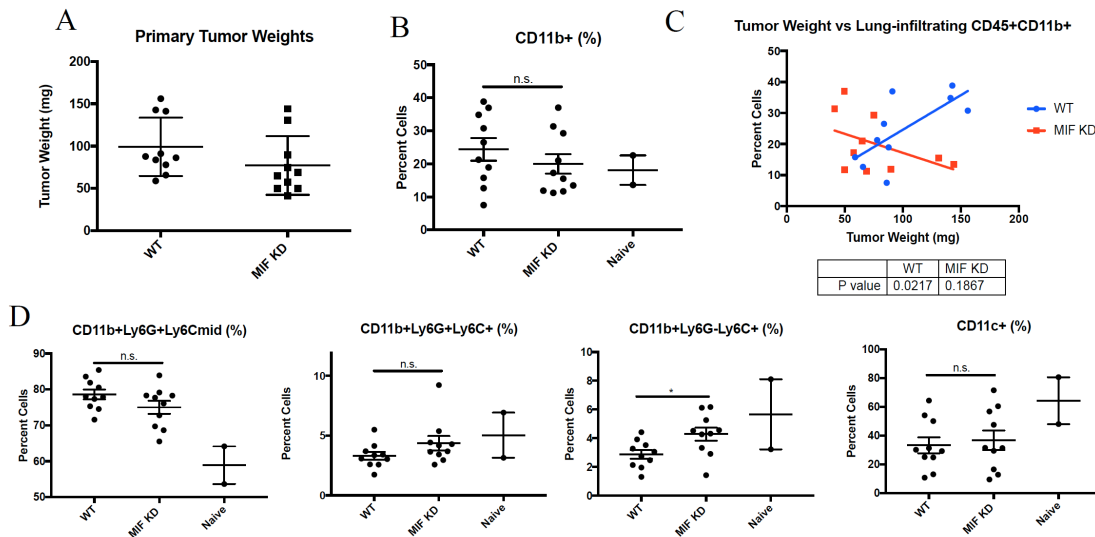


Figure 3.7: MIF expression in the primary tumor does not promote accumulation of CD11b+ myeloid cells in the lungs during early tumor development by flow cytometry. 1.0×10^4 WT or MIF KD 4T1-luc cells were implanted in the mammary fat pad of female Balb/c mice. **A**, Tumors were removed at day 12 of growth and weighed. **B**, Lungs from tumor-bearing mice were removed at day 12 of tumor growth, digested, and analyzed for the presence of CD11b+ cells by flow cytometry. **C**, Tumor weight was analyzed for correlation with CD11b+ cells found in the lungs. **D**, Lungs were analyzed for MDSC subsets and DCs. Data are the accumulation of 2 independent experiments with $n=4$ mice/group in experiment 1, and $n=6$ mice/group in experiment 2. One-way ANOVA, $*p<0.05$.

CD11b⁺ cells in the lung with primary tumor size, there is a very strong positive correlation in mice with WT tumors, whereas in mice with MIF KD tumors, this positive correlation is not observed (**Fig 3.7C**). This suggests that MIF expression in the primary tumor is linked to CD11b⁺ myeloid cell accumulation in the lungs. When analyzing myeloid cell subsets, I saw no significant difference in Ly6G-expressing populations (either Ly6G⁺Ly6C^{mid} or Ly6G⁺Ly6C^{hi}) (**Fig 3.7D**). Surprisingly, I observed a greater frequency of CD11b⁺Ly6G⁻Ly6C⁺ cells (monocytic MDSCs) in the lungs of mice with MIF KD tumors (**Fig 3.7D**). I also saw no difference in CD11c⁺ DCs between lungs of WT and MIF KD tumor-bearing mice (**Fig 3.7D**). Taken together, these data show that while lungs from WT tumor-bearing mice may have greater accumulation of CD11b⁺ myeloid cells, no differences in MDSC subsets are seen. Given that I see no effect of MIF expression on metastasis in the lungs when tumor size is controlled for, I hypothesize that the subset(s) of cell(s) that are increased in the lungs of WT tumor-bearing mice do not contribute to metastasis formation in a MIF-dependent fashion.

Discussion

Despite our initial finding that loss of MIF expression in the primary tumor in the 4T1 model reduced pulmonary metastasis, this subsequent work demonstrates that, if MIF KD tumors are permitted to grow to the same size as WT tumors, pulmonary metastasis is no longer impaired. This suggests that it is in fact primary tumor size, rather than MIF expression per se, dictating metastasis. I also analyzed two key markers of metastatic niche formation (collagen crosslinking and myeloid cell accumulation) in the lung, and found that MIF expression in the primary tumor only impacted the latter, during both

early and late stages of tumor progression. Upon further phenotyping of the accumulated myeloid cells in lungs of early-stage WT and MIF KD tumor-bearing mice, I did not find a statistically significant difference in general myeloid cell accumulation between WT and MIF KD tumor-bearing mice. This is contradictory to my immunofluorescence results, and may be due to a large amount of variability in the flow cytometry samples (the data are trending towards significance), or IF may be detecting regional differences in CD11b⁺ cell accumulation that are being missed by flow cytometry analysis. Further analysis of lungs by both immunofluorescence and flow cytometry will be needed to clarify these results.

While MIF is clearly playing a role in primary tumor growth, our data suggest that MIF expression in the primary tumor does not directly affect overall metastasis or metastatic niche formation in the 4T1 model. I have shown that primary tumor size is a much stronger indicator of metastatic burden than MIF expression. This correlation has been extensively studied in human breast cancer, and primary tumor size and stage have been found time and again to strongly correlate with both local and distant metastasis, as well as with progression-free survival (189–193). I argue that many studies that claim to reduce metastasis through therapeutic modalities may in fact simply be reducing primary tumor size, which is the main cause of reduced metastasis. Oftentimes in studies specifically focused on metastasis, primary tumor size is not shown, making it difficult to determine what effect the therapy/genetic manipulation is having specifically on metastasis versus the observations being primarily an effect of impact on primary tumor size.

Collagen crosslinking is an important contributor to establishment of the pre-metastatic niche in the lung. Lysyl oxidase (LOX) is a key hypoxia-inducible factor secreted by tumor cells, which travels to the lungs via the bloodstream where it exerts its enzymatic activity to crosslink collagen IV (133). Numerous studies have linked the hypoxic response in cancer to MIF (56,58,59,61,194–199). This body of work led me to hypothesize that loss of MIF expression in the primary tumor would lead to a reduction in collagen-crosslinking in the lungs through the activity of LOX. However, when I assessed this both at early and late stages of primary tumor growth, I saw no effect of MIF (or primary tumor size) on intensity of collagen crosslinking in the lungs. We have also assessed LOX/LOX family member expression under hypoxic conditions *in vitro* in the 4T1 cell line, and no clear effect of MIF expression was found (data not shown). Together, this suggests that tumor-derived MIF expression is not important to the mechanism through which collagen crosslinking is being regulated *in vivo*.

Accumulation of CD11b⁺ bone marrow-derived cells (BMDCs) has been shown to occur downstream of collagen crosslinking in establishment of a pre-metastatic niche, and this process is dependent on LOX activity (134). While I did not observe any changes in collagen crosslinking in my studies, we do have evidence to suggest that MIF can influence myeloid cell accumulation in the primary tumor (32). This led me to hypothesize that MIF may also influence myeloid populations at distant sites. Interestingly, MIF expression in the primary tumor did lead to an increase in CD11b⁺ cell accumulation in the lungs, regardless of primary tumor size. This suggests that, in our

model, accumulation of CD11b⁺ cells in the lung is not entirely dependent on the level of collagen crosslinking.

Given our previous finding that MIF expression in the primary tumor leads to increased accumulation of monocytic MDSCs in the tumor microenvironment, I hypothesized that the increase in CD11b⁺ cells in the lungs of WT tumor-bearing mice was due specifically to an increase in this subset of MDSCs. However, upon further phenotyping the CD11b⁺ cells found in the lungs by flow cytometry, I found that the opposite was true: more monocytic MDSCs were found in the lungs of mice with MIF KD tumors. No differences were seen in the PMN-MDSC subset. By flow cytometry analysis, I also did not detect a statistically significant difference in total CD11b⁺ cells as I observed by IF (though the flow cytometry data are trending towards significance). This is likely due to the high amount of variability observed from mouse to mouse, and further repeats of this experiment would potentially result in significance between groups. My more detailed analysis of the CD11b⁺ cells in the lungs did not reveal a myeloid cell subset that is more highly represented in the lungs of mice with WT tumors, suggesting that another population of cells that was not examined in my analysis is responsible for this difference. A more comprehensive evaluation of other myeloid subsets in the lungs, such as M1-like and M2-like macrophage populations, may reveal a subset of cells that is influenced by MIF expression. In conclusion, these data continues to support a strong role for MIF expression in promoting primary tumor growth. However, I found that the reduction in primary tumor size, rather than MIF expression per se, is actually responsible for driving lung metastasis in the 4T1 model.

Chapter Four: MIF promotes primary tumor growth, but not metastasis or myeloid cell accumulation in the MMTV-PyMT murine model of breast cancer.

Abstract

Macrophage Migration Inhibitory Factor (MIF) has been shown to promote breast cancer growth and progression in both implantable mouse models and human disease. In this study, I aimed to more closely link these findings by utilizing the genetically engineered MMTV-PyMT model of breast cancer. When comparing WT and MIF KO mice, I observed that WT mice developed mammary tumors earlier in life than MIF KO mice. I also found that WT mice harbored significantly larger tumors, and greater numbers of tumors compared with MIF KO mice. However, when I assessed overall lung metastasis, I surprisingly found no difference between WT and MIF KO mice. Similar to my observations in the 4T1 model, I saw no difference between groups in terms of matrix remodeling in the lungs, but did see a reduction in myeloid cell accumulation in MIF KO lungs. I hypothesized that the difference in primary tumor size observed may be due to differences in accumulation of immunosuppressive myeloid cells, as we have reported previously in the 4T1 model. However, when I analyzed multiple myeloid cell subsets, I found no differences in any population between WT and MIF KO tumors. More detailed studies will need to be performed to elucidate the mechanism by which MIF is controlling tumor growth in this model.

Introduction

Macrophage Migration Inhibitory Factor (MIF) has frequently been found to promote tumor growth and progression in implantable mouse models of breast cancer. A number of mechanisms have been reported, including MIF-dependent enhancement of proliferation and invasiveness of murine breast cancer cell lines via autocrine signaling through CD74 (200), heightened AKT activation (201), induction of tumor angiogenesis through increased VEGF and IL-8 expression (54), and several reports involving interaction of MIF with the anti-tumor immune response promoting tumor growth and metastasis (32,60,107,108,110,111,176). MIF expression has also been correlated with advanced disease and poor outcomes in human breast cancer patients, supporting further work to understand how MIF functions as a pro-tumorigenic factor (54,55,202,203).

The MMTV-PyMT murine model of breast cancer is broadly used and is more clinically relevant than implantable models of murine cancer. The MMTV-PyMT model involves use of the polyoma virus middle T antigen, which is under direct transcriptional control of the mouse mammary tumor virus (MMTV) promoter. This activity results in the development of tumors in some or all of the 10 mammary fat pads of female mice carrying the transgene, with disease progression mimicking human disease, advancing from hyperplasia through adenocarcinoma over approximately a five month time period (149,151). Also as seen in human disease progression, primary tumors in this model spontaneously metastasize to the lungs (149). Lung metastasis can be observed at later time points macroscopically, or detected and quantified early and late through qRT-PCR for the MMTV-PyMT transgene. The high level of translation to human disease makes

the MMTV-PyMT model very useful in studying breast cancer progression and metastasis.

To date, no work has been published on the effects of MIF expression in this model. By generating a MIF KO strain of MMTV-PyMT transgenic mice, I was able to elucidate that MIF expression does promote primary tumor growth and progression in this model. However, I did not observe an effect of MIF expression on either spontaneous pulmonary metastasis or on accumulation of myeloid cell populations in the primary tumors. Further work will need to be done in order to determine the mechanism by which MIF is promoting tumor growth in this model.

Materials and Methods

MMTV-PyMT Mouse Tumor Model

Wild-type (WT) male C57Bl/6 MMTV-PyMT mice were crossed with established female MIF knock-out (MIF KO) C57Bl/6 mice generated as described previously (204) in order to generate both WT and MIF KO MMTV-PyMT lines. All mouse pups were genotyped for transgene expression as well as to determine MIF status. Primers used for genotyping were as follows: murine MIF (F:5'ACGCAGCGCGCTCTCATAGA CCAGG3' R:3'GGTCTCTTATAAACCATTTATTTCTCC5'), Neo (F:5'TGCTCCTG CCGAGAAAGTATCCATCATGGC3' R:3'CGCCAAGCTCTTCAGCAATATCACGG GTAG5') and murine MMTV (F:5'TGTGCACAGCGTGTATAATCC3' R:3'CAGAAT AGG TCGGGTTGCTC5'). MIF status was confirmed by PCR, with a heterozygous mouse shown as a control (**Supplementary Figure 4.1, top**). Presence of the MMTV-

PyMT transgene was also confirmed using PCR, with a mouse negative for the transgene shown as a control (**Supplementary Figure 4.1, bottom**).

Mice were monitored starting at 6 weeks of age for the presence of mammary tumors. Using calipers, tumor volumes were estimated from two perpendicular measurements using the formula $V = 0.4 \times L \times W^2$.

All animal studies were conducted in accordance with the University of Virginia Animal Care and Use Committee (ACUC) under protocol approval #4039 and all efforts were made to minimize suffering of animals in all experiments.

Analysis of Lung Metastatic Burden by qRT-PCR

Following euthanasia, lungs were excised and homogenized with a pestle, followed by addition of 1mL of Trizol per 100mg of tissue, from which total RNA was isolated. RNA (2ug) was converted into cDNA using the iScript cDNA synthesis kit (Bio-Rad).

Quantative real-time PCR (qRT-PCR) was performed to quantify PyMT expression in the lungs, and normalized to 18s ribosomal RNA using IQ SYBR Green Supermix according to the manufacturers' instructions (Bio-Rad). Primers for qRT-PCR were as follows:

murine PyMT (F:5'GGGGATATGCTGTCATCGGGCTCA3' R:3'AGCTACCAGTCGCCGCCTAAGA5'), and murine 18s (F:5'GTAACCCGTTGAACCCCAT3' R:3'CCATCCAATCGGTAGTAGCG5')

Lung Sectioning

Lungs were removed from each mouse, cut in half, and flash frozen in liquid nitrogen. After freezing, lung pieces were stored at -80C until sectioned. Lungs were embedded in optimum cutting temperature (OCT) medium (VWR). Lungs were then sectioned onto slides using a Leica CM3050 Research Cryostat.

Picrosirius Red Staining

Slides with frozen lung sections were fixed for 10 minutes in 10% formalin, followed by a rinse with deionized (DI) H₂O. Slides were then stained with 0.1% picrosirius red stain (AbCam) for 90 minutes. Slides were rinsed with 0.01N HCl in water for 1 minute, followed by another rinse in DI H₂O. Slides were dehydrated with 70% EtOH for 30 seconds, and then cover slipped for storage until imaged. Slides were imaged using the Olympus BX51 high magnification microscope with the polarizing filter attached.

CD11b Immunofluorescent (IF) Staining

Slides with frozen lung sections were fixed for 20 minutes in an ice-cold solution of 1:1 acetone and 100% EtOH, followed by two PBS washes. Slides were then blocked with an avidin-biotin blocking kit (Vector Labs) in 3% BSA in PBS according to the manufacturers instructions. Slides were washed with PBS, and stained with primary anti-CD11b PE antibody (1:200, eBiosciences) for 45 minutes. Slides were washed, followed by staining with secondary anti-rat biotinylated antibody for 30 minutes (1:200, BD Biosciences). Slides were washed, and stained with a Texas Red neutral avidin antibody (1:500, Southern Biotech) for 30 minutes. Slides were washed, and mounted with

Vectashield plus DAPI mounting medium (Vector Labs) according to the manufacturers instruction. All staining was performed at room temperature. Following staining, slides were imaged with a Nikon Microphot-FXA fluorescent microscope and Nikon HB-10101AF Mercury Lamp and Olympus Q-Color5 camera.

Tumor Digestion and Flow Cytometry Analysis

At the time of euthanasia, tumors were excised from the mammary fat pads, weighed, and then digested with 10,000 U collagenase I (Worthington Biochemical) for 60 min at 37°C, followed by addition of 30U of DNase (Qiagen) for 10 minutes at RT. Cell suspensions were strained through a 70-um screen before use in experiments.

For flow cytometry analysis of T cells, single cell suspensions were stained with Live/Dead Fixable Yellow Dead Cell Stain (1:500, Invitrogen), as well as CD3-PE (1:200, Biolegend), CD4-APCCy7 (1:200, eBiosciences), CD8-PeCy7 (1:200, eBiosciences) and CD25-FITC (1:200, Biolegend).

For flow cytometry analysis of myeloid cells, single cell suspensions were stained with Live/Dead Fixable Yellow Dead Cell Stain (1:500, Invitrogen), as well as CD45-PerCP (1:100, BD Bioscience) or CD45-PE (1:100, eBiosciences), CD11b-PacBlue (1:100, Invitrogen), GR1-PE (1:500, Biolegend), F4/80-Alexafluor488 (1:100, AbDSerotec), CD11c-APCCy7 (1:200, Biolegend), Ly6G-APCCy7 (1:200, Biolegend) and Ly6C-PerCPCy5.5 (1:200, Biolegend).

All gating on cell surface markers was based on fluorescence minus one (FMO) controls. The cells were analyzed with the Beckman Coulter CyAN ADP LX 9 Color Flow Cytometer.

Image Quantification and Statistical Analysis

CD11b IF images were quantified using ImageJ software by calculating the area of mean pixel intensity of each image, with n=2 images per lung. All data are presented as mean +/- SEM. Data was analyzed either by Student's t-test or one-way ANOVA using the Graph-Pad Prism analysis software. P values are represented in the figures as * p<0.05, ** p<0.01, *** p<0.001, **** p<0.0001.

Results

MIF expression promotes tumor progression in the murine MMTV-PyMT spontaneous model of breast cancer.

To examine the role of MIF in tumor growth using this model, I compared female MIF-expressing (WT) and MIF-deficient (MIF KO) MMTV-PyMT transgenic mice. The average time to tumor occurrence was significantly delayed in MIF KO mice, though no significant difference in overall survival was seen (with "overall survival" indicating the point at which a mouse obtained the maximum allowable tumor burden, and needed to be humanely euthanized) (**Fig 4.1A**). When comparing age-matched 8-week-old mice, the point at which about half of the mice in my studies presented with at least one palpable tumor mass, MIF KO mice showed significantly fewer tumors per mouse and, in fat pads that did not yet harbor detectable tumors, smaller fat pads by weight (**Fig 4.1B**). While

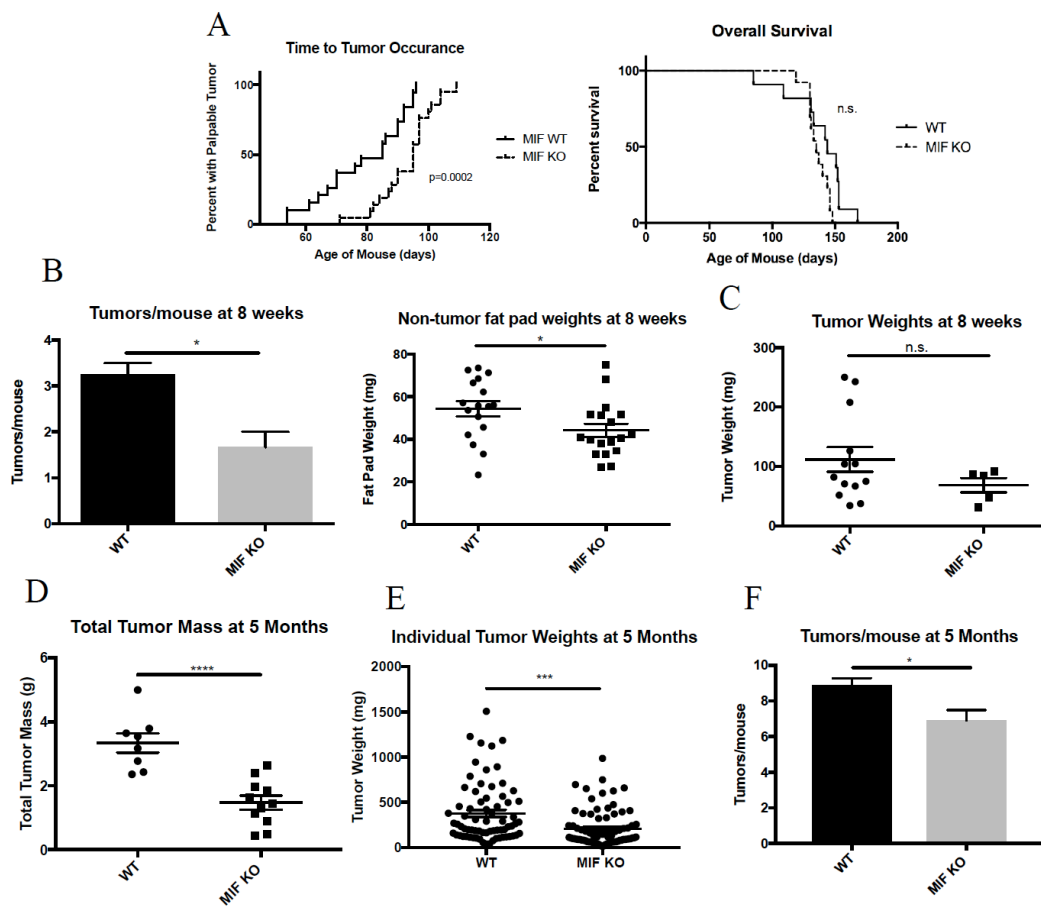


Figure 4.1: MIF expression promotes tumor progression in the murine MMTV-PyMT spontaneous model of breast cancer. Female WT and MIF KO MMTV-PyMT⁺ mice were monitored starting at 6 weeks of age for the presence of mammary tumors. **A**, Age was recorded on the day of appearance of the first tumor and age was recorded when mice reached the maximum allowable tumor size. n=19 for WT mice, n=21 for MIF KO mice. **B-C**, Mice were euthanized at 8 weeks of age. Detectable tumor material and non-tumor bearing fat pads were removed, weighed, and enumerated. Each data point on dot plots represents one individual fat pad or tumor, with some mice having multiple tumors. n=4 mice for WT and n=3 mice for MIF KO. **D-F**, Mice were euthanized at 5 months of age. Tumors were removed from the fat pads, enumerated, and weighed. Each data point in **(D)** represents one mouse. Each data point in **(E)** represents one tumor. n=8 mice for WT, n=11 mice for MIF KO.

the MIF KO mice had fewer tumors per mouse, there was no statistically significant difference between WT and MIF KO mice when comparing individual tumor sizes at this early time point (**Fig 4.1C**). When comparing late-stage, age-matched 5-month-old mice, MIF KO mice had significantly less total tumor burden compared to WT mice (**Fig4.1D**), as well as fewer tumors at the largest end of the size distribution (**Fig 4.1E**). MIF KO mice also developed significantly fewer tumors per mouse when compared to WT mice by 5 months of age (**Fig 4.1F**). Together, these data suggest that loss of MIF expression in the MMTV-PyMT model leads to a delay in tumor appearance and reduction in tumor growth.

MIF expression does not promote spontaneous lung metastasis.

As discussed previously, one of the major benefits of using this genetic model of breast cancer is that disease progression closely mimics that of human disease, including spontaneous metastasis to the lungs. Due to the expression of the PyMT oncogene specifically in tumor cells, metastasis can be quantified in the lungs using qRT-PCR for PyMT. When I quantified lung metastasis in WT and MIF KO mice, I found no significant difference between genotypes (**Fig 4.2A**). I did see increased expression of the transgene in lungs of tumor-bearing mice compared to lungs of a non-transgenic mouse as a negative control, and similar signal to that found in a tumor sample as a positive control (**Fig 4.2A**). I also observed no difference in total lung weight between WT and MIF KO groups, which again suggests no difference in metastatic burden between the two genotypes (**Fig 4.2B**).

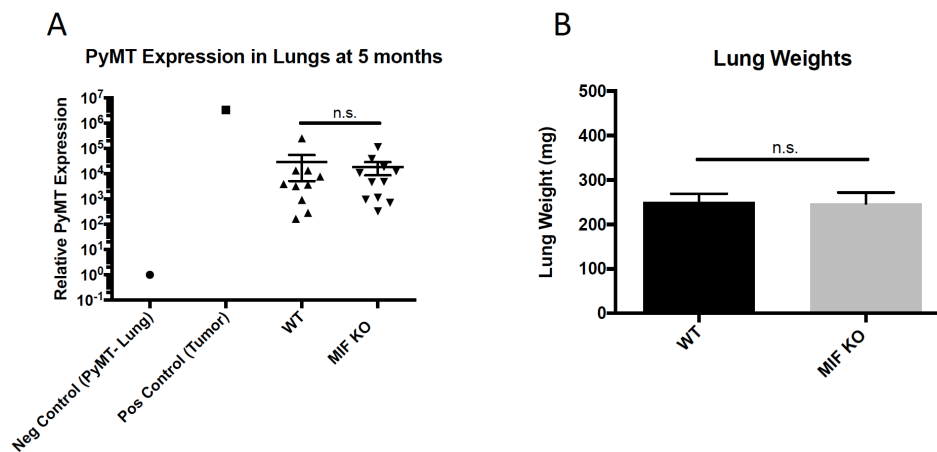


Figure 4.2: MIF expression does not promote spontaneous lung metastasis. **A**, Lungs were removed from female WT or MIF KO MMTV-PyMT mice at 5 months of age, RNA was extracted, and qRT-PCR was performed to detect expression of PyMT in the lungs. **B**, Lungs were weighed at the time of harvest. n=10 for WT mice, n=11 for MIF KO mice.

MIF expression does not promote collagen cross-linking in late-stage lungs.

Alongside assessing overall lung metastasis in this model, I also wanted to analyze metastatic niche formation between lungs of WT and MIF KO mice. Given that I saw no difference in overall metastasis (**Fig 4.2**), I hypothesized that no differences would be found in markers of niche formation. As discussed in Chapter 3, one of the key markers of formation of a metastatic niche in the lung is increased collagen crosslinking, which can be detected by staining lung sections with picrosirius red, followed by imaging with a polarized light microscope. I stained sections of lungs from 5 month-old WT and MIF KO MMTV-PyMT mice, and, as in the 4T1 model, saw no MIF-dependent difference in the amount of collagen crosslinking (**Fig 4.3A**). The tumors were also removed from all mice and weighed (**Fig 4.3B**). The tumor weight data supported previous experiments in that I saw significantly greater tumor burden in WT mice compared to MIF KO mice, both in terms of individual tumor weights as well as total tumor burden (**Fig 4.3B**).

MIF expression promotes CD11b⁺ cell accumulation in late-stage lungs.

A second marker of metastatic niche formation, also discussed in Chapter 3, is the accumulation of myeloid cells in the lungs following matrix remodeling. Using the 4T1 model, I previously observed significantly greater CD11b⁺ myeloid cell accumulation in the lungs of mice with WT primary tumors compared to MIF KD tumors, even though I saw no difference in overall lung metastasis when controlling for tumor size (**Fig 3.4 and Fig 3.6**). I therefore hypothesized that this phenotype may be recapitulated in the MMTV-PyMT model. I stained lungs from 5 month-old WT and MIF KO mice for

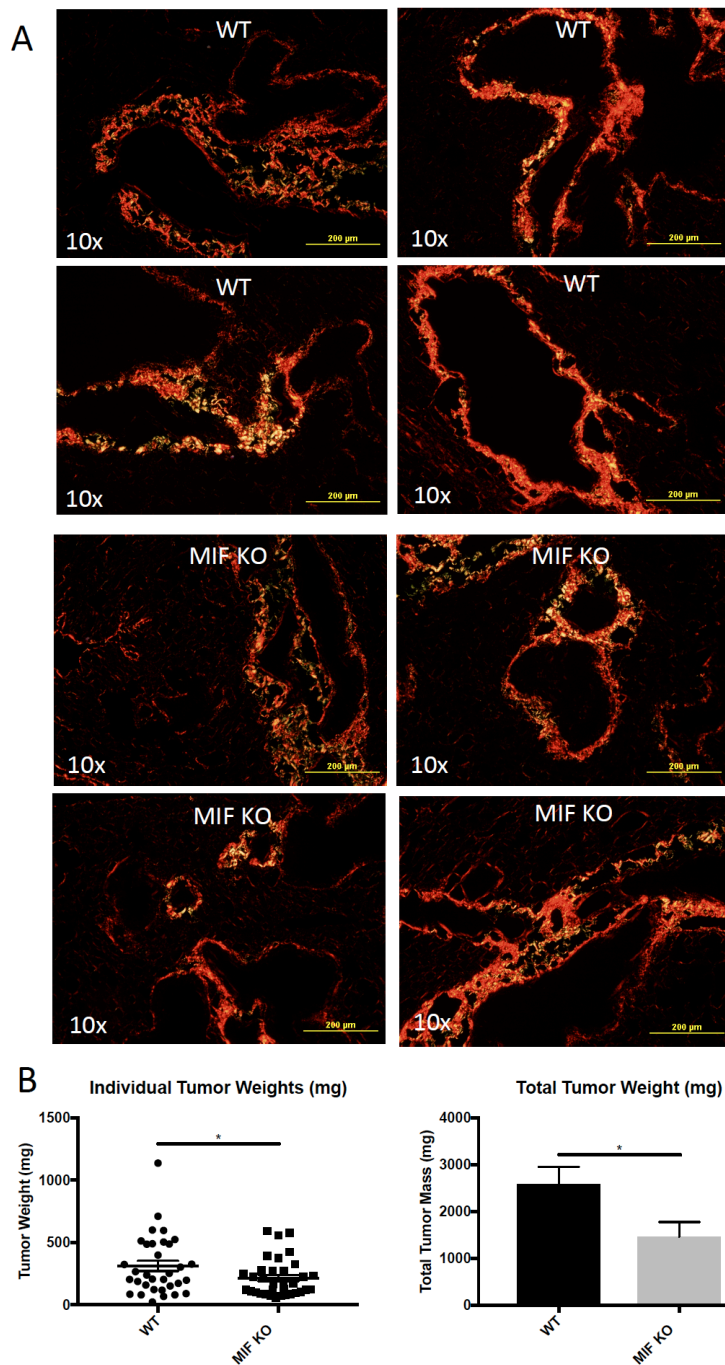


Figure 4.3: MIF expression does not promote collagen cross-linking in late-stage lungs. **A**, Lungs were removed from female WT or MIF KO MMTV-PyMT mice at 5 months of age, frozen sections were made, and stained with picrosirius red. All images were acquired using a polarized light microscope. **B**, Tumors were removed and were weighed individually and combined for total tumor weight per mouse. $n=4$ for WT mice and $n=5$ for MIF KO mice. Student's t-test, $*p<0.05$.

CD11b by IF, and, as hypothesized, found that WT mice had a greater accumulation of CD11b⁺ cells in their lungs at this late time point (**Fig 4.4A-B**).

Together, these data suggests that while MIF expression in this model does not affect overall metastatic burden in the lungs, MIF may be responsible for increasing accumulation of myeloid cells. Further study of these cells in the lung microenvironment will be needed to better understand their overall role in tumor growth and metastasis.

MIF expression does not affect intra-tumoral accumulation of myeloid cell subsets at 5 months.

I next wanted to determine if, as found in the 4T1 model, differences in the immune microenvironment of the primary tumors were apparent. This analysis could aid in understanding the mechanism by which the difference in tumor growth found between WT and MIF KO mice arises. I began assessment of immune infiltration by looking at accumulation of various myeloid cell subsets in late-stage, 5 month-old tumor-bearing mice. In order to minimize sample number (with up to 10 tumors per mouse, sample number can become a limiting factor), I categorized tumors as “small”, “medium” and “large” from each mouse based on the following criteria: “small”= <170mg, “medium”= 170-500mg, and “large”= >500mg. I then combined all of the “small” and “medium” tumors from an individual mouse and stained them as one sample representative of all tumors in that size range for that mouse. Large tumors were all stained individually as there are low numbers of tumors at that size in general, and the tumors are too large to combine when digesting. After separating tumors based on these size criteria, I found that

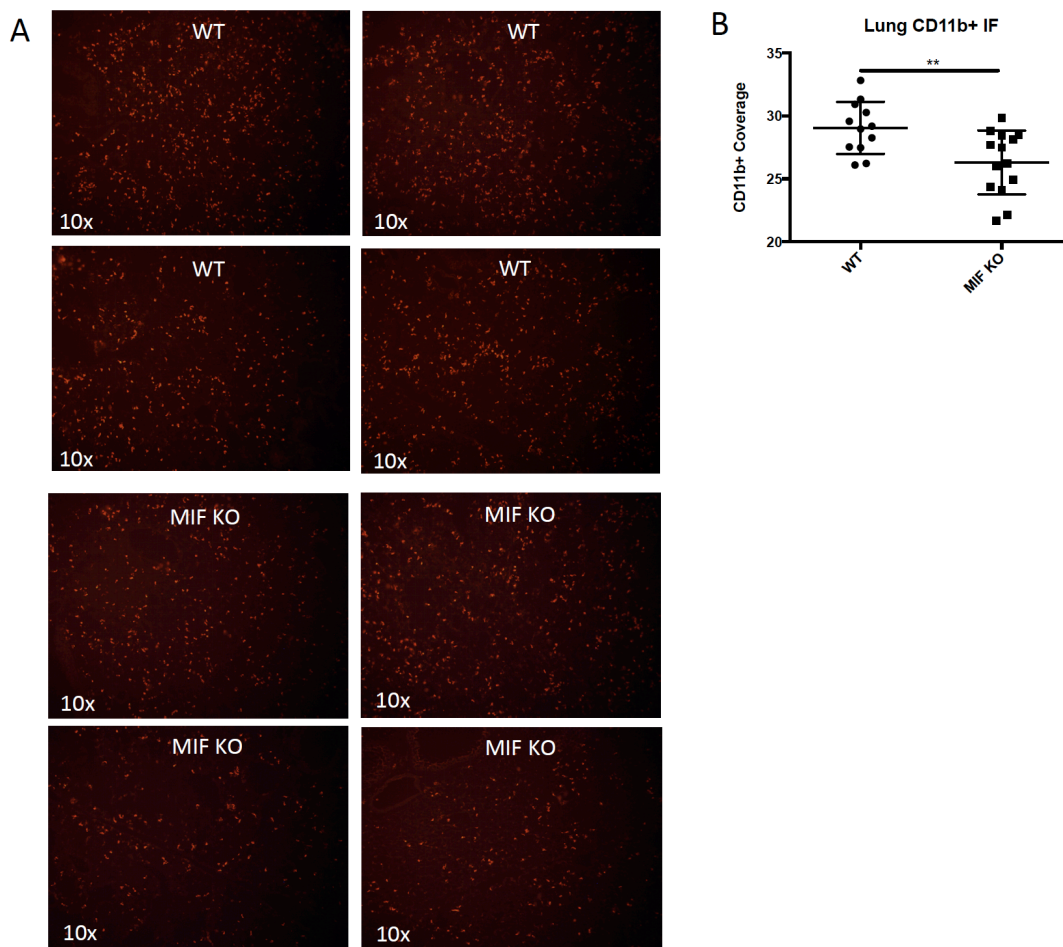


Figure 4.4: MIF expression promotes CD11b+ cell accumulation in late-stage lungs. **A**, Lungs were removed from female WT or MIF KO MMTV-PyMT mice at 5 months of age, frozen sections were made, and stained for CD11b by immunofluorescence. All images were acquired using a fluorescent light microscope **B**, Images were quantified for amount of CD11b positivity/image using ImageJ. n=4 for WT mice and n=5 for MIF KO mice, with 2 images per mouse quantified.

WT mice had significantly greater tumor burden than MIF KO mice in the “medium” and “large” tumor size groups (**Fig 4.5A**). There was no significant difference in tumor size between WT and MIF KO mice in the “small” size group (**Fig 4.5A**).

In order to analyze immune cell infiltrates in these tumors, I utilized flow cytometry staining for a number of myeloid cell markers, including CD11b, F4/80, Ly6C and Ly6G. When comparing percent and total number of cells per mg tumor, I found no differences in total myeloid cells (CD11b⁺) or macrophages (F4/80⁺) in any of the tumor size groups between WT and MIF KO mice (**Fig 4.5B-C**). I also observed very similar percentages of total myeloid cells in tumors of all sizes, at around 10-30%, and similarly for F4/80⁺ macrophages, at around 60%. However, when looking per mg of tumor, the number of these two cell populations trended towards being greater as tumor size increased (**Fig 4.5B-C**). This may indicate that the larger, more developed tumors are more greatly infiltrated by myeloid cells on a per-cell basis even though the percentage of total leukocytes remain similar across tumor size.

We have found previously in the 4T1 model that WT tumors have an increased accumulation of the monocytic subset of MDSCs compared to MIF KD tumors, and that these cells are at least partially responsible for the difference in tumor size found in the 4T1 model (32). I therefore hypothesized that MIF expression may also affect MDSC populations in the MMTV-PyMT model. In order to analyze these populations, I stained immune cells from WT and MIF KO tumors as discussed above for Ly6C and Ly6G, the two well-established markers for MDSCs in mice. CD11b⁺Ly6G⁺Ly6C^{lo} cells are

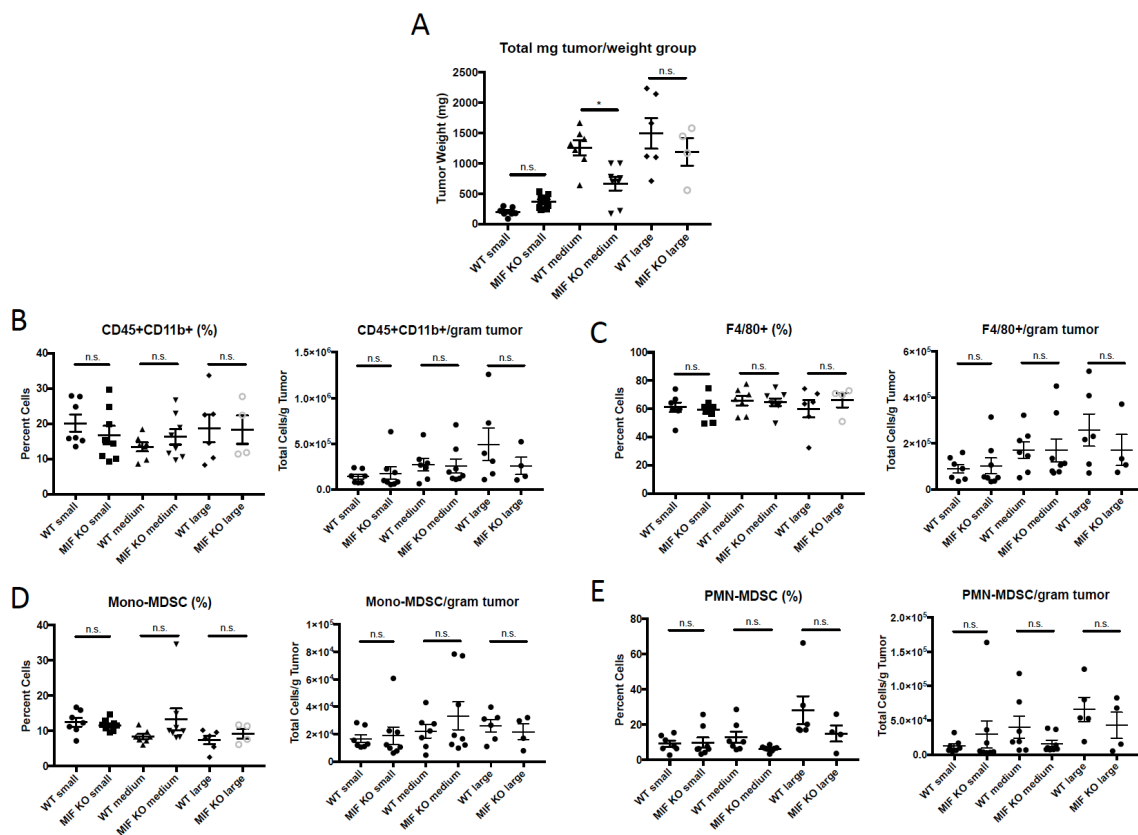


Figure 4.5: MIF expression does not affect intra-tumoral accumulation of myeloid cell subsets at 5 months. **A**, Tumors were removed from female WT or MIF KO MMTV-PyMT mice at 5 months of age, and all tumors from each mouse were weighed individually, and then sorted into weight groups per mouse as follows: small: <170mg, medium: 170-500mg and large: >500mg (large stained individually). **B-E**, Tumors were digested and stained for multiple myeloid cell markers by flow cytometry. n=7 for WT mice and n=8 for MIF KO mice. One-way ANOVA, *p<0.05.

generally accepted to represent the PMN-MDSC subset, while CD11b⁺Ly6G⁻Ly6C^{hi} cells are accepted to represent the mono-MDSC subset (99). When I assessed accumulation of these two subsets in WT and MIF KO MMTV-PyMT mice, I found no differences in either subset in terms of percent myeloid cells or cells per mg tumor (**Fig 4.5D-E**). As seen with total myeloid cells and macrophages, I observed similar percentages of these two subsets across all tumor sizes, with the exception of PMN-MDSCs, particularly in WT tumors. While not significantly different, large WT tumors did trend toward having more PMN-MDSCs, and larger tumors in general appear to have more of these cells, suggesting again that larger tumors may be more conducive to accumulation of this subset of MDSCs (**Fig 4.5E**).

MIF expression does not affect intra-tumoral accumulation of myeloid cell subsets at 4 months.

Given that I saw no difference in myeloid cells at the very late stage of 5 months of tumor growth in this model, I hypothesized that I may be missing any differences in important cell populations by looking this late, when the majority of tumor tissue is necrotic, especially in the largest tumors. I decided to analyze WT and MIF KO tumors from mice at 4 months of age to determine if any differences were seen at this earlier time point, when overall tumor sizes are much smaller. When measuring tumor size at this time point, I saw no difference in tumor burden by individual tumor weights between WT and MIF KO mice (**Fig 4.6A**). In this analysis, I also included a dendritic cell marker (CD11c), as we discovered that DC infiltration is strongly influenced by MIF at earlier points of tumor growth in the 4T1 model (**Fig 2.5**). I also used GR-1 as a general marker

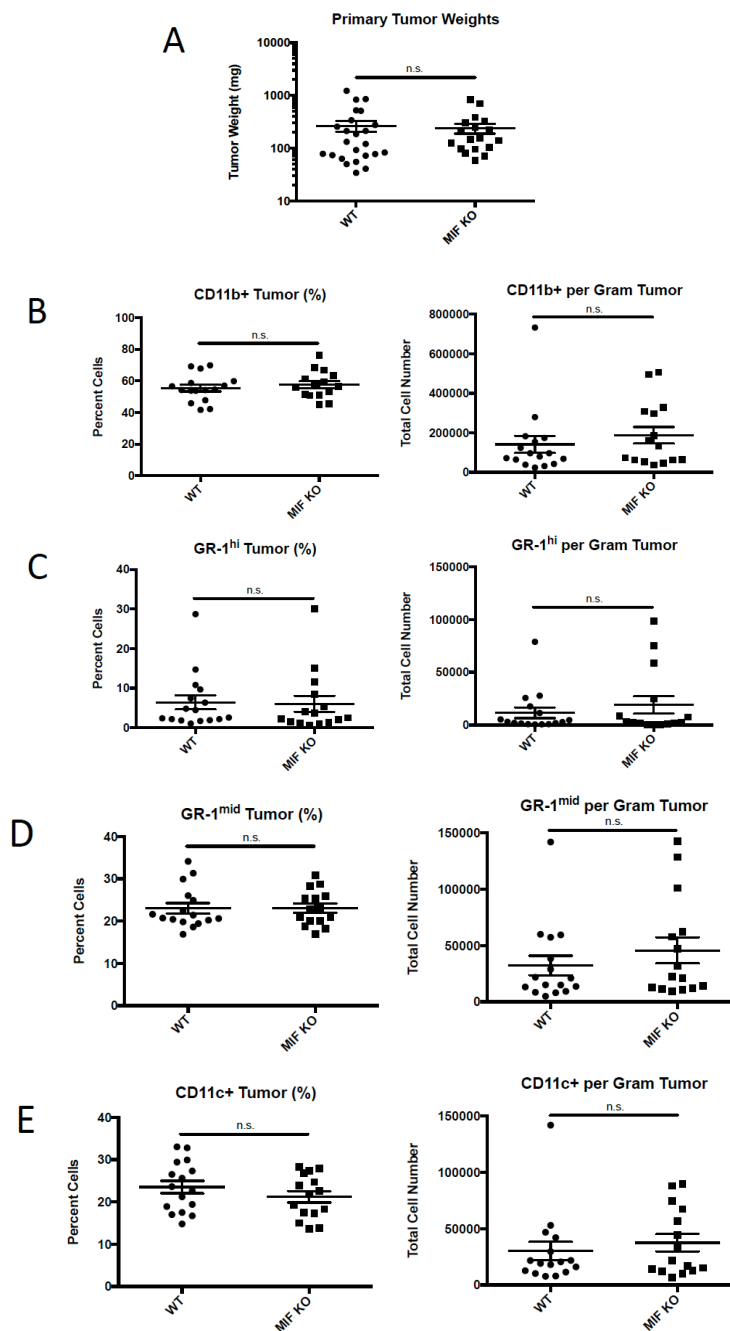


Figure 4.6: MIF expression does not affect intra-tumoral accumulation of myeloid cell subsets at 4 months. **A**, Tumors were removed from female WT or MIF KO MMTV-PyMT mice at 4 months of age, and all tumors from each mouse were weighed individually. **B-E**, All tumors were digested and stained for multiple myeloid cell markers by flow cytometry, with all tumors >100mg being stained individually and all tumors from a mouse that were <100mg being combined and treated as one data point per mouse. n=4 for WT mice and n=4 for MIF KO mice. Student's t-test revealed no statistically significant differences.

of MDSCs in this experiment (GR-1 recognizes both Ly6G and Ly6C epitopes). When quantifying total myeloid cells by CD11b expression, MDSCs by both GR-1^{hi} and GR-1^{mid}, and DCs by CD11c expression, I saw no significant differences in any population between WT and MIF KO mice either by percent or total cells per mg tumor (**Fig 4.6B-E**).

MIF expression does not affect intra-tumoral accumulation of T cells at 4 months.

While I found no differences in total myeloid cell infiltration, or in any of the subsets analyzed, I still observed a strong effect of MIF expression on total tumor size in this model. It is well established that T cells are important in tumor control, and we have evidence of enhanced T cell infiltration and activity in the 4T1 model at early time-points (**Fig 2.3**). I therefore wanted to analyze general T cell infiltration between WT and MIF KO mice at the earlier time point of 4 months. When examining total T cells (CD3⁺), as well as the CD4⁺, CD8⁺, and CD4⁺CD25⁺ (Treg) subsets, I observed no differences in any population between WT and MIF KO mice by percent or total cells per mg tumor (**Fig 4.7A-D**).

Overall, when analyzing the described immune cell infiltrates in WT versus MIF KO tumors, no significant differences were found in either 4 or 5 month-old mice in any population. This suggests that the cell populations I analyzed are likely not the major MIF-dependent influencers of tumor growth in this model, and further exploration will be needed to elucidate the mechanism by which MIF is strongly promoting tumor growth and progression in this model.

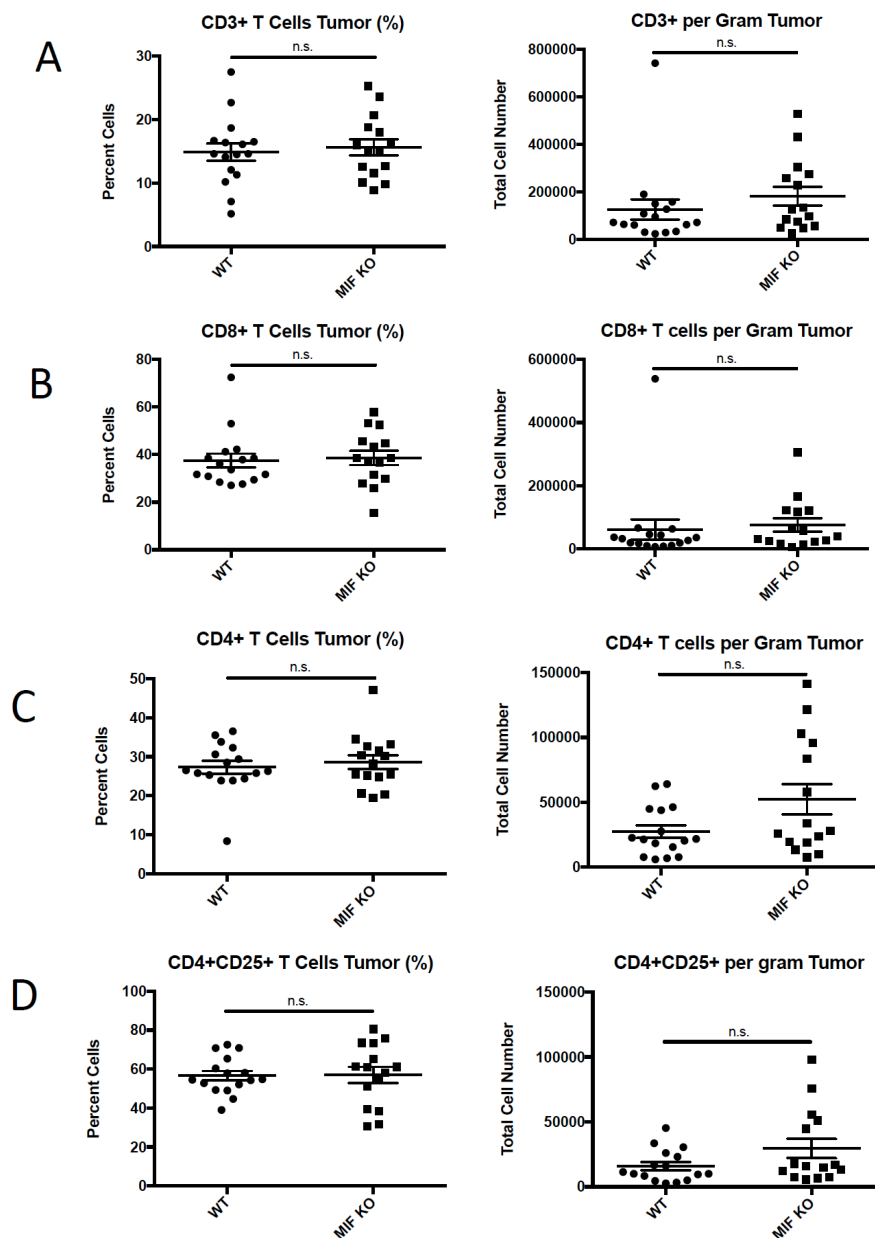


Figure 4.7: MIF expression does not affect intra-tumoral accumulation of T cells at 4 months. A-D, Tumors were digested and stained for T cell markers by flow cytometry, with all tumors >100mg being stained individually and all tumors from a mouse that were <100mg being combined and treated as one data point per mouse. n=4 for WT mice and n=4 for MIF KO mice. Student's t-test revealed no statistically significant differences.

Discussion

My results in the MMTV-PyMT murine model of breast cancer demonstrate a clear role for MIF in promotion of primary tumor growth. However, I did not observe an effect of MIF on spontaneous pulmonary metastasis in this model, nor did I identify an immune cell subset responsible for the primary tumor growth phenotype. Significantly more work will need to be done in this model to elucidate the mechanism by which MIF is promoting tumor growth (but not metastasis), either through an immune cell subset I have not detected yet, or through a tumor cell-intrinsic mechanism.

Seminal work in the MMTV-PyMT model by Lin *et al* strongly suggests that colony stimulating factor-1 (CSF-1) regulates metastasis in this model, but does not affect primary tumor growth (using a CSF-1 knockout model) (205). They also showed (using an overexpression system) that CSF-1 enhanced pulmonary metastasis and macrophage infiltration in the primary tumor, but had no effect on primary tumor growth overall (205). Another group studying the role of CXCR4 (a non-cognate MIF receptor) (36) in this model found that single-agent inhibition of CXCR4 reduced primary tumor growth, but did not significantly reduce metastasis, mimicking my results in MIF KO mice (206). However, when they combined CXCR4 inhibition with a VEGFR2 inhibitor, both primary tumor growth and pulmonary metastasis were significantly reduced (206). These studies and my data involving MIF further support that primary tumor growth and malignancy may be two separately regulated processes in this model. Given that this model more closely represents human disease progression, these studies also suggest that combination of MIF inhibition (or any other treatment that strongly inhibits primary

tumor growth) with another treatment modality like VEGFR2 inhibition may be better suited for treating both primary tumor growth and metastasis simultaneously.

Interestingly, while I did not see an overall difference in metastasis between WT and MIF KO tumor-bearing animals, I did detect an increase in accumulation of CD11b⁺ myeloid cells in the lungs of WT mice compared to MIF KO mice. This is similar to the findings by Lin *et al.*, in which CSF-1 modulation affected macrophage accumulation in the primary tumor, while having no effect on tumor growth itself (205). Based solely on CD11b as a marker, I do not know the specific type(s) of myeloid cells I am observing in the lungs, and the role they play, if any, in the metastatic process. While my data does not support a role for these cells in promoting metastasis, further examination of the myeloid population could shed more light on the mechanism by which MIF is promoting mammary tumor growth. Future studies will focus on immune phenotyping of lung-infiltrating myeloid cells at both early and late stages of tumor development by flow cytometry to elucidate if there is a particular myeloid subset that is more greatly represented in WT mice.

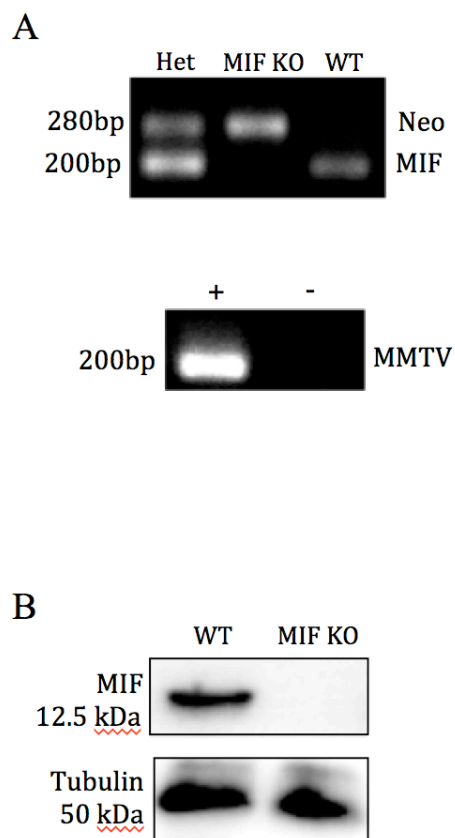
In my examination of the primary tumors of WT and MIF KO mice, I hypothesized that the difference in tumor growth may be due to the ability of MIF to promote accumulation of immunosuppressive MDSCs, as we have previously observed in the 4T1 model (32). I thoroughly screened tumors from WT and MIF KO MMTV-PyMT mice at various points during tumor growth, and found no significant differences in any of the myeloid (or lymphocyte) populations analyzed. This suggests that there is either a population(s) of

immune cells I did not detect that MIF is regulating to promote tumor growth, or that there is a tumor-intrinsic mechanism by which MIF is controlling tumor growth. (32,60,107,108,110,111,176). Future studies could utilize genetic methods to explore this (e.g. crossing our WT and MIF KO mice with various models of immune cell modulation, such as a Rag^{-/-} background), as well as performing antibody/cell depletion studies to determine if an intact immune response is necessary for our MIF-dependent tumor growth phenotype.

Based on the accumulating evidence in the literature using this model, I hypothesize that MIF is functioning through modulation of the immune system to control primary tumor growth. There is growing evidence for the role of tumor-associated macrophages (TAMs) in promoting both tumor growth and metastasis in the PyMT model. Boyle *et al.* has shown that CCR6 is responsible for maintaining TAMs in the mammary gland (207). DeNardo *et al.* reported that IL-4-secreting CD4⁺ T cells promote invasion and metastasis in this model through regulation of TAMs, which signal through EGFR to promote the invasiveness of mammary epithelial cells (208). Strachan *et al.* also found that CSF1R stimulation is required in this model for TAM turnover, and blockade of CSF1R decreases recruitment of new TAMs to the tumor microenvironment while simultaneously increasing CD8⁺ T cell recruitment (209). This body of work suggests that TAMs are a highly important immunosuppressive cell subset responsible for both primary tumor growth and metastasis. I postulate that MIF may play a role in regulating accumulation or turnover of these cells as well. My very basic analysis of macrophages in my studies, using only F4/80 as a marker, is not detailed enough to specifically detect

differences in this subset of macrophages. A more detailed analysis of macrophage subsets will need to be performed to assess if MIF is involved in macrophage accumulation or function in this model.

In conclusion, I have shown a clear role for MIF expression in primary tumor growth and progression in the MMTV-PyMT model. However, MIF expression does not control spontaneous pulmonary metastasis, accumulation of MDSCs, or overall myeloid cell numbers in the tumor microenvironment. It is still unclear if there are other myeloid (or general lymphocyte) populations that MIF is controlling, and further work will aim to uncover a subset(s) of cells MIF is regulating to promote tumor growth. Linking back to our previous work regarding MIF and immunogenic cell death (ICD) (33), I hypothesize that MIF expression could protect newly oncogenic tumor cells from undergoing cell death, which can elicit a strong anti-tumor immune response. Loss of MIF expression could promote cell death, therefore leading to a heightened anti-tumor immune response that I would expect to detect quite early during tumor development. Future studies will also aim to analyze DC activation as well as tumor cell death during the earliest phases of tumorigenesis to determine if a similar process is occurring in this model.



Supplementary Figure 4.1: Confirmation of MIF status in WT and MIF KO MMTV-PyMT mice. **A**, MIF gene deletion (top) and the MMTV-PyMT transgene (bottom) were detected by PCR. A MIF heterozygous mouse is shown as a control (top). **B**, MIF expression in WT and MIF KO mice was confirmed by immunoblot of lysate prepared from whole lung tissue.

Chapter 5: Discussion and Future Directions

The Role of MIF in Tumor Growth and Metastasis

Cumulatively, our work strongly supports a role for MIF in the promotion of tumor growth through modulation of the immunosuppressive microenvironment in the 4T1 model. We have shown that depletion of MIF expression in the 4T1 cell line leads to a reduction in primary tumor growth. This is consistent with previously published data using this model (32), as well as unpublished work in our laboratory in which depletion of MIF expression in a number of other cell lines also reduces primary tumor growth upon implant *in vivo*. I also show that global knock-out of MIF in the MMTV-PyMT murine model of breast cancer consistently leads to a delay in tumor occurrence, as well as decreased primary tumor burden throughout the time course of tumor progression. Importantly, I also demonstrate that increased primary tumor size, rather than expression of MIF in the primary tumor, dictates an increased abundance of pulmonary metastases. This is an important distinction, which is rarely made. However, it uncouples the role of MIF in primary tumor growth and metastasis. Further supporting this conclusion, we see no difference in overall metastasis in the lungs of WT versus MIF KO MMTV-PyMT mice. Upon further examination of the role of MIF in the metastatic process, I found that MIF expression in the primary tumor does not control the level of collagen crosslinking in the lungs during tumor progression, but may play a role in recruitment of myeloid cells during this process in both the 4T1 and MMTV-PyMT models. These results further support the role of MIF as an immune modulator during cancer progression, though in the setting of metastatic disease, this modulation may not directly affect disease outcomes.

MIF and ICD in the 4T1 model

The data presented in Chapter 2 suggest that MIF protects cancer cells from undergoing ICD under stressful culture conditions *in vitro*. However, the mechanism by which MIF is able to protect cells from undergoing ICD is still unknown. It will be important moving forward to dissect whether MIF is protecting from cell death in general, or if MIF is able to specifically suppress expression of the markers of ICD. Others have shown that execution of the ICD response requires both oxidative ER stress, as well as generation of reactive oxygen species (ROS) (125,210). When ER stress is experienced by a cancer cell, the three major ER stress sensors, inositol-requiring enzyme 1 alpha (IRE1a), protein kinase R-like ER kinase (PERK) and activating transcription factor 6 (ATF6) are activated, and the unfolded protein response (UPR) attempts to bring the cell back to homeostasis (211). However, if the level of ER stress is too great, the apoptotic signaling pathway is initiated downstream of PERK, driven by ATF4 and C/EBP homologous protein (CHOP) (212). This apoptotic ER stress response can lead to activation of signaling pathways that promote DAMP exposure, alerting the immune system to the presence of the dead and dying cell(s) (213). It is possible that MIF expression functions to protect cancer cells from responding to the chronic levels of ER stress necessary to induce ICD (115,214). To test this hypothesis, we could analyze the expression levels of proteins involved in the ER stress response in our WT versus MIF KD 4T1 cells under serum-free growth conditions. Increased expression of members of the ER stress pathway in MIF KD cells versus WT cells would suggest MIF expression protects cells from an increased ER stress response. If MIF expression does protect cells from initiating the chronic ER stress/UPR response, it would suggest that MIF is aiding in protection from

the apoptotic process brought about by cell stress, rather than having a direct involvement in the induction of ICD specifically. However, if no difference in the response to chronic ER stress is observed, this may suggest that MIF expression is functioning specifically to reduce expression of ICD markers downstream of the stress response.

One of the first events to occur under chronic ER stress is the translocation of calreticulin (CALR) to the cell surface (120,215). The exposure of CALR on the cell membrane is dependent on PERK-mediated phosphorylation of eIF2a, as well as activation of BAX/BAK via caspase-8 activation (216). Exposure of CALR on the surface of cancer cells undergoing ICD is required for DC-mediated phagocytosis of tumor material, and further activation of T cells (120). It will be important to determine if MIF expression is directly responsible for reduced exposure of CALR on the cell surface. This could be analyzed by monitoring eIF2a phosphorylation levels, BAX/BAK expression, and caspase-8 cleavage in WT and MIF KD 4T1 cells under serum starvation. Increased expression of these markers in MIF KD cells would suggest that MIF is directly suppressing exposure of CALR on the cell surface. One mechanism by which MIF could be controlling this pathway would be through upregulation of both PERK and the PI3k pathway, both of which are involved in the CALR exposure signaling pathway (123).

Similarly to CALR exposure, translocation of both HSP70 and HSP90 to the cell surface marks cells undergoing ICD (119,121,122). The mechanism by which these HSPs translocate to the cell surface is still unknown, but their ability to function as potent DAMPs has been reported (122,217). Both HSP70 and HSP90 have been shown to cross-

present tumor-derived peptides on MHC class I molecules, which leads to direct activation of anti-tumor CD8⁺ T cells (218–220). I have not yet analyzed HSP90 cell-surface expression in our WT and MIF KD 4T1 cells, but I hypothesize that MIF KD cells would show increased expression of HSP90 (similar to the result we see with HSP70).

Another essential marker of ICD induction we analyzed is secretion of ATP into the extracellular environment (124). As with CALR and HSP70 exposure, we found that MIF KD cells secrete more ATP than MIF-expressing cells under serum-free conditions. In the setting of ICD, ATP has been shown to bind purinergic receptors P₂X₇ and P₂Y₂, leading to secretion of IL-1beta and potent activation of an anti-tumor immune response (124,221). While we have confirmed that MIF KD cells demonstrate increased ATP secretion under serum-free conditions, we could also analyze IL-1beta expression in DCs from 4T1 tumor-bearing mice, with the hypothesis that we would see increased IL-1beta expression in DCs from MIF KD tumors when compared to MIF-expressing tumors. This would further support our hypothesis that loss of MIF expression under cell stress leads to enhanced ICD and downstream activation of an anti-tumor immune response.

Another important marker of ICD that we have not yet analyzed is secretion of the high mobility group 1 protein (HMGB1) into the extracellular environment, (222,223).

HMGB1 normally functions as a chromatin-binding protein involved in transcription (224), but once secreted, can bind to the receptor for advanced glycation endproducts (RAGE), and toll-like receptor 2 and 4 (TLR2/4) (225). Binding to these receptors on

DCs is critical for the activation of a tumor-specific T cell response (226,227). HMGB1 secretion into the extracellular environment can be analyzed via ELISA of cell supernatants from *in vitro* cultures. I hypothesize that we would see increased levels of HMGB1 in the supernatants of MIF KD cells cultured in serum-free culture conditions compared to WT cells, and this would further support our model in which loss of MIF expression in cell stress-inducing conditions leads to an enhanced ICD response.

Detection of ICD in vivo

While our studies strongly suggest that MIF expression in the 4T1 cell line protects cells from undergoing ICD *in vitro*, to date we have not confirmed this phenotype *in vivo*. We have supported this hypothesis by demonstrating that MIF KD tumors show enhanced DC and T cell infiltration and activation *in vivo*. However, detection of the markers of ICD *in vivo* has proven challenging. We hypothesize that the ICD response *in vivo* would occur within the first 2-3 days after tumor implant based on the timing we see in our *in vitro* studies (ICD is seen within 24-48 hours of serum starvation). It is extremely difficult to get enough tumor material out of the mammary fat pads this early, as we are only implanting 1×10^5 cells. It may be possible to analyze ICD *in vivo* by implanting a much larger number of tumor cells at the time of inoculation and analyzing the fat pads after 24-72 hours. That said, the absence of studies in the literature describing analysis of ICD markers *in vivo* suggests that this is a technically challenging issue to address, and further work in this field will hopefully result in better approaches to tackle this question.

The most well developed tool for detection of ICD *in vivo* to date is with vaccination experiments. This involves treating cancer cells *in vitro* with either ICD-inducing or non-ICD-inducing drugs, followed by vaccination of a mouse via injecting these dead/dying cells intraperitoneally or subcutaneously. This is followed by a re-challenge with the living version of the same cell line in a second tumor location of choice. If the cells used for vaccination were in fact undergoing ICD, the mouse will reject the re-challenge, as an anti-tumor immune response has been mounted through the initial vaccination. When the same cell line is treated *in vitro* using a non-ICD-inducing drug, the re-challenge will result in growth of a primary tumor at that site, as immunity was not initiated (123,162). It is possible that we could successfully vaccinate mice with 4T1 cells grown under serum-free conditions long enough to initiate cell death in the majority of cells. If MIF is in fact protecting cancer cells from undergoing ICD, I hypothesize that vaccination with MIF KD cells grown in serum-free media would lead to greater rejection of tumors upon re-challenge than vaccination with WT cells. Rejection of both WT and MIF KD tumors should be greater after vaccination with MIF KD tumors if a general immune response to the 4T1 cell line has been mounted.

MIF in combination with ICD inducers/non-inducers

As discussed in the introduction, others have determined that several classes of chemotherapeutics potentially induce an ICD response *in vitro*, including anthracyclines, mitoxantrone, cyclophosphamide, and oxaliplatin, while others such as mitomycin c and etoposide do not (120). It will be important to test the effect of MIF expression in cancer cell lines on the ICD response to treatment with both ICD-inducing and non-inducing

chemotherapies. We can utilize these previous studies to determine the optimal dosing range to induce ICD in our 4T1 cells, and then compare expression of the discussed ICD markers in WT versus MIF KD cells treated with each therapy. By comparing the effect of both ICD-inducing and non-inducing chemotherapies on WT and MIF KD cells, we can also further dissect if MIF is protecting cells from undergoing cell death in general, or from ICD specifically. If MIF expression does not protect cells from undergoing cell death upon treatment with non-ICD-inducing drugs, this would suggest that MIF is protecting cells specifically from undergoing ICD. However, if MIF protects cancer cells from undergoing cell death upon treatment with all chemotherapies tested, this would suggest that MIF is more generally protecting cancer cells from cell death. Early experiments would utilize the 4T1 cell line, as we have the most experience with the timing of ICD induction in this model, but expanding to other tumor cell lines would allow further analysis of the role of MIF in protection from cell death and the ICD response.

Role of CD4 versus CD8 T cells in tumor control in the 4T1 model

Our studies of the anti-tumor immune response in the 4T1 model show that, while there is an increase in abundance of only CD8 T cells (and not CD4 T cells) in MIF KD tumors, both CD8 and CD4 T cells isolated from these tumors are capable of producing more IFN γ upon *ex vivo* stimulation. Therefore, we hypothesized that both of these T cell subsets are important in the tumor control we observe in MIF KD tumors. In order to confirm the importance of T cells in the tumor control observed in mice with MIF KD tumors, we depleted both subsets of T cells simultaneously, rather than independently. It

will be important to further solidify this hypothesis by performing T cell depletion experiments in which CD8 and CD4 T cells are depleted independently in mice with WT or MIF KD tumors. I hypothesize that depletion of one T cell subset (but not both) will result in an intermediate phenotype, with some loss of growth control of MIF KD tumors, but not to the level seen in mice depleted of both T cell subsets simultaneously. Based on the increased abundance of CD8 T cells observed in MIF KD tumors, I hypothesize that depletion of this population will result in larger tumors than depletion of CD4 T cells, but that depletion of both subsets will be required in order to see growth restored to the level seen in mice with WT tumors.

MIF and the Metastatic Niche

My studies aimed at dissecting the role of MIF in metastasis led to the discovery that primary tumor size, rather than MIF expression, dictates overall pulmonary metastatic burden. When I generated MIF KD tumors comparable in size to MIF-expressing tumors by implanting a greater number of cells into the mammary fat pad, I found that the metastatic burden in the lungs of these mice was comparable to that in mice with MIF expressing tumors, and that primary tumor size correlated with metastatic burden. These data suggest that the decrease in metastatic burden we have observed previously in mice bearing MIF KD tumors is not necessarily due to loss of MIF expression directly, but rather indirectly, as a result of the reduction in primary tumor size following loss of MIF expression.

Concurrent with my studies of the effect of primary tumor size on metastatic burden, I was interested in determining if MIF expression in the primary tumor affected development of a pre-metastatic niche in the lungs. In these studies, I determined that MIF expression in the primary tumor has no effect on collagen crosslinking in the lung extracellular matrix (ECM), but does lead to an increase in myeloid cell accumulation that was independent of differences in primary tumor size. These observations in the lungs hold true at both early and late stages of tumor development. More detailed analysis of the myeloid cells in the lungs of early-stage tumor-bearing mice revealed no major differences in the MDSC subsets (or DCs) in the lungs. I did see a statistically significant increase in the $CD11b^+Ly6G^-Ly6C^+$ population in lungs of mice with MIF KD tumors compared to WT tumors, however the overall percentage of these cells among $CD45^+$ leukocytes in both groups was less than 8%. Given that we see a reduction in overall $CD11b^+$ myeloid cells in the lungs of MIF KD tumor-bearing mice by IF at both time points analyzed, I hypothesize that my current analysis strategy does not include the necessary markers to detect the myeloid cell population(s) accounting for the overall difference in $CD11b^+$ cell abundance in the lungs of mice bearing WT versus MIF KD tumors. More detailed dissection of the myeloid compartment (including macrophage and dendritic cell subsets as a starting point) will need to be performed. However, based on the observation that tumor size (and not MIF expression directly) dictates overall metastatic burden, I hypothesize that the myeloid cell population(s) that are increased in abundance in mice with WT tumors are not affecting overall metastatic burden. Therefore, I would not expect to see any differences in the ability of myeloid cells from

the lungs of WT versus MIF KD tumor-bearing mice to inhibit anti-tumor immune cell function.

Further analysis of the role of MIF on matrix remodeling in the metastatic niche

While I did not see an effect of MIF expression on the amount of collagen crosslinking found in the lungs of mice bearing 4T1 tumors at any time point analyzed, I have not ruled out the possibility that MIF expression in the primary tumor may affect matrix remodeling through other mechanisms. Increased fibronectin expression has been shown to be important for the migration and adherence of VEGFR1⁺ cells from the bone marrow to the lungs in a mouse model of lung metastasis (130). Much like my analysis of collagen crosslinking, fibronectin deposition in the lungs can be analyzed using immunofluorescent staining of frozen lung sections. Because fibronectin deposition in the lungs has been shown to increase accumulation of BMDCs at that location, I hypothesize that MIF expression in the primary tumor may enhance fibronectin expression in the lungs, which could be responsible for the increase in CD11b⁺ cells I observe in the lungs. Increased hyaluronan expression is another ECM factor that has been linked to increased metastasis in breast cancer (228–230). Hyaluronan binds to its cell surface receptor CD44, and this activity has been shown to decrease apoptosis and enhance invasiveness of cancer cells (228,231). Hyaluronan expression in the lungs can be analyzed using immunohistochemical techniques, allowing for analysis of all discussed ECM components in the same lung tissue using serial sectioning. I hypothesize that MIF expression in the primary tumor would not lead to increased hyaluronan expression in the

lungs due to the lack of effect of MIF expression on metastasis observed in the 4T1 model.

Role of MIF in Tumor Progression in the MMTV-PyMT Model

To date, I have shown that a global knockout of MIF expression in the MMTV-PyMT model leads to a delay in development of mammary tumors, as well as reduced overall tumor burden at both 8 weeks and 5 months. I have also shown that MIF expression in this model does not affect the presence of late-stage lung metastases. Consistent with my findings in the 4T1 model, MIF expression does not affect overall collagen crosslinking in the lungs of the MMTV-PyMT model, but does lead to increased accumulation of CD11b⁺ myeloid cells in the lungs (which seems to have no effect on overall metastatic burden in either model). Analysis of the myeloid compartment for MDSCs, macrophages, and DCs at both 4 and 5 months revealed no differences in abundance of any cell subset between WT and MIF KO mice.

Further dissection of immune cell subsets in WT and MIF KO MMTV-PyMT tumors

I initially hypothesized that the difference in tumor growth between WT and MIF KO mice in this model was due to differences in intratumoral MDSC accumulation as seen in the 4T1 model. However, upon detailed analysis of total MDSCs, as well as the mono- and PMN-MDSC subsets at both 4 and 5 months (chosen based on similarity in tumor size to late-stage tumors in the 4T1 model), I consistently found no difference in MDSCs between WT and MIF KO tumors at either time point. I also segregated tumors based on

weight (small, medium, or large) at 5 months, and did not see any differences in MDSCs between WT and MIF KO mice in any one tumor size category. Further analysis of general DC (CD11c⁺) and macrophage (F4/80⁺) accumulation in WT versus MIF KO tumors again revealed no differences between groups. Together, these data suggest that there is either no effect of MIF expression on myeloid cell accumulation in the primary tumors in this model, or I am missing an important subpopulation with my more generalized myeloid cell analysis.

While no differences in cell abundance were seen in the MDSC subpopulations analyzed in this model, I have not assessed their suppressive activity *ex vivo*. In the 4T1 model, we found that MIF-expressing tumors had both increased mono-MDSC accumulation, and that MDSCs isolated from MIF-expressing tumors had greater suppressive activity on T cell proliferation when compared to MDSCs from MIF-depleted tumors (32). We may discover that MDSCs sorted from WT MMTV-PyMT mice similarly show an increased T cell suppressive function when compared to MDSCs from MIF KO mice. This result would at least partially explain the difference in tumor growth I have observed between WT and MIF KO mice in this model.

Additional studies focusing on the macrophage compartment in this model may also reveal differences between WT and MIF KO mice. Tumor-associated macrophages (TAMs) have been shown to be an important myeloid cell subset involved in promoting tumor progression (232–234). This population of cells is also referred to as “M2-like”, or “alternatively activated”, macrophages and is distinct from classical “M1-like”

macrophages (234,235). TAMs are a subset of macrophages that display tumor-promoting characteristics, such as poor antigen presentation and secretion of the immunosuppressive molecules IL-10, TGFbeta, and prostaglandins (236–239). TAMs originate from circulating monocytes, which are recruited to tumor tissue where they differentiate into bona fide TAMs (240). Fully differentiated TAMs are characterized in mice as CD11b^{low}CD11c⁺MHCII⁺Ly6C⁻VCAM⁺ (240). I will need to expand my immunophenotyping panel to accommodate these markers in order to assess if MIF expression promotes accumulation of TAMs in the MMTV-PyMT model.

If I do detect differences in TAM accumulation when comparing WT and MIF KO tumors, further analysis of the immunosuppressive function of these cells will be important to confirm their effect on T cell function and tumor growth control. By flow sorting or using magnetic separation techniques to isolate these cells from WT and MIF KO tumors, I can acquire a relatively pure population. The sorted TAMs can then be cultured with activated T cells *in vitro* to assess their ability to inhibit T cell proliferation and cytokine production. Work by Yaddanapudi *et al.* suggests that macrophage-derived MIF may in fact drive TAM differentiation in a mouse model of melanoma. Macrophages derived from WT (MIF-expressing) mice show an enhanced TAM/M2-like phenotype compared to MIF KO mice, and the WT TAMs also possess an increased ability to suppress T cell proliferation compared to MIF KO TAMs (241). This work suggests that it may not be solely MIF expression in the primary tumor that is important in modulating the immunosuppressive microenvironment. It will be important for future studies in our MMTV-PyMT mice to deconvolute the role of tumor-derived MIF from MIF expression

in other cell types. We can utilize the Cre-LoxP system to generate tumor cell-specific MIF knockout mice (MIF^{fl/fl} crossed with MMTV-Cre) or a myeloid/macrophage specific MIF knockout (MIF^{fl/fl} crossed with LysM-Cre or F4/80-Cre, among other options). Analysis of tumor growth in these mice would begin to shed light on whether MIF derived from the tumor cells, myeloid cells, or both cell types are important to the tumor growth phenotype observed in global MIF KO mice.

Analysis of ICD/anti-tumor immunity in the MMTV-PyMT model

Interestingly, I observed a difference in fat pad weight between WT and MIF KO mice at 8 weeks, before palpable tumor masses were present at those sites. I hypothesize that there is an increased cellularity in the WT fat pads at this time point, which may be indicative of increased tumor material not yet palpable or visible by eye. Analysis of these fat pads histologically (utilizing H&E and cytokeratin stains, along with the help of a well-trained pathologist) will help determine if there is in fact enhanced tumorigenesis occurring in the early WT fat pads. This hypothesis is supported by the early difference in tumor growth we observe in the 4T1 model when comparing MIF-expressing and MIF-depleted tumors. Based on our analysis in the 4T1 model, I hypothesize that the early difference in tumor size observed is due to increased ICD in implanted MIF KD tumors compared to WT tumors. The increase in ICD leads to an enhanced DC/T cell activation phenotype in these tumors, resulting in greater tumor control over the course of tumor growth. It will be important to determine if this phenomenon is observed in the MMTV-PyMT model. Analysis of the fat pads from WT and MIF KO mice around the 8-week time point (where I hypothesize the initial difference in tumor size is occurring) for DC

and T cell accumulation/activation will begin to reveal if a similar phenomenon is occurring in this model. I hypothesize that I would observe an increase in both DC and T cell activation in immune cells *ex vivo* from MIF KO mice compared to WT mice. It may also be possible to recover enough tumor material from the early fat pads in this model to analyze markers of ICD on WT versus MIF KO tumor cells by flow cytometry. Here, I hypothesize that I would see increased markers of ICD on tumor cells from MIF KO mice compared to WT mice. Similarly, an assay for detection of ICD in histological sections of tumors would be informative in both models. However, to the best of our knowledge, no such assay exists to date.

MIF, metastasis, and the metastatic niche in the MMTV-PyMT model

My analysis of the lung metastatic niche in the MMTV-PyMT model further supported the results I observed in the 4T1 model. MIF expression in the MMTV-PyMT model did not affect collagen crosslinking in the lungs of late-stage tumor bearing mice, but did lead to an increased accumulation of total CD11b⁺ myeloid cells. Also similar to the results found in the 4T1 model, I observed no effect of MIF expression on total lung metastatic burden at a late point in tumor development (5 months). However, unlike in the 4T1 model, I saw no effect of MIF expression on overall metastasis even though I did observe increased total tumor burden in WT mice. Because of the very late time point at which I have analyzed lung metastatic burden, I may be missing a window during which MIF KO mice show reduced metastasis compared to WT mice, but once the tumors start to reach their maximum allowable size, the difference disappears due to an overwhelming amount of tumor material, leading to significant metastasis in the lungs. I could further dissect the

role of MIF in metastasis in the model by measuring metastasis by qRT-PCR or histological techniques earlier during tumor development. However, it is possible that MIF expression does not play a role in metastasis during any point of tumor development. Other groups have shown that factors such as CXCR4 and CSF-1 play a role in primary tumor development or metastasis, but not both (36,205). Detailed analysis of both overall metastasis as well as features of the metastatic niche (discussed previously) throughout the course of tumor progression will be important in determining if MIF plays a role in metastasis in this model.

MIF as a cell survival factor and translational implications

The cumulative support in the literature, and in the studies conducted by our laboratory, strongly suggests that MIF is involved in promoting the process of cancer development through supporting cell survival. MIF has been shown in multiple non-cancerous cell types (including neural progenitor cells, fibroblasts, and B cells) to signal via CD74 to the downstream PI3K/AKT and MAPK pathways, which promote survival and proliferation (242-244). The ability of MIF to signal through these same pathways resulting in increased survival has been observed in cancer cell lines as well (52, 201, 245), suggesting that cancer cells may have hijacked this important normal function of MIF to enhance their survival (52, 201, 245). Combined with the data supporting MIF's ability to inhibit accumulation of p53 (9,53), it would appear advantageous for tumor cells to overexpress MIF. The addition of my studies suggesting that MIF also protects cancer cells from undergoing ICD in the 4T1 model adds another layer of complexity to the mechanism by which MIF promotes cell survival.

My studies also revealed several discrepant observations when comparing the 4T1 and MMTV-PyMT models. In the MMTV-PyMT model, no difference in lung metastasis is observed regardless of the difference in primary tumor size observed between WT and MIF KO mice. However, in the 4T1 model, mice bearing smaller, MIF KD tumors exhibit a decreased lung metastatic burden. We also observe a decreased accumulation of mono-MDSCs in MIF KD tumors in the 4T1 model, while this phenotype is not observed when comparing WT and MIF KO tumors in the MMTV-PyMT model. The implantable nature of the 4T1 model, when compared with the spontaneously arising MMTV-PyMT model, may explain the observed difference in immune activation based on MIF expression. Implantation of tumor cells to the mammary fat pad is likely more immunogenic than a tumor arising from the tissue itself, leading to the enhanced immune activation I observe in the 4T1 model. We did not observe evidence of an enhanced immune response to MIF KO tumors in the MMTV-PyMT model, suggesting this is not the mechanism by which MIF is controlling tumor growth in this model. I hypothesize that the role of MIF as a cancer cell survival factor is the dominant function of MIF in this model, and that loss of MIF expression in the tumor cells results in an overall decreased ability of the tumor cells to survive and proliferate. This would result in smaller tumors, independent of a role for the immune response. To test this hypothesis, we would need to generate WT and MIF KO cell lines derived from the tumors in this model, and analyze their ability to survive *in vitro* by assessing their apoptotic and proliferative characteristics in culture. However, if we do not observe differences in intrinsic tumor cell survival between WT and MIF KO cells derived from tumors in this model, it is also still possible that the increased tumor control observed in MIF KO mice

is due to a more activated immune response. We have not assessed T cell activation status in this model, so while there are no differences in T cell numbers, they could be more functional in a MIF KO mouse. We could test this hypothesis by analyzing T cell activation status (IFN γ , CD44 and CD25 expression at the least), and also by depleting T cells in this model. If T cells are responsible for providing tumor control in the MIF KO mice, T cell depletion would result in increased tumor growth to the level observed in a WT mouse.

As discussed previously, development of a clinical MIF inhibitor has been unsuccessful to date. However, based on the discussion of MIF and its role in cancer provided here, there is clearly an unmet need for a potent inhibitor to progress to the clinical setting. Blockade of a critical cancer cell survival factor like MIF, which may simultaneously result in enhancement of the anti-tumor immune response, is a compelling combination. Coupled with immunotherapeutic modalities already in the clinic (such as anti-PD1-1), MIF inhibition could result in robust and lasting responses. However, given that MIF is not the only survival factor used by cancer cells, resistance would likely arise through dependence on other factors with subsequent loss of therapeutic efficacy.

MIF expression has been implicated as a potential biomarker for an aggressive disease course and poor prognosis for the patient. Our work suggests that MIF could potentially also serve as a biomarker for a tumor with a dampened anti-tumor immune response. Therefore, addition of MIF expression to the screening process for patients undergoing a cancer diagnosis and staging could provide valuable insight into which treatment options

might be most beneficial for the patient. I hypothesize that increased MIF expression in either the patient's serum or primary tumor (if a biopsy is taken) would suggest that that patient will experience an impaired anti-tumor immune response, and would not respond as well to treatment with an anti-PD-1/PD-L1 therapy (or other immunotherapies) as someone with low MIF expression. This would argue for combining T cell activating immunotherapy with other methods of immune activation (or a MIF inhibitor if one becomes available) to provide the patient with a greater chance of mounting a robust immune response to the tumor.

Most of the technical issues associated with progression of MIF inhibitors to the clinic have been due to undesirable off-target effects and toxicities once a potential inhibitor is tested *in vivo*. Because MIF expression is observed in a variety of cell types, MIF inhibition may be resulting in decreased survival in "normal" cell types, leading to toxicities in other organs (3-7). One potential avenue moving forward could be developing a method to deliver a MIF inhibitor specifically to the target tissue, like a tumor in the setting of solid cancers. Liposomal encapsulation of a MIF inhibitor could provide a safer mechanism to deliver the inhibitor to the tumor (by targeting the liposome to a tumor-specific cell-surface marker, such as HER2 in breast cancer, for example).

Our studies implicate MIF expression in multiple aspects of tumor progression. Early during tumor development, MIF functions by increasing cancer cell survival, resulting in impaired development of the anti-tumor immune response initiated by dying cancer cells. In late-stage tumors, MIF modulates the immunosuppressive microenvironment through

increased accumulation of MDSCs, leading to dampened T cell activation in the tumor.

All of these factors suggest that treatment of a cancer patient with a MIF inhibitor could be beneficial either at the earliest time of detection or in patients who are diagnosed with late-stage disease that may not have as many treatment options available to them.

References

1. Bloom BR, Bennett B. Mechanism of a Reaction in Vitro Associated with Delayed-Type Hypersensitivity. *Science*. 1966;153:80 LP-82.
2. David J. Delayed Hypersensitivity in Vitro: Its Mediation By Cell-Free Substances Formed By Lymphoid Cell-Antigen Interaction. *Pathology*. 1966;72-7.
3. Rossi AG, Haslett C, Hirani N, Greening AP, Rahman I, Metz CN, *et al*. Human circulating eosinophils secrete macrophage migration inhibitory factor (MIF): Potential role in asthma. *J Clin Invest*. 1998;101(12):2869-74.
4. Bacher M, Metz CN, Calandra T, Mayer K, Chesney J, Lohoff M, *et al*. An essential regulatory role for macrophage migration inhibitory factor in T-cell activation. *Proc Natl Acad Sci U S A*. 1996;93(15):7849-54.
5. Bernhagen J, Mitchell RA, Calandra T, Voelter W, Cerami A, Bucala R. Purification, Bioactivity, and Secondary Structure Analysis of Mouse and Human Macrophage Migration Inhibitory Factor (MIF). *Biochemistry*. 1994;33(47):14144-55.
6. Imamura K, Nishihira J, Suzuki M, Yasuda K, Sasaki S, Kusunoki Y, *et al*. Identification and immunohistochemical localization of macrophage migration inhibitory factor in human kidney. *Biochem Mol Biol Int*. 1996;40(6):1211-9.
7. Nishihira J, Koyama Y, Mizue Y. Identification of macrophage migration inhibitory factor (MIF) in human vascular endothelial cells and its induction by lipopolysaccharide. *Cytokine*. 1998;10(3):199-205.
8. Fingerle-Rowson GR, Bucala R. Neuroendocrine properties of macrophage migration inhibitory factor (MIF). *Immunol Cell Biol*. 2001;79:368-75.
9. Mitchell RA, Liao H, Chesney J, Fingerle-Rowson G, Baugh J, David J, *et al*. Macrophage migration inhibitory factor (MIF) sustains macrophage proinflammatory function by inhibiting p53: Regulatory role in the innate immune response. *Proc Natl Acad Sci*. 2002;99(1):345-50.
10. Gregersen PK, Bucala R. Macrophage migration inhibitory factor, MIF alleles, and the genetics of inflammatory disorders: Incorporating disease outcome into the definition of phenotype. *Arthritis Rheum*. 2003;48(5):1171-6.
11. Donn RP, Ray DW. Macrophage migration inhibitory factor: Molecular, cellular and genetic aspects of a key neuroendocrine molecule. *J Endocrinol*. 2004;182(1):1-9.
12. Calandra T, Roger T. Macrophage migration inhibitory factor: a regulator of innate immunity. *Nat Rev Immunol*. 2003;3(10):791-800.
13. Calandra T, Bernhagen J, Metz CN, Spiegel LA, Bacher M, Donnelly T, *et al*. MIF as a glucocorticoid-induced modulator of cytokine production. *Nature*. 1995;337(6544):68-71.
14. Calandra T, Echtenacher B, Roy DL, Pugin J, Metz CN, Hültner L, *et al*. Protection from septic shock by neutralization of macrophage migration inhibitory factor. *Nat Med*. 2000;6(2):164-70.
15. Mikulowska A, Metz CN, Bucala R, Holmdahl R. Macrophage migration inhibitory factor is involved in the pathogenesis of collagen type II-induced

- arthritis in mice. *J Immunol.* 1997;158(11).
16. Leech M, Metz C, Santos L, Peng T, Holdsworth SR, Bucala R, *et al.* Involvement of macrophage migration inhibitory factor in the evolution of rat adjuvant arthritis. *Arthritis Rheum.* 1998;41(5):910–7.
 17. Jong YP, Abadia-Molina a C, Satoskar a R, Clarke K, Rietdijk ST, Faubion W a, *et al.* Development of chronic colitis is dependent on the cytokine MIF. *Nat Immunol.* 2001;2(11):1061–6.
 18. Lin SG, Yu XY, Chen YX, Huang XR, Metz C, Bucala R, *et al.* De novo expression of macrophage migration inhibitory factor in atherogenesis in rabbits. *Circ Res.* 2000;87(12):1202–8.
 19. Dayawansa NH, Gao X-M, White DA, Dart AM, Du X-J. Role of MIF in myocardial ischaemia and infarction: insight from recent clinical and experimental findings. *Clin Sci.* 2014;127(3):149–61
 20. Yamaguchi E, Nishihira J, Shimizu T, Takahashi T, Kitashiro N, Hizawa N, *et al.* Macrophage migration inhibitory factor (MIF) in bronchial asthma. *Clin Exp allergy.* 2000;30(9):1244–9.
 21. Conroy H, Mawhinney L, Donnelly SC. Inflammation and cancer: macrophage migration inhibitory factor (MIF)--the potential missing link. *QJM.* 2010 Nov;103(11):831–6.
 22. Kleemann R, Kapurniotu A, Frank RW, Gessner A, Mischke R, Flieger O, *et al.* Disulfide analysis reveals a role for macrophage migration inhibitory factor (MIF) as thiol-protein oxidoreductase. *J Mol Biol.* 1998;280(1):85–102.
 23. Rosengren E, Åman P, Thelin S, Hansson C, Ahlfors S, Björk P, *et al.* The macrophage migration inhibitory factor MIF is a phenylpyruvate tautomerase. *FEBS Lett.* 1997;417(1):85–8.
 24. Rosengren E, Bucala R, Aman P, Jacobsson L, Odh G, Metz CN, *et al.* The immunoregulatory mediator macrophage migration inhibitory factor (MIF) catalyzes a tautomerization reaction. *Mol Med.* 1996 Jan;2(1):143–9.
 25. Hermanowski-Vosatka A, Mundt SS, Ayala JM, Goyal S, Hanlon WA, Czerwinski RM, *et al.* Enzymatically inactive macrophage migration inhibitory factor inhibits monocyte chemotaxis and random migration. *Biochemistry.* 1999;38(39):12841–9.
 26. Dickerhof N, Schindler L, Bernhagen J, Kettle AJ, Hampton MB. Macrophage migration inhibitory factor (MIF) is rendered enzymatically inactive by myeloperoxidase-derived oxidants but retains its immunomodulatory function. *Free Radic Biol Med.* Elsevier; 2015;89:498–511.
 27. Lubetsky JB. The Tautomerase Active Site of Macrophage Migration Inhibitory Factor Is a Potential Target for Discovery of Novel Anti-inflammatory Agents. *J Biol Chem.* 2002;277(28):24976–82.
 28. Bendrat K, Al-Abed Y, Callaway DJE, Peng T, Calandra T, Metz CN, *et al.* Biochemical and mutational investigations of the enzymatic activity of macrophage migration inhibitory factor. *Biochemistry.* 1997;36(49):15356–62.
 29. Winner M, Meier J, Zierow S, Rendon BE, Crichlow G V., Riggs R, *et al.* A novel, macrophage migration inhibitory factor suicide substrate inhibits motility and growth of lung cancer cells. *Cancer Res.* 2008;68(18):7253–7.
 30. Onodera S., Kaneda K., Mizue Y., Koyama Y., Fujinaga M., Nishihira J. Macrophage migration inhibitory factor up-regulates expression of matrix

- metalloproteinases in synovial fibroblasts of rheumatoid arthritis. *J Biol Chem.* 2010;1(275):444–50.
31. Al-Abed Y, Dabideen D, Aljabari B, Valster A, Messmer D, Ochani M, *et al.* ISO-1 binding to the tautomerase active site of MIF inhibits its pro-inflammatory activity and increases survival in severe sepsis. *J Biol Chem.* 2005;280(44):36541–4.
 32. Simpson KD, Templeton DJ, Cross J V. Macrophage migration inhibitory factor promotes tumor growth and metastasis by inducing myeloid-derived suppressor cells in the tumor microenvironment. *J Immunol.* 2012;189(12):5533–40.
 33. Balogh KN, Templeton DJ, Cross J V. Macrophage Migration Inhibitory Factor protects cancer cells from immunogenic cell death and impairs anti-tumor immune responses. *PLoS One.* 2018;1–20.
 34. Leng L, Metz CN, Fang Y, Xu J, Donnelly S, Baugh J, *et al.* MIF Signal Transduction Initiated by Binding to CD74. *J Exp Med.* 2003;197(11):1467–76. Available from: <http://www.jem.org/lookup/doi/10.1084/jem.20030286>
 35. Shi X, Wang T, Wang W, Du X, Li J, McDonald C, *et al.* CD44 is the signaling component of the macrophage migration inhibitory factor-CD74 receptor complex. *Dev Psychobiol.* 2013;55(5):539–50.
 36. Bernhagen J, Krohn R, Lue H, Gregory JL, Zernecke A, Koenen RR, *et al.* MIF is a noncognate ligand of CXC chemokine receptors in inflammatory and atherogenic cell recruitment. *Nat Med.* 2007;13(5):587–96.
 37. Lacy M, Kontos C, Brandhofer M, Hille K, Gröning S, Sinitski D, *et al.* Identification of an Arg-Leu-Arg tripeptide that contributes to the binding interface between the cytokine MIF and the chemokine receptor CXCR4. *Sci Rep.* 2018;8(1):1–17.
 38. Tarnowski M, Grymula K, Liu R, Tarnowska J, Drukala J, Ratajczak J, *et al.* Macrophage Migration Inhibitory Factor Is Secreted by Rhabdomyosarcoma Cells, Modulates Tumor Metastasis by Binding to CXCR4 and CXCR7 Receptors and Inhibits Recruitment of Cancer-Associated Fibroblasts. *Mol Cancer Res.* 2010;8(10):1328–43.
 39. Zhang X, Bucala R. Inhibition of macrophage migration inhibitory factor (MIF) tautomerase activity by dopachrome analogs. *Bioorg Med Chem Lett.* 1999;9(22):3193–8.
 40. Garai J, Lorand T. Macrophage Migration Inhibitory Factor (MIF) Tautomerase Inhibitors as Potential Novel Anti-Inflammatory Agents: Current Developments. *Curr Med Chem.* 2009;16(9):1091–114.
 41. Cross J V, Rady JM, Jr FWF, Lyons C, Timothy L, Templeton DJ. Nutrient Isothiocyanates Covalently Modify and Inhibit the Inflammatory Cytokine Macrophage Migration Inhibitory Factor (MIF). *Biochem J.* 2010;423(3):315–21.
 42. Bai F, Asojo OA, Cirillo P, Ciustea M, Ledizet M, Aristoff PA, *et al.* A novel allosteric inhibitor of macrophage migration inhibitory factor (MIF). *J Biol Chem.* 2012;287(36):30653–63.
 43. Schinagl A, Thiele M, Douillard P, Volkel D, Kenner L, Kazemi Z, *et al.* Oxidized macrophage migration inhibitory factor is a potential new tissue marker and drug target in cancer. *Oncotarget.* 2016;7(45):73486-73496.
 44. Guo P, Wang J, Liu J, Xia M, Li W. Macrophage immigration inhibitory factor

- promotes cell proliferation and inhibits apoptosis of cervical adenocarcinoma. *Tumor Biol.* 2015;5095–102.
45. He X-X, Yang J, Ding Y-W, Liu W, Shen Q-Y, Xia HH-X. Increased epithelial and serum expression of macrophage migration inhibitory factor (MIF) in gastric cancer: potential role of MIF in gastric carcinogenesis. *Gut.* 2006;55(6):797–802.
 46. Kamimura a, Kamachi M, Nishihira J, Ogura S, Isobe H, Dosaka-Akita H, *et al.* Intracellular distribution of macrophage migration inhibitory factor predicts the prognosis of patients with adenocarcinoma of the lung. *Cancer.* 2000;89(2):334–41.
 47. White ES, Flaherty KR, Carskadon S, Brant A, Iannettoni MD, Yee J, *et al.* Macrophage Migration Inhibitory Factor and CXC Chemokine Expression in Non-Small Cell Lung Cancer: Role in Angiogenesis and Prognosis. *Clin Cancer Res.* 2003;9(February):853–60.
 48. Hagemann T, Robinson SC, Thompson RG, Charles K, Kulbe H, Balkwill FR. Ovarian cancer cell-derived migration inhibitory factor enhances tumor growth, progression, and angiogenesis. *Mol Cancer Ther.* 2007;6(7):1993–2002.
 49. He X-X, Chen K, Yang J, Li X-Y, Gan H-Y, Liu C-Y, *et al.* Macrophage migration inhibitory factor promotes colorectal cancer. *Mol Med.* 2009;15(1–2):1–10.
 50. Hira E, Ono T, Dhar DK, El-Assal ON, Hishikawa Y, Yamanoi A, *et al.* Overexpression of macrophage migration inhibitory factor induces angiogenesis and deteriorates prognosis after radical resection for hepatocellular carcinoma. *Cancer.* 2001;103(3):588–98.
 51. Funamizu N, Hu C, Lacy C, Schetter A, Zhang G, He P, *et al.* Macrophage migration inhibitory factor induces epithelial to mesenchymal transition, enhances tumor aggressiveness and predicts clinical outcome in resected pancreatic ductal adenocarcinoma. *Int J Cancer.* 2013;132(4):785–94.
 52. Wang C, Zhou X, Li W, Li M, Tu T, Ba X, *et al.* Macrophage migration inhibitory factor promotes osteosarcoma growth and lung metastasis through activating the RAS / MAPK pathway. *Cancer Lett. Elsevier Ltd;* 2017;403:271–9.
 53. Hudson JD, Shoaibi M a, Maestro R, Carnero a, Hannon GJ, Beach DH. A proinflammatory cytokine inhibits p53 tumor suppressor activity. *J Exp Med.* 1999;190(10):1375–82.
 54. Xu X, Wang B, Ye C, Yao C, Lin Y, Huang X, *et al.* Overexpression of macrophage migration inhibitory factor induces angiogenesis in human breast cancer. *Cancer Lett.* 2008;261(2):147–57.
 55. Bando H, Matsumoto G, Bando M, Muta M, Ogawa T, Funata N, *et al.* Expression of macrophage migration inhibitory factor in human breast cancer: association with nodal spread. *Jpn J Cancer Res.* 2002 Apr;93(4):389–96.
 56. Winner M, Koong AC, Rendon BE, Zundel W, Mitchell RA. Amplification of Tumor Hypoxic Responses by Macrophage Migration Inhibitory Factor – Dependent Hypoxia-Inducible Factor Stabilization. *Cancer Res.* 2007;(1):186–93.
 57. Ren Y, Tsui H-T, Poon RT-P, Ng IO-L, Li Z, Chen Y, *et al.* Macrophage migration inhibitory factor: roles in regulating tumor cell migration and expression of angiogenic factors in hepatocellular carcinoma. *Int J Cancer.* 2003;107(1):22–9.
 58. Baugh JA, Gantier M, Li L, Byrne A, Buckley A, Donnelly SC. Dual regulation of

- macrophage migration inhibitory factor (MIF) expression in hypoxia by CREB and HIF-1. *Biochem Biophys Res Commun.* 2006;347(4):895–903.
59. Koong AC, Denko NC, Hudson KM, Schindler C, Swiersz L, Koch C, *et al.* Candidate Genes for the Hypoxic Tumor Phenotype Candidate Genes for the Hypoxic Tumor Phenotype 1. *Cancer Res.* 2000;60(4):883–7.
 60. Lv W, Chen N, Lin Y, Ma H, Ruan Y, Li Z, *et al.* Macrophage migration inhibitory factor promotes breast cancer metastasis via activation of HMGB1/TLR4/NF kappa B axis. *Cancer Lett. Elsevier Ireland Ltd;* 2016;375(2):245–55.
 61. Dessein AF, Stechly L, Jonckheere N, Dumont P, Monté D, Leteurtre E, *et al.* Autocrine induction of invasive and metastatic phenotypes by the MIF-CXCR4 axis in drug-resistant human colon cancer cells. *Cancer Res.* 2010;70(11):4644–54.
 62. Costa-Silva B, Aiello NM, Ocean AJ, Singh S, Zhang H, Thakur BK, *et al.* Pancreatic cancer exosomes initiate pre-metastatic niche formation in the liver. *Nat Cell Biol.* 2015;17(6):816-26.
 63. Dunn GP, Bruce AT, Ikeda H, Old LJ, Schreiber RD. Cancer immunoeediting: From immunosurveillance to tumor escape. *Nat Immunol.* 2002;3(11):991–8.
 64. Burkholder B, Huang RY, Burgess R, Luo S, Jones VS, Zhang W, *et al.* Tumor-induced perturbations of cytokines and immune cell networks. *Biochim Biophys Acta - Rev Cancer.* 2014;1845(2):182–201.
 65. Ha T-Y. The Role of Regulatory T Cells in Cancer. *Immune Netw.* 2009;9(6):209.
 66. Solinas G, Schiarea S, Liguori M, Fabbri M, Pesce S, Zammataro L, *et al.* Tumor-Conditioned Macrophages Secrete Migration-Stimulating Factor: A New Marker for M2-Polarization, Influencing Tumor Cell Motility. *J Immunol.* 2010;185(1):642–52.
 67. Gabrilovich DI, Nagaraj S. Myeloid-derived suppressor cells as regulators of the immune system. *Nat Rev Immunol.* 2009;9(3):162–74.
 68. Dong H, Strome SE, Salomao DR, Tamura H, Hirano F, Flies DB, *et al.* Tumor-associated B7-H1 promotes T-cell apoptosis: A potential mechanism of immune evasion. *Nat Med.* 2002;8(8):793–800.
 69. Nishimura H, Nose M, Hiai H, Minato N, Honjo T. Development of lupus-like autoimmune diseases by disruption of the PD-1 gene encoding an ITIM motif-carrying immunoreceptor. *Immunity.* 1999;11(2):141–51.
 70. Butte MJ, Keir ME, Phamduy TB, Sharpe AH, Freeman GJ. Programmed Death-1 Ligand 1 Interacts Specifically with the B7-1 Costimulatory Molecule to Inhibit T Cell Responses. *Immunity.* 2007;27(1):111–22.
 71. Francisco LM, Salinas VH, Brown KE, Vanguri VK, Freeman GJ, Kuchroo VK, *et al.* PD-L1 regulates the development, maintenance, and function of induced regulatory T cells. *J Exp Med.* 2009;206(13):3015–29.
 72. Chen L, Han X. Anti-PD-1/PD-L1 therapy of human cancer : past, present, and future. *J Clin Invest.* 2015;125(9):3384–91.
 73. Cripps, James G.; Gorham JD. MDSC in Autoimmunity. *Int Immunopharmacol.* 2011;31(9):1713–23.
 74. Rodriguez PC, Zea AH, Culotta KS, Zabaleta J, Ochoa JB, Ochoa AC. Regulation of T Cell Receptor CD3 ζ Chain Expression by l-Arginine. *J Biol Chem.* 2002;277(24):21123–9.

75. Bingisser RM, Tilbrook PA, Holt PG, Bingisser RM, Kees UR. Macrophage-Derived Nitric Oxide Regulates T Cell Activation via Reversible Disruption of the Jak3/STAT5 Signaling Pathway. *J Immunol.* 1998;160(20):5729–34.
76. Harari O, Liao JK. Inhibition of MHC II gene transcription by nitric oxide and antioxidants. *Curr Pharm Des.* 2004;10(8):893–8.
77. Kusmartsev S, Nefedova Y, Yoder D, Gabrilovich DI. Antigen-Specific Inhibition of CD8+ T Cell Response by Immature Myeloid Cells in Cancer Is Mediated by Reactive Oxygen Species. *J Immunol.* 2004;172(2):989–99.
78. Bronte V, Zanovello P. Regulation of immune responses by L-arginine metabolism. *Nat Rev Immunol.* 2005;5(8):641–54.
79. Rodríguez PC, Ochoa AC. Arginine regulation by myeloid derived suppressor cells and tolerance in cancer: Mechanisms and therapeutic perspectives. *Immunol Rev.* 2008;222(1):180–91.
80. Zea AH, Rodriguez PC, Atkins MB, Hernandez C, Signoretti S, Zabaleta J, *et al.* Arginase-Producing Myeloid Suppressor Cells in Renal Cell Carcinoma Patients : A Mechanism of Tumor Evasion. *Cancer Res.* 2005;65(8):3044–8.
81. Gehad AE, Lichtman MK, Schmults CD, Teague JE, Calarese AW, Jiang Y, *et al.* Nitric oxide-producing myeloid-derived suppressor cells inhibit vascular e-selectin expression in human squamous cell carcinomas. *J Invest Dermatol.* 2012;132(11):2642–51.
82. Schmielau J, Finn OJ. Activated Granulocytes and Granulocyte-derived Hydrogen Peroxide Are the Underlying Mechanism of Suppression of T-Cell Function in Advanced Cancer Patients. *Cancer Res.* 2001;61(12):4756–60.
83. Nagaraj S, Gupta K, Pisarev V, Kinarsky L, Sherman S, Kang L, *et al.* Altered recognition of antigen is a novel mechanism of CD8+ T cell tolerance in cancer. *Nat Med.* 2008;13(7):828–35.
84. Toh B, Wang X, Keeble J, Sim WJ, Khoo K, Wong WC, *et al.* Mesenchymal transition and dissemination of cancer cells is driven by myeloid-derived suppressor cells infiltrating the primary tumor. *PLoS Biol.* 2011;9(9).
85. Engels, Boris; Rowley, Donald A.; Schreiber H. Targeting stroma to treat cancers. *Semin Cancer Biol.* 2012;22(1):41–9.
86. Yang L, DeBusk LM, Fukuda K, Fingleton B, Green-Jarvis B, Shyr Y, *et al.* Expansion of myeloid immune suppressor Gr⁺CD11b⁺ cells in tumor-bearing host directly promotes tumor angiogenesis. *Cancer Cell.* 2004;6(4):409–21.
87. Sinha P, Okoro C, Foell D, Freeze HH, Ostrand-Rosenberg S, Srikrishna G. Proinflammatory S100 Proteins Regulate the Accumulation of Myeloid-Derived Suppressor Cells. *J Immunol.* 2008;181(7):4666–75.
88. Ichikawa, Mie; Williams, Roy; Wang, Ling; Vogl, Thomas; Srikrishna G. S100A8/A9 activate key genes and pathways in colon tumor progression. *Mol Cancer Res.* 2011;9(2):133–48.
89. Burke M, Choksawangkarn W, Edwards N, Ostrand-Rosenberg S, Fenselau C. Exosomes from Myeloid-Derived Suppressor Cells Carry Biologically Active Proteins. *J Proteome Res.* 2014;13(2):836–43.
90. Shi H, Zhang J, Han X, Li H, Xie M, Sun Y, *et al.* Recruited monocytic myeloid-derived suppressor cells promote the arrest of tumor cells in the premetastatic niche through an IL-1B-mediated increase in E-selectin expression. *Int J cancer.*

- 2017;1383:1370–83.
91. Noman MZ, Desantis G, Janji B, Hasmim M, Karray S, Dessen P, *et al.* PD-L1 is a novel direct target of HIF-1 , and its blockade under hypoxia enhanced MDSC-mediated T cell activation. *J Exp Med.* 2014;211(5):781–90.
 92. Pan PY, Ma G, Weber KJ, Ozao-Choy J, Wang G, Yin B, *et al.* Immune stimulatory receptor CD40 is required for T-cell suppression and T regulatory cell activation mediated by myeloid-derived suppressor cells in cancer. *Cancer Res.* 2010;70(1):99–108.
 93. Mao Y, Sarhan D, Steven A, Seliger B, Kiessling R, Lundqvist A. Inhibition of tumor-derived prostaglandin-E2 blocks the induction of myeloid-derived suppressor cells and recovers natural killer cell activity. *Clin Cancer Res.* 2014;20(15):4096–106.
 94. Habibi M, Kmiecik M, Graham L, Morales JK, Harry D. Radiofrequency thermal ablation of breast tumors combined with intralesional administration of IL-7 and IL-15 augments anti-tumor immune responses and inhibits tumor development and metastasis. *Breast Cancer Res Treat.* 2009;114(3):423–31.
 95. Yang L, Huang J, Ren X, Gorska AE, Chytil A, Carbone DP, *et al.* Abrogation of TGFB signaling in mammary carcinomas recruits Gr-1+CD11b+ myeloid cells that promote metastasis. *Cancer Cell.* 2008;13(1):23–35.
 96. Bronte V, Serafini P, De Santo C, Marigo I, Tosello V, Mazzoni A, *et al.* IL-4-induced arginase 1 suppresses alloreactive T cells in tumor-bearing mice. *J Immunol.* 2003;170(1):270–8.
 97. Kapanadze T, Gamrekelashvili J, Ma C, Chan C, Zhao F, Hewitt S, *et al.* Regulation of accumulation and function of myeloid derived suppressor cells in different murine models of hepatocellular carcinoma. *J Hepatol* [Internet]. European Association for the Study of the Liver; 2013 Jun 21 [cited 2013 Jul 1]; Available from: <http://www.ncbi.nlm.nih.gov/pubmed/23796475>
 98. Youn Je-In, Nagaraj Srinivas, Collazo Michelle GDI. Subsets of Myeloid- derived Suppressor Cells in Tumor Bearing Mice. *J Immunol.* 2009;181(8):5791–802.
 99. Bronte V, Brandau S, Chen S, Colombo MP, Frey AB, Greten TF, *et al.* Recommendations for myeloid-derived suppressor cell nomenclature and characterization standards. *Nat Commun.* 2016;7:1–10.
 100. Sun H-L, Zhou X, Xue Y-F, Wang K, Shen Y-F, Mao J-J, *et al.* Increased frequency and clinical significance of myeloid-derived suppressor cells in human colorectal carcinoma. *World J Gastroenterol.* 2012;18(25):3303–9.
 101. Diaz-montero CM, Salem ML, Nishimura MI, Garrett-Mayer E, Cole DJ, Montero AJ. Increased circulating myeloid-derived suppressor cells correlate with clinical cancer stage, metastatic burden, and doxorubicin-cyclophosphamide chemotherapy. *Cancer Immunol Immunother.* 2009;58(1):49–59.
 102. Wang L, Chang EWY, Wong SC, Ong S-M, Chong DQY, Ling KL. Increased Myeloid-Derived Suppressor Cells in Gastric Cancer Correlate with Cancer Stage and Plasma S100A8/A9 Proinflammatory Proteins. *J Immunol.* 2013;190(2):794–804.
 103. Arihara F, Mizukoshi E, Kitahara M, Takata Y, Arai K, Yamashita T, *et al.* Increase in CD14+HLA-DR-/low myeloid-derived suppressor cells in hepatocellular carcinoma patients and its impact on prognosis. *Cancer Immunol*

- Immunother. 2013;62(8):1421–30.
104. Khaled YS, Ammori BJ, Elkord E. Increased levels of granulocytic myeloid-derived suppressor cells in peripheral blood and tumour tissue of pancreatic cancer patients. *J Immunol Res*. Hindawi Publishing Corporation; 2014;2014:879897.
 105. Eruslanov E, Neuberger M, Daurkin I, Perrin GQ, Algood C, Dahm P, *et al*. Circulating and tumor-infiltrating myeloid cell subsets in patients with bladder cancer. *Int J Cancer*. 2012;130(5):1109–19.
 106. Huang A, Zhang B, Wang B, Zhang F, Fan K-X, Guo Y-J. Increased CD14(+)HLA-DR (-/low) myeloid-derived suppressor cells correlate with extrathoracic metastasis and poor response to chemotherapy in non-small cell lung cancer patients. *Cancer Immunol Immunother*. 2013;62(9):1439-51.
 107. Yan X, Orentas RJ, Johnson BD. Tumor-derived macrophage migration inhibitory factor (MIF) inhibits T lymphocyte activation. *Cytokine*. 2006;33(4):188–98.
 108. Zhou Q, Yan X, Gershan J, Orentas RJ, Johnson BD. Expression of macrophage migration inhibitory factor by neuroblastoma leads to the inhibition of antitumor T cell reactivity in vivo. *J Immunol*. 2008;181(3):1877–86.
 109. Choi S, Kim H-R, Leng L, Kang I, Jorgensen WL, Cho C-S, *et al*. Role of Macrophage Migration Inhibitory Factor in the Regulatory T Cell Response of Tumor-Bearing Mice. *J Immunol*. 2012;189(8):3905–13.
 110. Yaddanapudi K, Rendon BE, Lamont G, Kim EJ, Al Rayyan N, Richie J, *et al*. MIF Is Necessary for Late-Stage Melanoma Patient MDSC Immune Suppression and Differentiation. *Cancer Immunol Res*. 2016;4(2):101-112.
 111. Xu S, Guo X, Gao X, Xue H, Zhang J. Macrophage migration inhibitory factor enhances autophagy by regulating ROCK1 activity and contributes to the escape of dendritic cell surveillance in glioblastoma. *Int J Oncol*. 2016;49(5):2105–15.
 112. Ghoochani A, Schwarz MA, Yakubov E, Engelhorn T, Doer A, Buchfelder M, *et al*. MIF-CD74 signaling impedes microglial M1 polarization and facilitates brain tumorigenesis. *Oncogene*. 2016;35(48):6246–61.
 113. Krockenberger M, Dombrowski Y, Weidler C, Ossadnik M, Honig A, Hausler S, *et al*. Macrophage Migration Inhibitory Factor Contributes to the Immune Escape of Ovarian Cancer by Down-Regulating NKG2D. *J Immunol*. 2008;180(11):7338–48.
 114. Mittelbronn M, Platten M, Zeiner P, Dombrowski Y, Frank B, Zachskorn C, *et al*. Macrophage migration inhibitory factor (MIF) expression in human malignant gliomas contributes to immune escape and tumour progression. *Acta Neuropathol*. 2011;122(3):353–65.
 115. Tesniere A, Panaretakis T, Kepp O, Apetoh L, Ghiringhelli F, Zitvogel L, *et al*. Molecular characteristics of immunogenic cancer cell death. *Cell Death Differ*. 2008;15(1):3–12.
 116. Kepp O, Senovilla L, Vitale I, Vacchelli E, Adjemian S, Agostinis P, *et al*. Consensus guidelines for the detection of immunogenic cell death. *Oncoimmunology*. 2014;3(9).
 117. Galluzzi L, Buqué A, Kepp O, Zitvogel L, Kroemer G. Immunogenic cell death in cancer and infectious disease. *Nat Publ Gr*. 2016;17(2):97–111.
 118. Sims GP, Rowe DC, Rietdijk ST, Herbst R, Coyle AJ. HMGB1 and RAGE in Inflammation and Cancer. *Annu Rev Immunol*. 2010;28(1):367–88.

119. Fucikova J, Kralikova P, Fialova A, Brtnicky T, Rob L. Human Tumor Cells Killed by Anthracyclines Induce a Tumor-Specific Immune Response. *Cancer Res.* 2011;4:4821–34.
120. Obeid M, Tesniere A, Fimia GM, Apetoh L, Panaretakis T, Casares N, *et al.* Calreticulin exposure dictates the immunogenicity of cancer cell death. *Nat Med.* 2007;13(1):54–61.
121. Garg AD, Krysko D V, Vandenabeele P, Agostinis P. Hypericin-based photodynamic therapy induces surface exposure of damage-associated molecular patterns like HSP70 and calreticulin. *Cancer Immunol Immunother.* 2012;70:215–21.
122. Spisek R, Charalambous A, Mazumder A, Vesole H. D, Jagannath Sundar, Dhodapkar V. M. Bortezomib enhances dendritic cell (DC)–mediated induction of immunity to human myeloma via exposure of cell surface heat shock protein 90 on dying tumor cells: therapeutic implications. *Blood.* 2007;109(11):4839–45.
123. Kroemer G, Galluzzi L, Kepp O, Zitvogel L. Immunogenic Cell Death in Cancer Therapy. *Annu Rev Immunol.* 2013;31:51–72.
124. Ghiringhelli F, Apetoh L, Tesniere A, Aymeric L, Ma Y, Ortiz C, *et al.* Activation of the NLRP3 inflammasome in dendritic cells induces IL-1 β –dependent adaptive immunity against tumors. *Nat Med.* 2009;15(10):1170–9.
125. Garg AD, Krysko D V., Vandenabeele P, Agostinis P. The emergence of phox-ER stress induced immunogenic apoptosis. *Oncoimmunology.* 2012;1(5):786–8.
126. Dudek AM, Garg AD, Krysko D V, Ruyscher D De, Agostinis P. Inducers of immunogenic cancer cell death. *Cytokine Growth Factor Rev.* 2013;24(4):319–33.
127. Suzuki Y, Mimura K, Yoshimoto Y, Watanabe M, Ohkubo Y, Izawa S, *et al.* Immunogenic tumor cell death induced by chemoradiotherapy in patients with esophageal squamous cell carcinoma. *Cancer Res.* 2012;72(16):3967–76.
128. Garg AD, Krysko D V., Verfaillie T, Kaczmarek A, Ferreira GB, Marysael T, *et al.* A novel pathway combining calreticulin exposure and ATP secretion in immunogenic cancer cell death. *EMBO J.* 2012;31(5):1062–79.
129. Paget S. The distribution of secondary growths in cancer of the breast. *Lancet.* 1889;133(3421):571–3.
130. Kaplan RN, Riba RD, Zacharoulis S, Bramley AH, Vincent L, Costa C, *et al.* VEGFR1-positive haematopoietic bone marrow progenitors initiate the pre-metastatic niche. *Nature.* 2005;438(7069):820–7.
131. Harris AL. Hypoxia—a Key Regulatory Factor in Tumour Growth. *Nat Rev Cancer.* 2002;2(1):38–47.
132. Semenza GL. Molecular mechanisms mediating metastasis of hypoxic breast cancer cells. *Trends Mol Med.* 2012;18(9):534–43.
133. Levental KR, Yu H, Kass L, Lakins JN, Erler JT, Fong SFT, *et al.* Matrix Crosslinking Forces Tumor Progression By Enhancing Integrin Signaling. *Cell.* 2009;139(5):891–906.
134. Erler JT, Bennewith KL, Cox TR, Lang G, Bird D, Koong A, *et al.* Hypoxia-induced lysyl oxidase is a critical mediator of bone marrow cell recruitment to form the premetastatic niche. *Cancer Cell.* 2009;15(1):35–44.
135. Erler JT, Bennewith KL, Nicolau M, Dornhöfer N, Kong C, Le Q-T, *et al.* Lysyl oxidase is essential for hypoxia-induced metastasis. *Nature.*

- 2006;440(7088):1222–6.
136. Le Q-T, Harris J, Magliocco AM, Kong CS, Diaz R, Shin B, *et al.* Validation of Lysyl Oxidase As a Prognostic Marker for Metastasis and Survival in Head and Neck Squamous Cell Carcinoma: Radiation Therapy Oncology Group Trial 90-03. *J Clin Oncol.* 2009;27(26):4281–6.
 137. Barker HE, Chang J, Cox TR, Lang G, Bird D, Nicolau M, *et al.* LOXL2-mediated matrix remodeling in metastasis and mammary gland involution. *Cancer Res.* 2011;71(5):1561–72.
 138. Hiratsuka S, Watanabe A, Aburatani H, Maru Y. Tumour-mediated upregulation of chemoattractants and recruitment of myeloid cells predetermines lung metastasis. *Nat Cell Biol.* 2006;8(12):1369–75.
 139. Kowanetz M, Wu X, Lee J, Tan M, Hagenbeek T, Qu X, *et al.* Granulocyte-colony stimulating factor promotes lung metastasis through mobilization of Ly6G+Ly6C+ granulocytes. *PNAS.* 2010;107(50):21248–55.
 140. Chioda M, Peranzoni E, Desantis G, Papalini F, Falisi E, Samantha S, *et al.* Myeloid cell diversification and complexity: An old concept with new turns in oncology. *Cancer Metastasis Rev.* 2011;30(1):27–43.
 141. Sceneay J, Chow MT, Chen A, Halse HM, Wong CSF, Andrews DM, *et al.* Primary Tumor Hypoxia Recruits CD11b+/Ly6Cmed/Ly6G+ Immune Suppressor Cells and Compromises NK Cell Cytotoxicity in the Premetastatic Niche. *Cancer Res.* 2012;72(16):3906–11.
 142. Yan HH, Pickup M, Pang Y, Gorska AE, Li Z, Chytil A, *et al.* Gr-1+CD11b+ myeloid cells tip the balance of immune protection to tumor promotion in the premetastatic lung. *Cancer Res.* 2010;70(15):6139–49.
 143. Granot, Zvi; Henke, Erik; Comen, Elizabeth; King, Tari; Norton, Larry; Benezra R. Tumor entrained neutrophils inhibit seeding in the premetastatic lung. *Cancer Cell.* 2011;31(9):1713–23.
 144. Gao D, Joshi N, Choi H, Ryu S, Hahn M, Catena R, *et al.* Myeloid progenitor cells in the premetastatic lung promote metastases by inducing mesenchymal to epithelial transition. *Cancer Res.* 2012;72(6):1384–94.
 145. Dexter DL, Kowalski HM, Blazar BA, Fligiel Z, Vogel R, Heppner GH. Heterogeneity of tumor cells from a single mouse mammary tumor. *Cancer Res.* 1978;38(October):3174–81.
 146. Pulaski B a, Ostrand-Rosenberg S. Mouse 4T1 breast tumor model. *Curr Protoc Immunol.* 2001;Chapter 20:Unit 20.2.
 147. Pulaski B a, Ostrand-Rosenberg S. Reduction of Established Spontaneous Mammary Carcinoma Metastases following Immunotherapy with Major Histocompatibility Complex Class II and B7.1 Cell-based Tumor Vaccines. *Cancer Res.* 1998;1486–93.
 148. Lelekakis M, Moseley JM, Martin TJ, Hards D, Williams E, Lowen D, *et al.* A novel orthotopic model of breast cancer metastasis to bone. *Clin Exp metastasis.* 1999;17(2):163–70.
 149. Guy CT, Cardiff RD, Muller WJ. Induction of mammary tumors by expression of polyomavirus middle T oncogene: a transgenic mouse model for metastatic disease. *Mol Cell Biol.* 1992;12(3):954–61.
 150. Rodriguez-Viciano P, Collins C, Fried M. Polyoma and SV40 proteins

- differentially regulate PP2A to activate distinct cellular signaling pathways involved in growth control. *Proc Natl Acad Sci.* 2006;103(51):19290–5.
151. Fluck MM, Schaffhausen BS. Lessons in signaling and tumorigenesis from polyomavirus middle T antigen. *Microbiol Mol Biol Rev.* 2009;73(3):542–63.
 152. Ichiyama H, Onodera S, Nishihira J, Ishibashi T, Nakayama T, Minami A, *et al.* Inhibition of joint inflammation and destruction induced by anti-type II collagen antibody/lipopolysaccharide (LPS)-induced arthritis in mice due to deletion of macrophage migration inhibitory factor (MIF). *Cytokine.* 2004;26(5):187–94.
 153. Bini L, Magi B, Marzocchi B, Arcuri F, Tripodi S, Cintonino M, *et al.* Protein expression profiles in human breast ductal carcinoma and histologically normal tissue. *Electrophoresis.* 1997;18(15):2832–41.
 154. Meyer-Siegler, Katherine; Fattor, Ron; Hudson PB. Expression of Macrophage Migration Inhibitor Factor in the Human Prostate. *Diagn Mol Path.* 1998;7(1):44–50.
 155. Shimizu T, Abe R, Nakamura H, Ohkawara a, Suzuki M, Nishihira J. High expression of macrophage migration inhibitory factor in human melanoma cells and its role in tumor cell growth and angiogenesis. *Biochem Biophys Res Commun.* 1999 Nov 2;264(3):751–8.
 156. Meyer-Siegler, Katherine; Hudson PB. Enhanced Expression of Macrophage Migration Inhibitory Factor in Prostatic Adenocarcinoma Metastases. *Adult Urol.* 1996;4295(96).
 157. Xia HHX, Yang Y, Chu KM, Gu Q, Zhang YY, He H, *et al.* Serum macrophage migration-inhibitory factor as a diagnostic and prognostic biomarker for gastric cancer. *Cancer.* 2009;115(23):5441–9.
 158. Swope M, Sun HW, Blake PR, Lolis E. Direct link between cytokine activity and a catalytic site for macrophage migration inhibitory factor. *EMBO J.* 1998;17(13):3534–41.
 159. Ouertatani-Sakouhi, Hajer; El-Turk, Farah; Fauvet, Bruno; Roger, Thierry; Le Roy, Didier; Karpinar, *et al.* A new class of isothiocyanate-based irreversible inhibitors of Macrophage Migration Inhibitory Factor (MIF). *Biochemistry.* 2009;70(4):646–56.
 160. Aslakson CJ, Miller FR. Selective Events in the Metastatic Process Defined by Analysis of the Sequential Dissemination of Subpopulations of a Mouse Mammary Tumor. *Cancer Res.* 1992;52(6):1399–405.
 161. Ullrich E, Bonmort M, Mignot G, Kroemer G, Zitvogel L. Tumor stress, cell death and the ensuing immune response. *Cell Death Differ.* 2008;15(1):21–8.
 162. Casares N, Pequignot MO, Tesniere A, Ghiringhelli F, Roux S, Chaput N, *et al.* Caspase-dependent immunogenicity of doxorubicin-induced tumor cell death. *J Exp Med.* 2005;202(12).
 163. Kazama H, Ricci J, Herndon JM, Hoppe G, Green DR, Ferguson TA. Induction of Immunological Tolerance by Apoptotic Cells Requires Caspase-Dependent Oxidation of High-Mobility Group Box-1 Protein. *Immunity.* 2008;21–32.
 164. Guo Y, Hou J, Luo Y, Wang D. Functional disruption of macrophage migration inhibitory factor (MIF) suppresses proliferation of human H460 lung cancer cells by caspase-dependent apoptosis. *Cancer Cell Int.* 2013;13(1):28.
 165. Maria S, Jörg J, Guido F, Sorin S, Ebinger A. Macrophage migration inhibitory

- factor (MIF) is induced by cytotoxic drugs and is involved in immune escape and migration in childhood rhabdomyosarcoma. *Cancer Immunol Immunother.* 2016;65(12):1465–76.
166. Qiu C-H, Miyake Y, Kaise H, Kitamura H, Ohara O, Tanaka M. Novel Subset of CD8 + Dendritic Cells Localized in the Marginal Zone Is Responsible for Tolerance to Cell-Associated Antigens. *J Immunol.* 2009;182(7):4127–36.
 167. Nakajima C, Uekusa Y, Iwasaki M, Yamaguchi N, Mukai T, Gao P, *et al.* A role of IFN γ in Tumor Immunity: T cells with the capacity to reject tumor cells are generated but fail to migrate to tumor sites in IFN γ deficient mice. *Cancer Res.* 2001;61(8):3399–405.
 168. Schreiber RD, Celada A, Buchmeier N. The role of interferon gamma in the induction of activated macrophages. *Forum D'Immunologie.* 1983;0:203-206.
 169. Matsushita H, Hosoi A, Ueha S, Abe J, Fujieda N. Cytotoxic T Lymphocytes Block Tumor Growth Both by Lytic Activity and IFN γ -Dependent Cell-Cycle Arrest. *Cancer Immunol Res.* 2015;3:26–37.
 170. Chin YE, Kitagawa M, Su W-CS, You Z-H, Iwamoto Y, Fu X-Y. Cell Growth Arrest and Induction of Cyclin-Dependent Kinase Inhibitor p21WAF1/CIP1 Mediated by STAT1. *Science.* 1996;272(5262):719-722.
 171. Braumuller H, Wieder T, Brenner E, Abmann S, Hahn M, Alkhaled M, *et al.* T-helper-1-cell cytokines drive cancer into senescence. *Nat Lett.* 2013;494(7437):361-5.
 172. Gupta GP, Massagué J. Cancer Metastasis: Building a Framework. *Cell.* 2006;127(4):679–95.
 173. Klein CA. The Metastasis Cascade. *Science.* 2008;9(4):1785–7.
 174. Ren Y, Chan HM, Fan J, Xie Y, Chen YX, Li W, *et al.* Inhibition of tumor growth and metastasis in vitro and in vivo by targeting macrophage migration inhibitory factor in human neuroblastoma. *Oncogene.* 2006;25(25):3501–8.
 175. Liu G, Xu Z, Hao D. MicroRNA-451 inhibits neuroblastoma proliferation, invasion and migration by targeting macrophage migration inhibitory factor. *Mol Med Rep.* 2016;13(3):2253–60.
 176. Zhang M, Yan L, Kim JA. Modulating mammary tumor growth, metastasis and immunosuppression by siRNA-induced MIF reduction in tumor microenvironment. *Cancer Gene Ther.* 2015;22(10):463-74.
 177. Filipazzi P, Valenti R, Huber V, Pilla L, Canese P, Iero M, *et al.* Identification of a new subset of myeloid suppressor cells in peripheral blood of melanoma patients with modulation by a granulocyte-macrophage colony-stimulation factor-based antitumor vaccine. *J Clin Oncol.* 2007;25(18):2546–53.
 178. Almand B, Clark JI, Nikitina E, van Beynen J, English NR, Knight SC, *et al.* Increased production of immature myeloid cells in cancer patients: a mechanism of immunosuppression in cancer. *J Immunol.* 2001;166(1):678–89.
 179. Gabitass RF, Annels NE, Stocken DD, Pandha H a, Middleton GW. Elevated myeloid-derived suppressor cells in pancreatic, esophageal and gastric cancer are an independent prognostic factor and are associated with significant elevation of the Th2 cytokine interleukin-13. *Cancer Immunol Immunother.* 2011;60(10):1419–30.
 180. Verschoor CP, Johnstone J, Millar J, Dorrington MG, Habibagahi M, Lelic A, *et*

- al.* Blood CD33(+)HLA-DR(-) myeloid-derived suppressor cells are increased with age and a history of cancer. *J Leukoc Biol.* 2013;93(4):633-7.
181. Duffy A, Zhao F, Haile L, Gamrekelashvili J, Fioravanti S, Ma C, *et al.* Comparative analysis of monocytic and granulocytic myeloid-derived suppressor cell subsets in patients with gastrointestinal malignancies. *Cancer Immunol Immunother.* 2013;62(2):299–307.
 182. Zhang B, Wang Z, Wu L, Zhang M, Li W, Ding J, *et al.* Circulating and Tumor-Infiltrating Myeloid-Derived Suppressor Cells in Patients with Colorectal Carcinoma. *PLoS One.* 2013;8(2).
 183. Condamine T, Gabrilovich DI. Molecular mechanisms regulating myeloid-derived suppressor cell differentiation and function. *Trends Immunol.* 2011;32(1):19–25.
 184. Movahedi K, Guillems M, Van den Bossche J, Van den Bergh R, Gysemans C, Beschin A, *et al.* Identification of discrete tumor-induced myeloid-derived suppressor cell subpopulations with distinct T cell-suppressive activity. *Blood.* 2008;111(8):4233–44.
 185. Murata Y. Study of Splenic Enlargement in Tumor-bearing Mice. 1959;50(1):89–105.
 186. Giles AJ, Reid CM, Evans JD, Murgai M, Highfill SL, Kasai M, *et al.* Activation of hematopoietic stem/progenitor cells promotes immunosuppression within the pre-metastatic niche. 2015;76(6):1335-47.
 187. Sharma SK, Chintala NK, Vadrevu SK, Patel J, Karbowniczek M, Markiewski MM. Pulmonary Alveolar Macrophages Contribute to the Premetastatic Niche by Suppressing Antitumor T Cell Responses in the Lungs. *J Immunol.* 2015;194(11):5529-38.
 188. Yu PF, Huang Y, Han YY, Lin LY, Sun WH, Rabson AB, *et al.* TNF α -activated mesenchymal stromal cells promote breast cancer metastasis by recruiting CXCR2⁺ neutrophils. *Oncogene.* 2016;36(4):482-490.
 189. Ahlgren J, Westman G, Stål O, Arnesson L-G. Prediction of axillary lymph node metastases in a screened breast cancer population. *Acta Oncol.* 1994;33(6):603–8.
 190. Foulkes WD. Size surprise? Tumour size, nodal status, and outcome after breast cancer. *Curr Oncol.* 2012;19(5):241–3.
 191. Gajdos C, Tartter PI, Bleiweiss IJ. Lymphatic invasion, tumor size, and age are independent predictors of axillary lymph node metastases in women with T1 breast cancers. *Ann Surg.* 1999;230(5):692–6.
 192. Orang E, Marzony ET, Afsharfard A. Predictive Role of Tumor Size in Breast Cancer with Axillary Lymph Node Involvement - Can Size of Primary Tumor be used to Omit an Unnecessary Axillary Lymph Node Dissection? *Asian Pacific J Cancer Prev.* 2013;14(2):717–22.
 193. Westenend PJ, Meurs CJC, Damhuis RAM. Tumour size and vascular invasion predict distant metastasis in stage I cancer. Grade distinguishes early and late metastasis. *J Clin Pathol.* 2005;58(2):196–201.
 194. Welford SM, Bedogni B, Gradin K, Poellinger L, Powell MB, Giaccia AJ. HIF1 α delays premature senescence through the activation of MIF. *Genes Dev.* 2006;20(24):3366–71.
 195. Copple, Bryan L., Bai, Shan, Burgoon, Lyle D., Moon J-O. Hypoxia-inducible Factor-1 α Regulates Expression of Genes in Hypoxic Hepatic Stellate Cells

- Important for Collagen Deposition and Angiogenesis. *Liver Int.* 2011;29(10):1883–9.
196. Fu H, Luo F, Yang L, Wu W, Liu X. Hypoxia stimulates the expression of macrophage migration inhibitory factor in human vascular smooth muscle cells via HIF-1 α dependent pathway. *BMC Cell Biol.* 2010;11:66.
 197. Simons D, Grieb G, Hristov M, Pallua N, Weber C, Bernhagen J, *et al.* Hypoxia-induced endothelial secretion of macrophage migration inhibitory factor and role in endothelial progenitor cell recruitment. *J Cell Mol Med.* 2011;15(3):668–78.
 198. Larsen M, Tazzyman S, Lund EL, Junker N, Lewis CE, Kristjansen PEG, *et al.* Hypoxia-induced secretion of macrophage migration-inhibitory factor from MCF-7 breast cancer cells is regulated in a hypoxia-inducible factor-independent manner. *Cancer Lett.* 2008;265(2):239–49.
 199. Oda S, Oda T, Nishi K, Takabuchi S, Wakamatsu T, Tanaka T, *et al.* Macrophage migration inhibitory factor activates hypoxia-inducible factor in a p53-dependent manner. *PLoS One.* 2008;3(5):e2215.
 200. Verjans E, Noetzel E, Bektas N, Schütz AK, Lue H, Lennartz B, *et al.* Dual role of macrophage migration inhibitory factor (MIF) in human breast cancer. *BMC Cancer.* 2009;9:230.
 201. Lue H, Thiele M, Franz J, Dahl E, Speckgens S, Leng L, *et al.* Macrophage migration inhibitory factor (MIF) promotes cell survival by activation of the Akt pathway and role for CSN5/JAB1 in the control of autocrine MIF activity. *Oncogene.* 2007;26(35):5046–59.
 202. Richard V, Kindt N, Decaestecker C, Gabius HJ, Laurent G, Noël JC, *et al.* Involvement of macrophage migration inhibitory factor and its receptor (CD74) in human breast cancer. *Oncol Rep.* 2014;32(2):523–9.
 203. Fersching DMI, Nagel D, Siegele B, Salat C, Heinemann V, Holdenrieder S, *et al.* Apoptosis-related biomarkers sFAS, MIF, ICAM-1 and PAI-1 in serum of breast cancer patients undergoing neoadjuvant chemotherapy. *Anticancer Res.* 2012;32(5):2047–58.
 204. Conine SJ, Cross J V. MIF Deficiency Does Not Alter Glucose Homeostasis or Adipose Tissue Inflammatory Cell Infiltrates during Diet-Induced Obesity. *Obesity.* 2014;22(2):418–25.
 205. Lin EY, Nguyen a V, Russell RG, Pollard JW. Colony-stimulating factor 1 promotes progression of mammary tumors to malignancy. *J Exp Med.* 2001;193(6):727–40.
 206. Hassan S, Buchanan M, Jahan K, Aguilar-Mahecha A, Gaboury L, Muller WJ, *et al.* CXCR4 peptide antagonist inhibits primary breast tumor growth, metastasis and enhances the efficacy of anti-VEGF treatment or docetaxel in a transgenic mouse model. *Int J Cancer.* 2011;129(1):225–32.
 207. Boyle ST, Faulkner JW, McColl SR, Kochetkova M. The chemokine receptor CCR6 facilitates the onset of mammary neoplasia in the MMTV-PyMT mouse model via recruitment of tumor-promoting macrophages. *Mol Cancer.* 2015;14(1):1–14.
 208. DeNardo DG, Barreto JB, Andreu P, Vasquez L, Tawfik D, Kolhatkar N, *et al.* CD4(+) T cells regulate pulmonary metastasis of mammary carcinomas by enhancing protumor properties of macrophages. *Cancer Cell.* 2009;16(2):91–102.

209. Strachan DC, Ruffell B, Oei Y, Bissell MJ, Coussens LM, Pryer N, *et al.* CSF1R inhibition delays cervical and mammary tumor growth in murine models by attenuating the turnover of tumor-associated macrophages and enhancing infiltration by CD8⁺T cells. *Oncoimmunology*. 2013;2(12).
210. Galluzzi L, Pedro JMB, Demaria S. Activating autophagy to potentiate immunogenic chemotherapy and radiation therapy. *Nat Publ Gr*. 2016;14(4):247–58.
211. Ron D, Walter P. Signal integration in the endoplasmic reticulum unfolded protein response. *Nat Rev Mol Cell Biol*. 2007;8(7):519–29.
212. Maurel M, McGrath EP, Mnich K, Healy S, Chevet E, Samali A. Controlling the unfolded protein response-mediated life and death decisions in cancer. *Semin Cancer Biol*. 2015;33:57–66.
213. Menu P, Mayor A, Zhou R, Tardivel A, Ichijo H, Mori K, *et al.* ER stress activates the NLRP3 inflammasome via an UPR-independent pathway. *Cell Death Dis*. 2012;3(1):e261-6.
214. Rufo N, Garg AD, Agostinis P. The Unfolded Protein Response in Immunogenic Cell Death and Cancer Immunotherapy. *Trends in Cancer*. 2017;3(9):643–58.
215. Martin SJ, Reutelingsperger CP, McGahon a J, Rader J a, van Schie RC, LaFace DM, *et al.* Early Redistribution of Plasma Membrane Phosphatidylserine is a General Feature of Apoptosis Regardless of the Initiating Stimulus: Inhibition by Overexpression of Bcl-2 and Abl. *J Exp Med*. 1995;182:1545–56.
216. Panaretakis T, Kepp O, Brockmeier U, Tesniere A, Bjorklund AC, Chapman DC, *et al.* Mechanisms of pre-apoptotic calreticulin exposure in immunogenic cell death. *EMBO J*. 2009;28(5):578–90.
217. Asea A, Kabingu E, Stevenson MA, Calderwood SK. HSP70 peptide-bearing and peptide-negative preparations act as chaperokines. *Cell Stress Chaperones*. 2000;5(5):425–31.
218. Schild H, Arnold-Schild D, Lammert E, Rammensee HG. Stress proteins and immunity mediated by cytotoxic T lymphocytes. *Curr Opin Immunol*. 1999;11(1):109–13.
219. Srivastava PK, Menoret A, Basu S, Binder RJ, McQuade KL. Heat shock proteins come of age: Primitive functions acquire new roles in an adaptive world. *Immunity*. 1998;8(6):657–65.
220. Binder RJ, Blachere NE, Srivastava PK. Heat Shock Protein-chaperoned Peptides but not Free Peptides Introduced into the Cytosol are Presented Efficiently by Major Histocompatibility Complex I Molecules. *J Biol Chem*. 2001;276(20):17163–71.
221. Elliott MR, Chekeni FB, Tramont PC, Lazarowski ER, Kadl A, Walk SF, *et al.* Nucleotides released by apoptotic cells act as a find-me signal to promote phagocytic clearance. *Nature*. 2009;461(7261):282–6.
222. Scaffidi P, Misteli T, Bianchi ME. Release of chromatin protein HMGB1 by necrotic cells triggers inflammation. *Nature*. 2002;418(6894):191–5.
223. Yamazaki T, Hannani D, Poirier-Colame V, Ladoire S, Locher C, Sistigu A, *et al.* Defective immunogenic cell death of HMGB1-deficient tumors: Compensatory therapy with TLR4 agonists. *Cell Death Differ*. 2014;21(1):69–78.
224. Bianchi ME, Beltrame M, Paonessa G. Specific Recognition of Cruciform DNA

- by Nuclear Protein HMG1. *Science*. 1989;243(4894):1056–9.
225. Park JS, Gamboni-robertson F, He Q, Svetkauskaite D, Kim J, Strassheim D, *et al.* High mobility group box 1 protein interacts with multiple Toll-like receptors. *Am J Physiol Cell Physiol*. 2006;3:917–24.
 226. Apetoh L, Ghiringhelli F, Tesniere A, Obeid M, Ortiz C, Criollo A, *et al.* Toll-like receptor 4-dependent contribution of the immune system to anticancer chemotherapy and radiotherapy. *Nat Med*. 2007;13(9):1050–9.
 227. Tian J, Avalos AM, Mao SY, Chen B, Senthil K, Wu H, *et al.* Toll-like receptor 9-dependent activation by DNA-containing immune complexes is mediated by HMGB1 and RAGE. *Nat Immunol*. 2007;8(5):487–96.
 228. Yu Q, Toole B, Stamenkovic I. Induction of apoptosis of metastatic mammary carcinoma cells in vivo by disruption of tumor cell surface CD44 function. *J Exp Med*. 1997;186(12):1985–96.
 229. Li Y, Li L, Brown TJ, Heldin P. Silencing of hyaluronan synthase 2 suppresses the malignant phenotype of invasive breast cancer cells. *Int J Cancer*. 2007;120(12):2557–67.
 230. Auvinen P, Tammi R, Kosma VM, Sironen R, Soini Y, Mannermaa A, *et al.* Increased hyaluronan content and stromal cell CD44 associate with HER2 positivity and poor prognosis in human breast cancer. *Int J Cancer*. 2013;132(3):531–9.
 231. Todaro M, Gaggianesi M, Catalano V, Benfante A, Iovino F, Biffoni M, *et al.* CD44v6 is a marker of constitutive and reprogrammed cancer stem cells driving colon cancer metastasis. *Cell Stem Cell*. 2014;14(3):342–56.
 232. Mantovani A, Bottazzi B, Colotta F, Sozzani S, Ruco L. The origin and function of tumor-associated macrophages. *Immunol Today*. 1992;13(7):265–70.
 233. Liu Y, Cao X. The origin and function of tumor-associated macrophages. *Cell Mol Immunol*. 2015;12(1):1–4.
 234. Mantovani A, Sozzani S, Locati M, Allavena P, Sica A. Macrophage polarization: Tumor-associated macrophages as a paradigm for polarized M2 mononuclear phagocytes. *Trends Immunol*. 2002;23(11):549–55.
 235. Mills CD, Kincaid K, Alt JM, Heilman MJ, Hill AM. M-1/M-2 Macrophages and the Th1/Th2 Paradigm. *J Immunol*. 2000;164(12):6166–73.
 236. Sica A, Saccani A, Bottazzi B, Polentarutti N, Vecchi A, Damme J V., *et al.* Autocrine Production of IL-10 Mediates Defective IL-12 Production and NF- κ B Activation in Tumor-Associated Macrophages. *J Immunol*. 2000;164(2):762–7.
 237. Loercher AE, Nash MA, Kavanagh JJ, Platsoucas CD, Freedman RS. Identification of an IL-10-Producing HLA-DR-Negative Monocyte Subset in the Malignant Ascites of Patients with Ovarian Carcinoma That Inhibits Cytokine Protein Expression and Proliferation of Autologous T Cells. *J Immunol*. 1999;163(11):6251–60.
 238. Kim J, Modlin RL, Moy RL, Dubinett SM, McHugh T, Nickoloff BJ, *et al.* IL-10 production in cutaneous basal and squamous cell carcinomas. A mechanism for evading the local T cell immune response. *J Immunol*. 1995;155:2240–7.
 239. Kambayashi R, Alexander H, Fong M, Strassman G. Potential involvement of IL-10 in suppressing tumor-associated macrophages. Colon-26-derived prostaglandin E2 inhibits TNF-alpha release via a mechanism involving IL-10. *J Immunol*.

- 2015;154(7):3383-90.
240. Franklin R a, Liao W, Sarkar A, Kim M V, Bivona MR, Liu K, *et al.* The Cellular and Molecular Origin of Tumor-Associated Macrophages. *Science*. 2014 May 8 [cited 2014 May 23];921.
 241. Yaddanapudi K, Putty K, Rendon BE, Lamont GJ, Faughn JD, Satoskar A, *et al.* Control of Tumor-Associated Macrophage Alternative Activation by Macrophage Migration Inhibitory Factor. *J Immunol*. 2013;190(6):2984-93.
 242. Gore Y, Starlets D, Maharshak N, Becker-Herman S, Kaneyuki U, Leng L, *et al.* Macrophage migration inhibitory factor induces B cell survival by activation of a CD74-CD44 receptor complex. *J Biol Chem*. 2008;283(5):2784–92.
 243. Kim J-Y, Kwok S-K, Hur K-H, Kim H-J, Kim NS, Yoo S, *et al.* Up-regulated macrophage migration inhibitory factor protects apoptosis of dermal fibroblasts in patients with systemic sclerosis. *Clin Exp Immunol*. 2008;152(2):328–35. 252.
 244. Ohta S, Misawa A, Fukaya R, Inoue S, Kanemura Y, Okano H, *et al.* Macrophage migration inhibitory factor (MIF) promotes cell survival and proliferation of neural stem/progenitor cells. *J Cell Sci*. 2012;125(13):3210–20.
 245. Li G-Q., Xia J, Lei X-Y, Zhang L. Macrophage migration inhibitory factor regulates proliferation of gastric cancer cells via the PI3K/Akt pathway. *World J Gastroenterol*. 2009;15(44):5541.